Equilibrium of the CO_2-NH_3-Urea-H_2O System under High Temperature and Pressure. II. Liquid-Vapor Equilibrium in the Loading Mole Ratio of $2NH_3$ to CO_2[1]

By Schōhachi KAWASUMI

(Received December 17, 1951)

It is an established experimental fact that the yield of urea in urea-synthesis from ammonia and carbon dioxide depends upon the loading density or ratio of the weights of the materials to the total volume of the reaction vessel at a given temperature. The writer showed in the previous paper[2] that the equilibrium pressure as well as the urea-yield is a fnnction of the loading density at a given temperature, and explained that the diversity of the equilibrium pressure is based upon that of the equilibrium composition of the liquid and vapor phase.

The object of the present paper is to show the relations within the equilibrium composition of the liquid and vapor phase, the loading density and the temperature, by analysing the composition of the two phases under high temperature and pressure. For this purpose the vapor composition, or mole ratios of ammonia, carbon dioxide and water in the vapor-phase, the liquid composition, or mole ratio of unconverted ammonia to carbon dioxide in the liquid-phase, the converted amount to urea, and liquid-vapor volume ratio have been determined respectively by the following analytical methods in the loading mole ratio of 2 ammonia to 1 carbon dioxide.

The liquid- and vapor-phase compositions in the equilibrium state of the system have been calculated from these data. From these results the effects of the loading density and the temperature respectively on the calculated equilibrium compositions and the equilibrium constant of the following reaction have been discussed.

$$CO_2+2NH_3 \rightleftarrows CO(NH_2)_2+H_2O \qquad (1)$$

Experimental Procedure

Method of Determining the Vapor Compositions.—It is concluded that the reaction in urea-synthesis from ammonia and carbon dioxide takes place in the liquid phase, with which the vapor phase composed of CO_2, NH_3 and H_2O is in a state of equilibrium in the reaction vessel. The writer investigated the mole ratio of CO_2, NH_3 and H_2O is in a state of equilibrium in the reaction vessel. The writer investigated the mole ratio of CO_2, NH_3 and H_2O in the vapor phase by the following method.

(1). **Experimental Apparatus.**—The experimental apparatus consists of the reaction vessel (A), vapor holder (B), and gas-analyzing apparatus (C) as shown in Fig. 1. A is just the same as the apparatus used for pressure measurement reported in the previous paper[2]. The vapor and liquid were kept in a state of equilibrium in the reaction vessel (A-3). The readings of equilibrium pressure by the pressure gauge (A-2) became constant after 5 to 6 hours at such a high temperature as 160°C. The gas sample was withdrawn from the vapor phase after 20 hours of being in a state of equilibrium. The vapor-holder (B) is a bottle of 3 liter capacity (B-1), which is dipped in the thermo-regulated water bath at 90°C. and provided with a mercury-dropping apparatus. A part of the vapor in A-3 which is under high temperature and pressure is discharged into B-1 at the state of 90°C. and 1 atm. The gas-analyzing apparatus (C) consists of a washing bottle of 1 normal sulphuric acid aqueous solution (C-1), which is kept in the thermostat at 70°C., U-tules with calcium chloride (C-2 and C-4) and kali-bulb (C-3). The mole ratio of CO_2, NH_3 and H_2O in the vapor was analyzed, sending the vapor in B-1 through this apparatus (C) gradually.

(2). **Procedure of Vapor Sampling.**—After heating the reaction vessel at a given temperature for 20 hours, the vapor in a state of equilibrium with the liquid was gently withdrawn through a 4 mm. high pressure valve (A-1) into a previously evacuated vapor-holder (B-1), which had been kept at the constant temperature of 90°C. to avoid the condensation of ammonium carbamate. To keep the condition of equilibrium between the vapor and the liquid in A-3, the valve (A-1) was adjusted by the reading of mercury head in a closed mercury manometer (B-6).

The sampling procedure through the valve (A-1) as described above—a method to get a gas sample at 90°C. and at the ordinary pressure—is the most

(1) A part of this paper was presented at the annual meeting of the Chemical Society of Japan held at Tokyo, on 6 April 1951.

(2) S. Kawasumi, This Bulletin, **24**, 148 (1951).

CHEMISTRY HALL LIBRARY

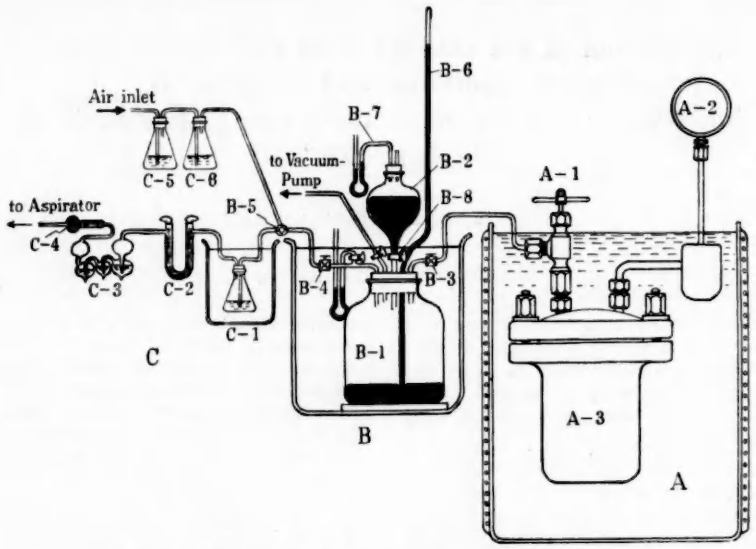

Fig. 1. –Apparatus for measuring the vapor compositions.

important. When the pressure of B-1 reached about 760 mmHg, the valve (A-1) and a screw-cock (B-3) were closed. At the temperature of 160°C. and the equilibrium pressure 70 to 150 kg./cm.², the readings of pressure drop were constantly between 5 and 7 kg./cm². The pipe between A-1 and B-3 which is exposed in the air, was heated to more than 70°C. by gas heating in order to avoid the condensation of the ammonium carbamate while withdrawing the vapor.

(3). **Determination of Mole Ratios of CO_2, NH_3 and H_2O.**—After the vapor was withdrawn, the vapor in B-1 was sent into an analyzing apparatus (C) at the constant velocity by dropping mercury in B-2 into B-1. The dropping velocity of mercury was regulated by a cock (B-8) according to pressure difference of a manometer (B-7). The dropping rate of mercury at each time was regulated on the average to about 40 cc. per minute. Ammonia was absorbed in C-1, water vapor in C-2 and C-4, and carbon dioxide in C-3. After the mercury-dropping procedure was finished, ammonia, carbon dioxide and water vapor in the dead space of C were completely driven into the absorbers by sending air which was introduced after being washed by concentrated KOH solution (C-5) and H_2SO_4 solution (C-6), by manipulating a three-way cock (B-5).

After the gas-absorbing procedure was finished, the four apparatuses C-1, C-2, C-3 and C-4 were weighed to obtain their increments. The increments of the kali-bulb (C-3) is the amount of carbon dioxide absorbed. And the amount of ammonia absorbed was found by titrating the solution in C-1 with 1-x NaOH solution. The amount of water vapor absorbed in C is the difference between the sum of the increments of both C-1 and C-2 and the absorbed amount of ammonia. In one gas-sampling procedure, the average value of the gas-analysis of two or three times was taken by dividing the sample in B-1 into two or three parts.

C-1 was kept at the constant temperature of 70°C. to minimize the absorption or solution of carbon dioxide into the dilute H_2SO_4 solution (C-1). The writer examined the analytical error which happened by the absorption or solution of carbon dioxide in the preliminary experiment, in which C-1 was kept over the temperature range 10 to 80°C. The amount of carbon dioxide absorbed in the kali-bulb (C-3) was measured by sending the decomposition gas which had been generated by heating 0.50 g. (0.00641 Mole) of ammonium carbamate, into the apparatus (C). The amount of $x/2$ H_2SO_4 solution in C-1 was 130 cc. The experimental results showed that the temperature of C-1 has to be kept at 70 to 80°C. by all means.

(4) **Accuracy of analysis.**—The above-mentioned analysis requires skill in the procedure, especially in the quantitative analysis of water vapor, or else the error becomes larger. It was confirmed by analyzing samples of known composition that the experimental error of this analytical procedure was less than 1 % in ammonia, but about 3 to 5 % in carbon dioxide and water vapor respectively. Obviously in most cases, carbon dioxide shows a tendency to negative error and water vapor to positive error.

Method of Determining Liquid Compositions.—A liquid sample which had been withdrawn from the equilibrium vessel under high temperature and pressure was analyzed by the following

procedure to study the mole ratio of the unconverted ammonia to carbon dioxide in it.

(1). **Experimental Apparatus.**—The experimental apparatus consists of the equilibrium vessel of the urea-synthesis reaction (A) and of the apparatus of withdrawing the liquid sample (B) as given in Fig. 2. A is just the same as the

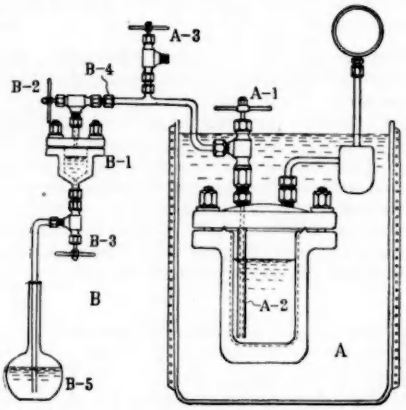

Fig. 2.—Apparatus for measuring the liquid compositions.

apparatus used for the pressure measurement described in the previous paper[3], with the exception that the cover of the equilibrium vessel is fitted with a lead pipe (A-2) of inner diameter 3 mm., outer diameter 10 mm. and length 12 cm. to discharge the liquid through the high pressure valve (A-1). B-1 is a high pressure vessel of capacity 56 cc. made of stainless steel and provided with two high pressure valves (B-2 and B-3), employed for introducing and withdrawing the liquid sample respectively, since the liquid discharged into B-1 exerts more than atmospheric pressure even at the ordinary temperature.

(2) **Procedure of Sampling.**—The procedure of withdrawing the liquid sample is more difficult than that of the sampling of vapor. The least analysable quantity of the liquid sample must be withdrawn without disturbing the liquid-vapor equilibrium by the opening of the valve (A-1), and it must be accomplished as quickly as possible, since a slow manipulation will bring about the vaporisation of the liquid through the valve (A-1). Moreover, the liquid in B-1 at the ordinary temperature is solidified too readily to be discharged from B-1. But these difficulties were nearly overcome by the following method. After the contents of the reaction vessel (A) had arrived at a condition of equilibrium at a given temperature, a very small liquid sample was expelled through the two valves (A-1 and A-3), and then the liquid was driven into B-1 through the two valves (A-1 and B-2) and the steel pipe between A-1 and B-2. This steel pipe had previously been heated at 80 to 100°C. by gas heating. A suitable amount of water had previously been charged in B-1 in order to prevent the solidification of the liquid sample. The amount of the liquid sample could be regulated by the amount of water in B-1. Under a condition of the equilibrium vessel at 160°C. and 90 kg./cm², for example, the pressure falls to 85 kg./cm². by the withdrawal of the liquid sample, but recovers and rises again after a while. After B had been separated from A by disconnecting the nut (B-4), B-1 was intensely shaken to make the contents in it homogeneous, and then by opening the valve (B-3) gently, the aqueous solution in B-1 was discharged into a measuring flask (B-5) of capacity 500 cc., in which some water had previously been charged to catch even a small amount of the vapor from the solution. By pouring the washing water into B-1 through the valve (B-2), the sample in B-1 was completely washed out to make the total amount of the sample 500 cc.

(3). **Determination of the Mole Ratio of Ammonia to Carbon Dioxide.**—The mole ratio of ammonia to carbon dioxide in the aqueous solution withdrawn by such a method as stated above was determined by the following method. An aliquot portion (50 cc.) of the sample 500 cc. was taken for determination of the unconverted ammonia by titration with 1-N sulphuric acid. Unconverted carbon dioxide in the sample was analyzed in an apparatus as shown in Fig. 3.

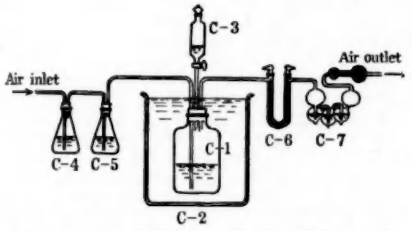

Fig. 3.—Apparatus for determination of carbon dioxide.

The other aliquot portion (50 cc.) was taken into a bottle (C-1), together with a few drops of methyl-orange as the indicator. Carbon dioxide generated by dropping concentrated sulphuric acid from a funnel (C-3) after the bottle (C-1) was immersed into a thermostat (C-2) at 70°C., was absorbed in potassium hydroxide solution (C-7) through a U-tube with calcium chloride (C-6). The dropping of sulphuric acid was continued until the color of the indicator in C-1 changed. After the generation of carbon dioxide had ended, carbon dioxide in the dead space was completely made to absorb in C-7 by sending air refined through concentrated potassium hydroxide solution (C-4) and sulphuric acid (C-5) by means of an aspirator. The increment of kali-bulb (C-7) is equal to the amount of carbon dioxide absorbed. Each sample was analyzed three times and the mean value was taken.

(4). **Accuracy of Analysis.**—At the above

method of analysis, though the excess addition of sulphuric acid for the generation of carbon dioxide after the neutralisation was reached, should result in a hydrolysis of urea and a consequent increase in the analytical value of carbon dioxide, an experiment showed that even when 50 cc. more sulphuric acid than necessary for the neutralisation was used, the value of carbon dioxide was only 0.15 % higher than theoretical. Therefore, it has become evident that the above method is not made invalid by the reaction of urea-decomposition.

Experimental Results

Relation between Vapor Composition and Loading Density.—As mentioned in detail in the previous paper[2], the equilibrium pressure of the urea-synthesis reaction greatly depends upon the loading density, that is to say, the former increases with the latter at a given temperature under a condition in which the loading mole ratio of carbon dioxide to ammonia is one by two. It is an important problem to clear up how the vapor composition depends upon the loading density in this case. The writer studied the relation between the vapor composition and the loading density at 160°C.

The experimental results showed that the mole ratio of ammonia to carbon dioxide in the vapor is less than two at each loading density, and the more loading density increases, the richer the carbon dioxide in the vapor composition becomes,

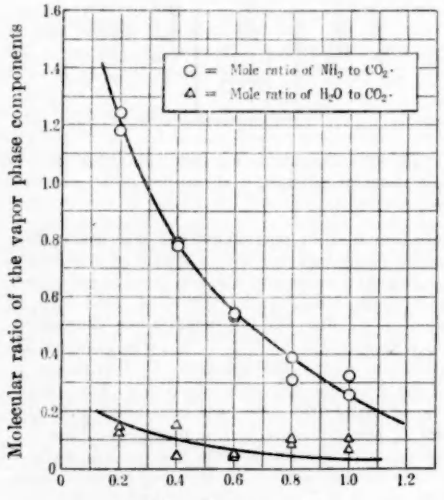

Fig. 4.—Relation between the vapor composition and the loading density at 160°C.

as shown in Fig. 4. Therefore, it is clear that the equilibrium pressure increases with the loading density, as the increase of the loading density accompanies at the same time the increase of carbon dioxide content in the vapor phase. These experimental results are based on the fact that the solubility of ammonia into the liquid phase is more than that of carbon dioxide. Moreover, the experimental results showed that the measured mole ratio of water to carbon dioxide in the vapor,—though there exists a very small quantity of water vapor—, is nearly within the range of 0.03 to 0.16.

Relation between Vapor Composition and Temperature.—The equilibrium pressure rises with temperature at a constant loading density as explained in the previous paper.[2] At the same time, it is expected in this case that the vapor composition undergoes a change with the change in temperature. The result of the experiments in which the vapor composition was measured at the loading density 0.60 g./cc. and over the temperature range of 140 to 180°C., is shown in Fig. 5. The observed mole ratio of ammonia to carbon

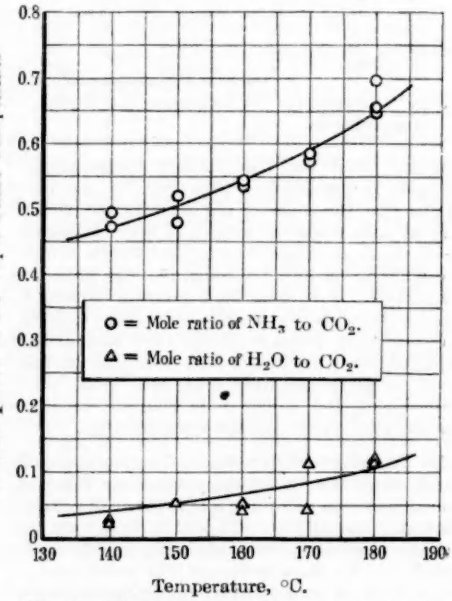

Fig. 5.—Relation between the vapor composition and the temperature at a loading density of 0.60 g./cc.

dioxide ranges from 0.47 to 0.65 under this condition and the vapor composition becomes richer in ammonia with the rise of temperature. The relation between the mole ratio of carbon dioxide to ammonia and temperature is nearly linear within the range of the experiments. Mole ratio of water to carbon dioxide ranges from 0.02 to 0.12.

Relation between Liquid Composition and Loading Density.—The effect of the variation of

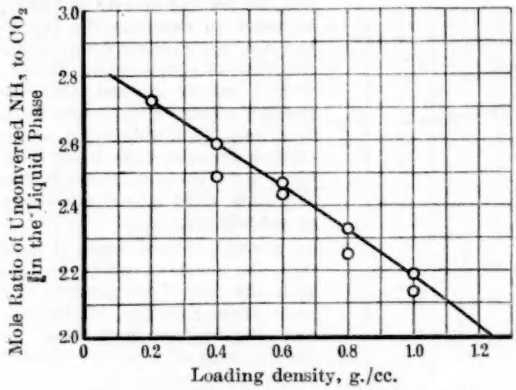

Fig. 6.—Relation between the liquid composition and the loading density at 160°C.

the loading density on the mole ratio of ammonia to carbon dioxide in the liquid phase which is in equilibrium with the vapor was studied at 160°C. and the loading densities of 0.20 to 1.00 g./cc. The experimental results are shown in Fig. 6. The mole ratio of ammonia to carbon dioxide increases from 2.18 to 2.72 within the range of the experiments; thus the liquid composition becomes richer in ammonia, with decrease of the loading density. This is closely connected with the facts that the vapor composition becomes richer in ammonia as described above and the yield of urea decreases, with decrease of the loading density. The point where the curve intersects the abscissa in Fig. 6 is nothing but the loading density where the mole ratio of ammonia to carbon dioxide in the liquid phase becomes equal to the loading mole ratio, or where the equilibrium vessel is filled up with only the liquid phase. This loading density is 1.24 g. per cc., being consistent with the maximum loading density which will be derived from the relation between the ratio of liquid volume to vessel volume and the loading density in the following section of this paper.

Relation between Liquid Composition and Temperature.—The effect of the change in temperature on the mole ratio of ammonia to carbon dioxide in the liquid phase was studied at the loading density 0.60 g./cc. and over the temperature range of 140 to 180°C. The experimental results are shown in Fig. 7. The mole ratio of unconverted ammonia to carbon dioxide increases from 2.26 to 2.67 within the range of the experiments; thus the liquid composition becomes richer in ammonia, with the rise of temperature. The mole ratio in the liquid composition is approximately a linear function of the temperature as shown in Fig. 7. This line intersects the abscissa at about 115°C. and this point is nothing but the temperature where the mole ratio of ammonia to carbon dioxide in the liquid phase becomes equal to the loading mole ratio, or the transition temperature, where the content in the equilibrium vessel undergoes a change from the solid- to the liquid-phase reaction. This transition temperature has been fully investigated by Kitawaki, Hori and Shimoda.[3] According to their investigations, a junction of the decomposition pressure-temperature curve of solid ammonium carbamate and the equilibrium pressure-temperature curve of the mixed solution of the CO_2-NH_3-Urea-H_2O system was 114.6°C., being consistent with the transition temperature from the solid- to the liquid-phase reaction, where a discontinuous point appears, in a plot of the yield of urea against the temperature, as shown in Fig. 8.

Relation among Urea-Yield, Loading Density and Temperature.—Fichter and Becker[4] discovered in 1911 that the

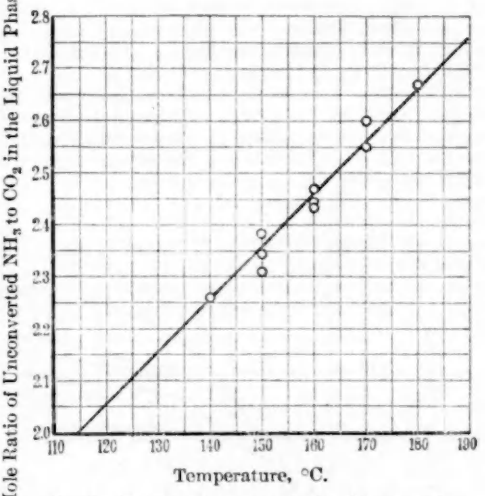

Fig. 7.—Relation between the liquid composition and the temperature at a loading density of 0.60 g./cc.

equilibrium yield of urea increaes with the loading density at a given temperature. Thereafter, the effect of the loading density on the equilibrium yield of urea was studied by Clark, Gaddy and Rist,[5] and M. Tokuoka,[6] the former specially studied the effect at such a higher loading density as 1.0 g./cc. over the temperature range of 135 to 200°C. The writer also studied the relation between the equilibrium yield of urea

(3) Kitawaki, Hori and Shimoda, *Bull. Gov. Chem. Ind. Res. Inst. Tokyo*, **32**, No. 6 and 10 (1937).
(4) Fichter and Becker, *Ber.*, **44**, 3473 (1911).
(5) Clark, Gaddy and Rist, *Ind. Eng. Chem.*, **25**, 1092 (1933).
(6) M. Tokuoka, *J. Agr. Chem. Soc. Japan*, **10**, 1334 (1934); *ibid.*, **11**, 107 (1935); *ibid.*, **11**, 174 (1935).

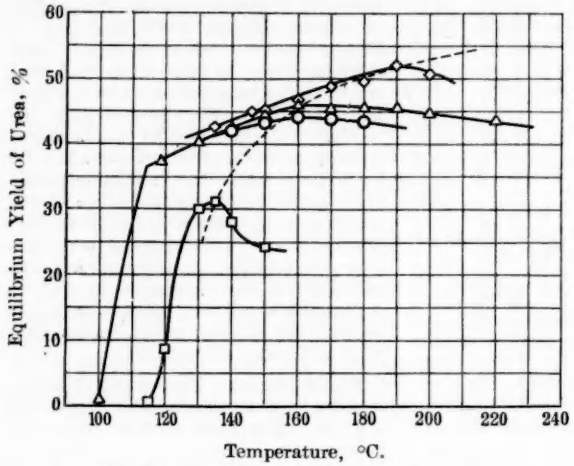

Fig. 8.—Relation between the yield of urea and the temperature.

Symbol	Loading density, g./cc.	Investigator
◇	1.00	Clark, Gaddy and Rist[5]
△	0.65	Kitawaki, Hori and Shimoda[3]
○	0.60	Present Measurement
□	0.11	Fichter and Becker[4]

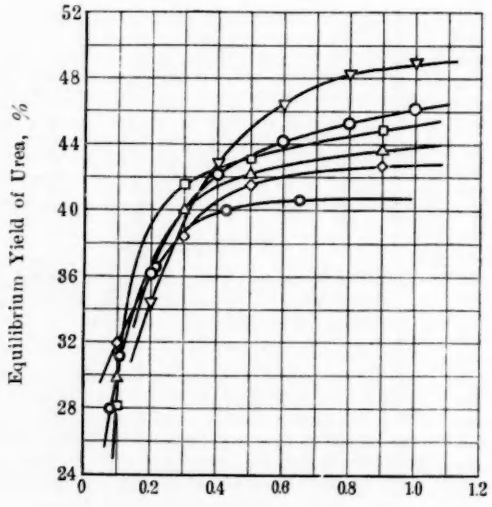

Fig. 9.—Relation between the yield of urea and the loading density.

Symbol	Temp. °C.	Investigator
▽	170	Clark, Gaddy and Rist[5]
○	160	Present Measurement
□	150	M. Tokuoka[6]
△	145	M. Tokuoka[6]
◇	140	M. Tokuoka[6]
◎	135	Fichter and Becker[4]

and the loading density at 160°C., in order to calculate the liquid- and the vapor-phase compositions in a state of equilibrium. Experimental results showed that the average yields of urea are 36.2, 42.2, 44.2, 45.3, and 46.2 % at the loading densities 0.20, 0.40, 0.60, 0.80, and 1.0 g./cc., respectively. The data cited above are shown graphically in Fig. 9.

In general it had been thought that the yield of urea increases with the rise of temperature at a given loading density, but Fichter, and Becker[4] showed that the yield of urea at a loading density of 0.11 g./cc. attains to the maximum at 135°C. Thereafter, the maximum yields of urea were experimentally shown at about 160°C. and 0.65 g./cc. by Kitawaki, Hori and Shimoda,[3] and at about 190°C. and 1.0 g./cc. by Clark, Gaddy and Rist,[5] respectively, as given in Fig. 8. The writer also studied the effect of the temperature on the equilibrium yield of urea at a loading density of 0.60 g./cc. Experimental results showed that the average yields of urea are 42.1, 43.3, 44.2, 44.0, and 43.5 % at 140°, 150°, 160°, 170°, and 180°C., respectively. Clark and others[5] explained that the lower yield of urea obtained above 190°C. may be attributed to the complications introduced by the more active corrosion of the reactor and to the increased tendency for the thermal dissociation of urea and the catalytic cracking of ammonia. However, the reason why these experiments showed increasing conversion of ammonium carbamate into urea with temperature up to the maximum at a given loading density, must essentially be attributed to the inevitable relations among the urea-yield, the loading density and the temperature, which result from the liquid- and the vapor-phase equilibrium of the CO_2-NH_3-Urea-H_2O system. Evidently, according to the data cited above, the temperatures where the equilibrium yield of urea attains to the maximum, rise with the increase of the loading density, drawing such a locus as a dotted line shown in Fig. 8.

In Fig. 10 which is a schematic expression of Fig. 9, it can readily be understood that the urea-yield Y_1 at the temperature T_1 is less than Y_2 at the lower temperature

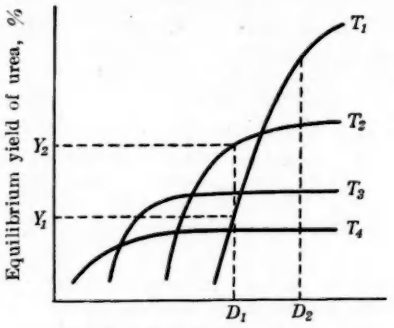

Fig. 10.—Schematic diagram of relation among the yield of urea, the loading density and the temperature.

Photo. 1

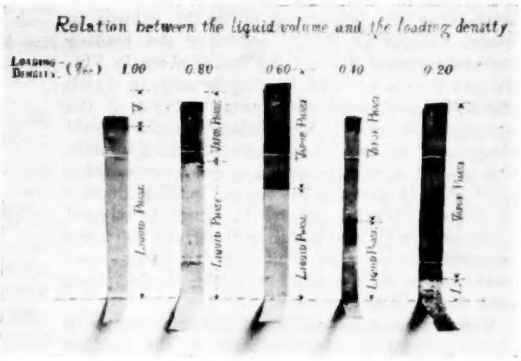
Relation between the liquid volume and the loading density
Loading Density (g./cc.) 1.00 0.80 0.60 0.40 0.20
Liquid Phase
Three Phases

T_2, and Y_2 is the maximum urea-yield at a given loading density of D_1. Therefore we must raise the temperature and increase the loading density at the same time in order to increase the yield of urea. It is because of the decrease of vapor-phase volume, or of the incrase of ratio of the liquid-phase weight to the initial loading weight, that the yields of urea increase, with the increase of the loading density at a given temperature, as pointed out by Matignon and Fréjacques.[7] Krase and Gaddy[8] have also explained that since the equilibrium is established in the liquid phase and presumably only a negligible amount, if any, of urea is in the gaseous phase, the extent of conversion of carbamate to urea is dependent on the ratio of the volumes of liquid and gas phases. Similarly the existence of the maximum yield of urea in a plot of the yield against the temperature at a given loading density is attributable to the circumstances; while the conversion of ammonium carbamate to urea in the liquid phase increases, the quantity of liquid phase itself decreases with the rise of temperature. Ultimately the reason why such relations as shown in Fig. 10 arise among the urea-yield, the loading density and the temperature, must be accounted for by the fact that the equilibrium yields of urea depend not only upon the equilibrium of the reaction of urea-synthesis in the liquid-phase, but also upon the liquid- and vapor-phase equilibrium.

Volume-Ratio of Vapor- to Liquid-Phase.—As the equilibrium state between the vapor and liquid in an autoclave under high temperature and pressure is difficult to survey with the naked eyes, the writer tried to measure the volume-ratio of the vapor to the liquid by the following method in order to calculate the vapor- and liquid-density.

In the urea-synthesis reaction from ammonia and carbon dioxide, the corrosive action of the reacting system for the materials of the reaction vessel is so violent, that there appears a distinct corrosive line on the material which corresponds to the boundary of the two phases. Aluminium or 18Cr-8Ni stainless steel of about 20 cm. long, 15 mm. wide and 1 to 2 mm. thick, was bent at right angles as shown in Photo. 1 and inserted into the reaction vessel so that the plate might not move in it. After heating the reaction vessel at a given temperature for about 20 hours, the plate was taken out from the vessel. As shown in Photo. 1, a part of the plate which was dipped in the molten reaction mixture suffered more corrosive action and grew thinner than the other part exposed in the vapor; especially at the boundary of the two phases it suffered a violent corrosion. We can readily determine the volume-ratio of the two phases with about ±1 % error

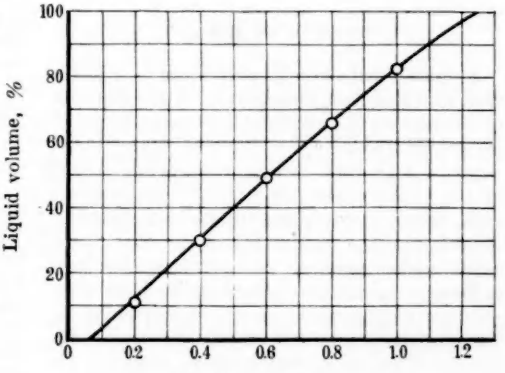

Fig. 11.—Relation between liquid volume and loading density at 160°C.

(7) Matignon and Fréjacques, *Bull. soc. chim.*, **31**, 394 (1922).

(8) Krase and Gaddy, *Ind. Eng. Chem.*, **14**, 611 (1922).

from the plate. The volume of the autoclave is about 750 cc. The data from these experiments concerning the percentage of liquid volume to vessel volume at 160°C. and over the loading density range of 0.2 to 1.0 g./cc., is given in Fig. 11 and Photo. 1. The loading density, in which the liquid volume to the total volume of the autoclave is 100 %, is nothing but the liquid density in the case of the autoclave filled up with the liquid. It will be sought by the extrapolation from Fig. 11 that the maximum loading density is about 1.24 g./cc. at 160°C. which is in good agreement with that which was derived from the relation between the mole ratio of unconverted ammonia to carbon dioxide in the liquid phase and the loading density.

The experimental results on the percentage of liquid volume to vessel volume at the loading density 0.60 g./cc. and over the temperature range of 140 to 180°C. is given in Table 1. The experiments showed that the percentage of liquid volume is nearly constant and independent of the temperature at a given loading density within the experimental error.

Table 1

Relation between Liquid Volume and Temperature at a Loading Density of 0.60 g./cc.

Temp., °C.	Equilibrium pressure, atm.	Leiquid volume to the vessel volume, %
140	52	48.2
150	67	47.1
160	88	48.8
170	115	48.5
180	149	47.5

Discussion of Results

Relation between Equilibrium Composition and Loading Density.—For the purpose of calculating the equilibrium compositions, it is assumed that the system consists of three components, ammonia, carbon dioxide and water, in the vapor phase and of four components, urea, water, unconverted ammonia and carbon dioxide, in the liquid phase, or that there exists neither gaseous- nor melted-ammonium carbamate in the two phases under high temperature and pressure, since it is impossible to measure the amount of ammonium carbamate distinguished from unconverted ammonia or carbon dioxide, although much amount of ammonium carbamate must exist in the liquid phase. In such a case that "c" gram moles of ammonium carbamate (equivalent of "$2c$" moles of ammonia and "c" moles of carbon dioxide) were initially loaded into a reaction vessel of 1 litre volume, we obtain from the material balance respectively;

$$n_{\text{urea}}+n_{CO_2}+n'_{CO_2}=c \tag{2}$$

$$2n_{\text{urea}}+n_{NH_3}+n'_{NH_3}=2c. \tag{3}$$

Let us put,

$$n'_{NH_3}/n'_{CO_2}=R' \tag{4}$$

$$n'_{H_2O}/n'_{CO_2}=S' \tag{5}$$

$$n_{NH_3}/n_{CO_2}=R \tag{6}$$

$$n_{\text{urea}}=cY \tag{7}$$

and

$$n_{H_2O}=n_{\text{urea}}-n'_{H_2O}. \tag{8}$$

From these seven equations (2) to (8), we can derive the following relations (9) to (14) which allow the equilibrium concentration of each component to be calculated.

$$n'_{CO_2}=\frac{c(1-Y)(R-2)}{R-R'} \tag{9}$$

$$n'_{NH_3}=\frac{cR'(1-Y)(R-2)}{R-R'} \tag{10}$$

$$n'_{H_2O}=\frac{cS'(1-Y)(R-2)}{R-R'} \tag{11}$$

$$n_{CO_2}=\frac{c(1-Y)(2-R')}{R-R'} \tag{12}$$

$$n_{NH_3}=\frac{cR(1-Y)(2-R')}{R-R'} \tag{13}$$

$$n_{\text{urea}}=cY \tag{7'}$$

$$n_{H_2O}=c\left\{Y-\frac{S'(1-Y)(R-2)}{R-R'}\right\}. \tag{14}$$

The compositions of the liquid- and vapor phase in the equilibrium state at a temperature of 160°C. and over the loading density range of 0.20 to 1.0 g./cc. are shown in Table 2. The equilibrium constants (K_{N_1}) of the reaction (1) represented by mole fraction (N_i) of each component in the liquid phase $K_{N_1}=\frac{N_{\text{urea}}N_{H_2O}}{N_{CO_2}N^2_{NH_3}}$ are also given in the last line of Table 2. These values of the equilibrium constant at 160°C. are approximately constant, independent of the loading density. A plot of mole fraction x_i of each component in two phases against the loading density is drawn in Fig 12. It is conjectured from Fig. 12 that the equilibrium yields of urea increase at a given temperature because the vapor-phase decreases or the boundary surface between the two phases rises up in the reaction vessel, with increasing loading density.

Effect of Loading Density on Liquid- and Vapor-Density.—The liquid- and vapor-density of the system under high temperature and pressure are given by dividing the weight

Table 2

Effect of Loading Density on Liquid- and Vapor-Phase Compositions in Equilibrium State at 160°C.

D, g./cc.	0.20	0.40	0.60	0.80	1.00
c, mole/l.	2.562	5.123	7.685	10.247	12.808
P, atm.	69	76.5	89	107.5	136.5
R'	1.347	0.816	0.547	0.405	0.325
S'	0.164	0.103	0.066	0.045	0.033
R	2.725	2.590	2.460	2.326	2.180
Y	0.362	0.422	0.442	0.453	0.462
Equilibrium Concentration, mole/l. n'_{CO_2}	0.859	0.984	1.031	0.951	0.669
n'_{NH_3}	1.158	0.803	0.564	0.385	0.217
n'_{H_2O}	0.141	0.102	0.068	0.043	0.022
n_{CO_2}	0.774	1.975	3.257	4.654	6.222
n_{NH_3}	2.109	5.115	8.012	10.823	13.563
n_{urea}	0.928	2.164	3.397	4.642	5.918
n_{H_2O}	0.787	2.063	3.329	4.599	5.895
Mole fraction N'_{CO_2}	0.398	0.521	0.620	0.690	0.737
N'_{NH_3}	0.537	0.425	0.339	0.279	0.239
N'_{H_2O}	0.065	0.054	0.041	0.031	0.024
N_{CO_2}	0.168	0.175	0.181	0.188	0.197
N_{NH_3}	0.459	0.452	0.445	0.438	0.429
N_{urea}	0.202	0.191	0.189	0.188	0.187
N_{H_2O}	0.171	0.182	0.185	0.186	0.187
K_{N_1}	0.976	0.977	0.974	0.968	0.963

of each phase obtained from Table 2 by the liquid- and vapor-volume respectively. The densities (d and d') of the two phases at 160°C. and over the loading density range 0.20 to 1.00 g./cc. increase with the loading density as shown in Fig. 13. The extrapolation of the liquid-density curve in Fig. 13 shows that the liquid density at the maximum loading density of 1.24 g./cc. is identical with the latter. The vapor density (d') is approximately a linear function of the equilibrium pressure as shown in Fig. 14.

Relation between Equilibrium Composition and Temperature.—The results of calculation of the liquid- and vapor-phase compositions in the equilibrium state at a loading density of 0.60 g./cc. and over the temperature range of 140 to 180°C. are shown in Table 3. A plot of mole fraction x_i against the temperature is shown in Fig. 15. It is conjectured from Fig. 15 that the maximum yield of urea in a plot of the yield against the temperature

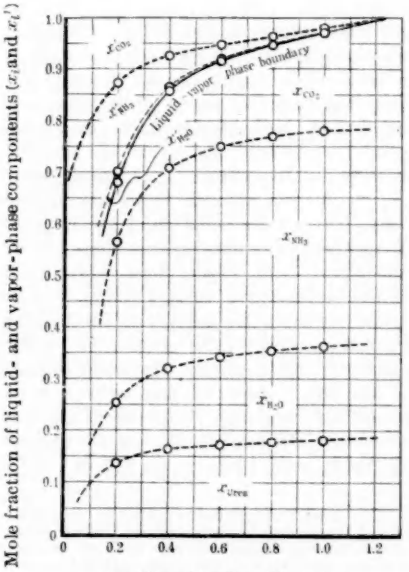

Fig. 12.—Liquid-vapor equilibria diagram of the CO_2-NH_3-Urea-H_2O system at a temperature of 160°C.

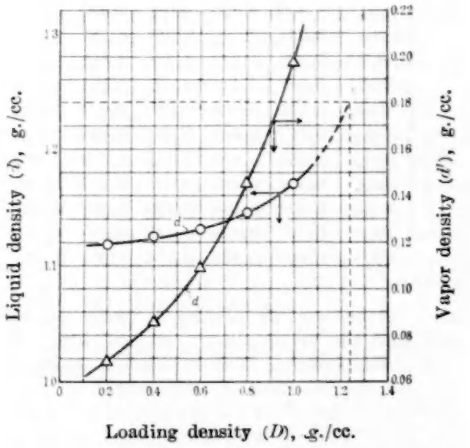

Fig. 13.—Effect of loading density on liquid- and vapor-density at 160°C.

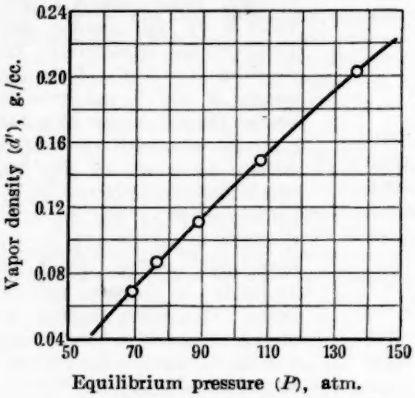

Fig. 14.—Relation between vapor density and equilibrium pressure at 160°C.

Table 3

Effect of Temperature on Liquid- and Vapor-Phase Compositions in Equilibrium State at a Loading Density of 0.60 g./cc.

	Temp., °C.	140	150	160	170	180
	c, mole/l.	7.685	7.685	7.685	7.685	7.685
	P, atm.	50.5	68	89	117	151
	R'	0.470	0.505	0.545	0.592	0.650
	S'	0.040	0.052	0.066	0.082	0.105
	R	2.260	2.360	2.460	2.562	2.665
	Y	0.421	0.433	0.442	0.440	0.435
Equilibrium Concentration, mole/l.	n'_{CO_2}	0.646	0.845	1.031	1.227	1.432
	n'_{NH_3}	0.303	0.427	0.564	0.726	0.931
	n'_{H_2O}	0.026	0.044	0.068	0.100	0.150
	n_{CO_2}	3.803	3.512	3.257	3.076	2.910
	n_{NH_3}	8.590	8.290	8.012	7.880	7.760
	n_{urea}	3.235	3.327	3.397	3.381	3.343
	n_{H_2O}	3.209	3.283	3.329	3.281	3.193
Equilibrium mole fraction	N'_{CO_2}	0.662	0.642	0.620	0.597	0.570
	N'_{NH_3}	0.311	0.324	0.339	0.354	0.370
	N'_{H_2O}	0.027	0.034	0.041	0.049	0.060
	N_{CO_2}	0.202	0.190	0.181	0.174	0.169
	N_{NH_3}	0.456	0.451	0.445	0.448	0.452
	N_{urea}	0.172	0.181	0.189	0.192	0.194
	N_{H_2O}	0.170	0.178	0.185	0.186	0.185
	K_{N_1}	0.697	0.833	0.974	1.021	1.046

at a given loading density is based on the fact that the vapor-phase increases with the rise of temperature. The equilibrium constants K_{N_1} of the reaction (1) represented by mole fraction N_i are shown in the last line of Table 3. There appears a discontinuous point at 160°C. in a plot of the equilibrium constant against the temperature. Hori and Ogami [9] have already found that a plot of the logarithm of the equilibrium constant[10] against the reciprocal of the temperature results in two straight lines intersecting at 154°C. This conclusion was reached in their experiment which was effected at a loading density of 0.65 g./cc. in a reaction vessel of sealed glass tube, and explained that the existence of the discontinuous point may possibly be based on the difference between the phases in the equilibrium state of the system at each temperature, that is to say, between the solid- and vapor-phase equilibrium at lower temperature than 154°C. and the liquid- and vapor-phase equilibrium at higher temperature than 154°C., because this point perfectly coincides with the melting point 153.5 to 155.8°C. of ammonium carbamate observed by Kitawaki, Hori and Shimoda[3]. The other values of the melting point of ammonium carbamate which were reported by Terres and Behrens[11], E. Jänecke[12], and Krase, Gaddy and Clark[13] are 147 to 150°C.,

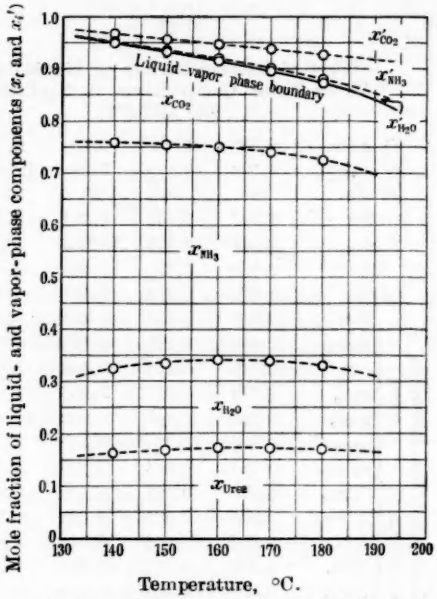

Fig. 15.—Liquid-vapor equilibria diagram of the CO_2-NH_3-Urea-H_2O system at a loading density of 0.60 g./cc.

(9) Hori and Ogami, *J. Soc. High Pressure Gas Ind. Japan*, **6**, 256 (1942).

(10) The equilibrium constant employed by Hori and Ogami was represented by mole fraction derived from the initial loading composition and the yield of urea without distinction between the liquid- and the vapor-compositions.

(11) Terres and Behrens, *Z. physik. Chem.*, **139 A**, 695 (1928).

(12) E. Jänecke, *Z. Elektrochem.*, **35**, 716 (1929).

(13) Krase, Gaddy and Clark, *Ind. Eng. Chem.*, **22**, 289 (1930).

153 and 145°C. respectively.

The fusion of ammonium carbamate, however, is a complicated phenomenon connected inevitably with the formation of equi-molar urea and water, as pointed out by Kitawaki and others,[3] because its melting point depends on the rate of heating carbamate and in cooling the molten ammonium carbamate, in which even a small quantity of urea was always detected, it is not solidified at the temperature where pure solid carbamate itself began to melt in heating it. In other words, the respective temperature observed in such a way is only an apparent melting point of carbamate, which may possibly depend upon the initial loading density of carbamate in a vessel. Since the equilibrium system, which is the subject under consideration, is a homogeneous liquid phase at a higher temperature than the transition point 115°C., the explanation that the discontinuous point corresponds to the melting point of ammonium carbamate is unreasonable. Preferably it ought to be considered that the discontinuous point corresponds to the maximum yield of urea in Fig. 8 and consequently varies depending on the initial loading density of carbamate.

This unaccountable relation between the equilibrium constant and the temperature might result from the inadequate initial assumption that the system consists of four components of urea, water, ammonia and carbon dioxide in the liquid phase. In other words, it seems to be impossible to represent the reaction of the urea formation by such a simple reaction as the equation (1). Therefore, for the complete explanation of the relation, further consideration should be tried from other stand-points and on other assumptions.

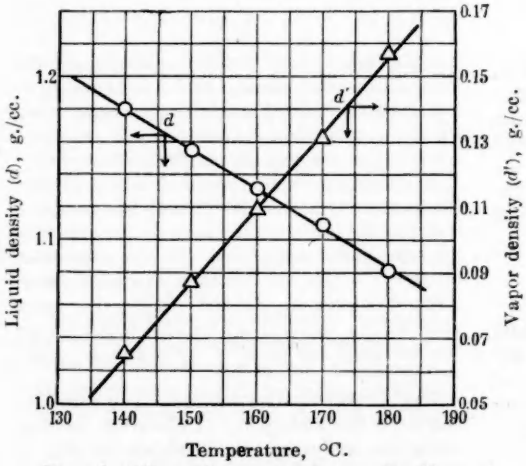

Fig. 16.—Effect of temperature on liquid- and vapor-density at a loading density of 0.60 g /cc.

Effect of Temperature on Liquid- and Vapor-Density.—From the weight of each phase obtained from Table 3 and the volume of each phase, the liquid- and vapor-density at a loading density of 0.60 g./cc. and over the temperature range of 140 to 180°C. has been calculated as shown in Fig. 16. The liquid-density decreases and the vapor-density increases linearly with the rise of temperature, respectively.

Summary

(1) For studying the liquid-and vapor-phase equilibrium of the CO_2-NH_3-Urea-H_2O system under high temperature and pressure, details of methods to determine mole ratios of ammonia, carbon dioixde and water in the vapor phase, mole ratio of ammonia to carbon dioxide in the liquid phase, and volume-ratio of the vapor-to liquid-phase in an autoclave have been described.

(2) Experimental results at temperatures between 140 and 180°C. and over the loading density range of 0.20 to 1.00 g./cc. have been shown in the case of the loading mole ratio of $2NH_3$ to 1 CO_2.

(3) The relations among the equilibrium yield of urea, the loading density and the temperature were discussed from the standpoint of the liquid- and vapor-phase equilibrium.

(4) The liquid- and vapor-phase compositions in the equilibrium state of the system have been calculated on an assumption that the system consists of three components, ammonia, carbon dioxide and water, in the vapor phase and of four components, urea, water, ammonia and carbon dioxide, in the liquid phase.

(5) The equilibrium constant of the following reaction represented by mole fraction of each component in the liquid phase is approximately constant independent of the loading density at a given temperature.

$$CO_2 + 2NH_3 \rightleftarrows CO(NH_2)_2 + H_2O$$

(6) A discontinuous point appearing in a plot of the equilibrium constant against the temperature at a given loading density has been discussed.

(7) The liquid- and vapor-densities of the system under high temperature and pressure have been calculated from

the equilibrium compositions.

Nomenclature

Symbols

c—Number of moles of ammonium carbamate loaded initially into the reaction vessel, gram mole per litre

d—Density of liquid, g. per cc.

D—Loading density, or ratio of the weights of materials to the total volume of the reaction vessel, gram per cc.

K_{N_1}—Equilibrium constant of the reaction(1) represented by mole fraction N_i, no units

n_i—Number of moles of a component "i" in the liquid phase per litre of the reaction vessel, gram mole per litre

N_i—Mole fraction of a component "i" in the liquid phase, or ratio of gram moles to the total gram moles in the liquid phase, no units

P—Equilibrium pressure, atm.

R—Mole ratio of unconverted ammonia to carbon dioxide in the liquid phase, no units

S—Mole ratio of water to carbon dioxide in the liquid phase, no units

x_i—Mole fraction of a component "i" in the liquid phase, or ratio of gram moles to the total gram moles in the two phases, no units

Y—Equilibrium yield of urea, or ratio of gram moles of urea to initial loading moles of ammonium carbamate ($= n_{urea}/c$), no units

Superscript

$'$ (dash)—sign to denote the vapor phase

The writer wishes to express appreciation for the kind guidance and the advice received throughout this work from Dr. Shinjiro Kodama, Prof. of Kyoto University, and for the encouragement received from Dr. Kenji Fujimura, the chief of the Research Department.

Research Department, Niihama Works,
Nissin Chemical Co., Ltd., Niihama

Studies on the Polarographic Analysis. XII. New Differential Polarography with One Dropping Electrode (2)

By Masayoshi Ishibashi and Taitiro Fujinaga

(Received February 27, 1952)

Introduction

In the previous paper,[1] the authors reported on the construction of the new differential polarograph and its application was discussed from the standpoint of qualitative analysis. Here, they discuss the differential technique from the standpoint of quantitative analysis and of electrode reactions there-of.

Results and Discussion

On the Relation between the Peak Current (i_h) of the Differential Method and the Diffusion Current (i_d) of the Ordinary Method.—As easily concluded from Eq. (4) shown in the previous paper,[1] the peak current should be proportional to the diffusion current, taking ΔE small enough to get the ideal differential curve. And also it would be less than one half of the diffusion current even though ΔE is taken as large enough to cover the whole increasing part of the ordinary wave.

However, in many cases it is observed that the peak current is several times the height of the ordinary diffusion current, proving the increase of the sensitivity. But in some cases, contrary to this, the diminishing of the sensitivity is observed. So the differential curve obtained by the authors' method is not always the resultant one of $E \sim i$ curve and $E - \Delta E \sim -i'$ curve.

The authors studied to clear these phenomena from the standpoint of electrode reaction, using the analysing circuit shown in Fig. 1. In the circuit of 1-a, when the switch is rotated, the electrolytic current i corresponding to the

(1) M. Ishibashi and T. Fujinaga, This Bulletin, **25**, 68 (1952).

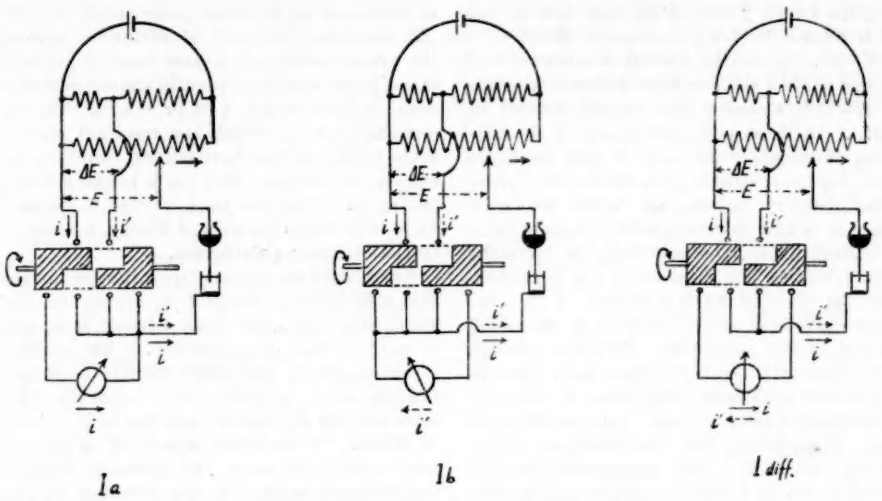

Fig. 1.—Scheme of the differential polarograph (1-diff.) and its analysing circuits (1-a and 1-b).

potential E flows through the galvanometer in the normal direction, while the current i' corresponding to the potential $E-\Delta E$ does not flow through it, but is short-circuited to the cell. We call the polarogram thus obtained by the rotation of the alternator in the circuit 1-a as $E\sim i$ rot. curve and to the contrary, in the circuit 1-b, the current i corresponding to E is short-circuited and i' corresponding to $E-\Delta E$ flows in the reverse direction through the galvanometer and we call this as $E-\Delta E\sim -i'$ rot. curve.

It is readily admitted that the differential polarogram obtained by the authors' method is the resultant curve of the $E\sim i$ rot. curve and $E-\Delta E\sim -i'$ rot. curve and that the experimental findings explain this point fairly well and are in good agreement with the considerations (see Fig. 2 and others). In addition, the scheme 1-a corresponds to the scheme 1-b in the experiment of Kalousek[2] and the scheme 1-b is a reversed circuit of the scheme 1-a in his experiment. Therefore, the authors' differential polarogram is explained to be the deduced curve of the two curves obtained by Kalousek's experiment.

(a) **A case when the electrode reaction is reversible and the dissociation rate of the reducible substances is fast.**—Cadmium and its ion can be oxidized or reduced reversibly at the dropping mercury electrode. The behavior of electrolytic dissolution and deposition of cadmium in potassium chloride solution is shown in Fig. 2. The curve 1 shows the ordinary polarogram i.e. the $E\sim i$ curve (taken with the switch stopped in 1-a or 1-

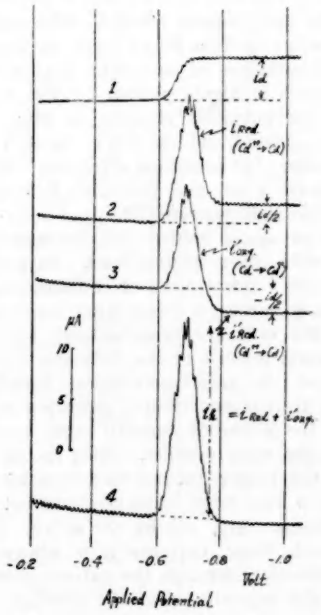

Fig. 2.—Polarograms of cadmium ion in potassium chloride:
ΔE= 50 millivolts, sensit. = 1:200.

(2) M. Kalousek, *Collection Czech. Chem. Communs.*, **13**, 105 (1948).

diff.), the curve 2 the $E\sim i$ rot. curve (the switch rotated in 1-a), the curve 3 the $E-\Delta E \sim -i'$ rot. curve (the switch rotated in 1-b) and the curve 4 the resultant differential curve *i.e.* $E\sim\Delta i/\Delta E$ curve (the switch rotated in 1-diff.). In these polarogram ΔE is 50 millivolts. Comparing the curve 1 with the curve 4, the diffusion current i_d is 4.1 microamperes in the ordinary polarogram while the peak current i_h is 18.3 microamperes in the differential one; in short, the sensitivity is increased by *ca.* 4.5 times. In the curve 2, the maximum is seen at the half-wave potential of the ordinary curve and the magnitude is about 2.7 $\times i_d$ and in the part of the diffusion current, the current falls down to about $i_d/2$. And in the curve 3 analogous maximum is seen and the current falls down to *ca.* $-i_d/2$ in the same part. Considering the isochronism of the rotating switch, it is well recognized that the current of *ca.* $i_d/2$ flows in normal and reverse directions in the part of diffusion current. As for the maximum at the halfwave potential, it could be explained, as Kalousek did, to depend on the reversibility of the electrode reactions. However, as for the curve 3, the current flows in the reverse direction contrary to Kalousek's scheme 1-a by the change of the switch connection. More precisely, the current caused by the reduction of cadmium ions flows in normal direction at the potential E, but in the next instant when E-ΔE is applied the reduction of them takes place no longer, but the dissolution of cadmium begins from the cadmium amalgam yielded by the reduction at the potential E thus effecting the oxidation current, which flows through the galvanometer still in normal direction. At the next instant when the potential E is again applied, the cadmium ions dissolved out of the electrode are again reduced at the same time together with other diffused ions. As a result of these, the concentration of cadmium ion at the electrode surface becomes much larger than it is in the ordinary polarography and the concentration instead of the diffusion layer is brought at the mercury-solution interface. Therefore the concentration of cadmium amalgam at the electrode surface also becomes larger in the same manner. Thus in the circuit 1-a the large reduction current and in the circuit 1-b the large oxidation current are yielded respectively, but by the action of the switch both these currents flow always in normal direction through the galvanometer in spite of the opposite electrode reaction. As the result, as shown in curve 4 of Fig. 2, the prominent maximum is seen in the differential method. Now, when the applied potential is so increased as both the potential E and $E-\Delta E$ come into the part of diffusion current, the above mentioned reverse reaction no longer takes place and consequently the currents have each definite value, $i_d/2$ or $-i_d/2$. The differential curve 4 which is a resultant curve of these curves 2 and 3, therefore, indicates zero current in the stationary parts before and after the wave. Thus the peak current (i_h) is larger by several times than the diffusion current (i_d) of the ordinary polarogram.

From the view-point of quantitative analysis this magnification ratio i_h/i_d would be constant, since then, the peak current is proportional to the concentration. In practice, however, taking ΔE small enough the magnification ratio is particularly large in dilute solution and it diminishes as the concentration increases. Nevertheless, when ΔE is taken as large enough to cover the potential width of the ordinary wave, the ratio becomes constant independently of the concentration and so the peak current is directly proportional to the concentration (see Fig.3). This increase in

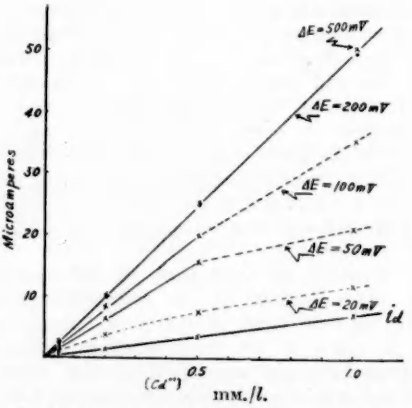

Fig. 3.—Relation between the peak current (i_h) and the diffusion current (i_d) of the cadmium ion in potassium chloride.

sensitivity based upon the reversibility is observed as well with the following ions and substances; free ions of copper, zinc, lead etc. and alkali-metal ions and ammonium ion also and oxygen.

(b) **A case when the electrode reaction is irreversible and the dissociation rate of the reducible substance is fast.**—Zinc ion indicates an irreversible electrode reaction in ammoniacal solution. Fig. 4 as well as Fig. 2 shows the normal order, curve 1; $E\sim i$ curve, curve 2; $E\sim i$ rot. curve, curve 3; $E-\Delta E\sim -i'$

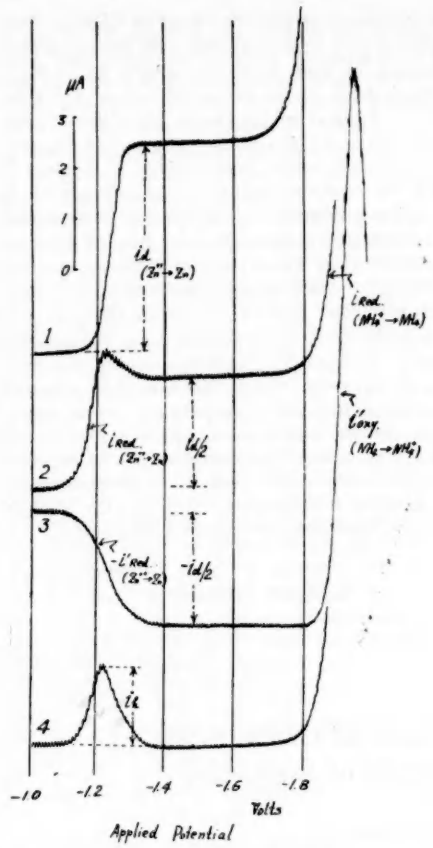

Fig. 4.—Polarograms of zinc ion in ammoniacal solution: ΔE=40 millivolts, sensit.=1:50.

rot. curve and curve 4; $E \sim \Delta i/\Delta E$ curve, which are all in regard to the same zinc ammine solution. The explanation about the case of such irreversible reaction is very easy and the differential curve in this case is in almost a perfect agreement with that in an ideal state. The electrode reaction is scarcely different from cases of ordinary polarography. It would be needless to discuss the curves 1 and 3. Though the curve 2 has likewise its maximum, this maximum is never beyond the height of diffusion current so long as ΔE is less than 300 millivolts. This maximum is explained as follows; the reduction takes place when the potential E is applied and the vacuum layer is formed on the electrode surface. In the next instant when the potential falls to $E-\Delta E$ its reduction still does not take place and also the oxidation does not happen due to the irreversible process. Therefore the vacuum layer is soon almost filled with zinc ions by the diffusion from the bulk of the solution at the potential $E-\Delta E$. In the next instant, when E is again applied, those zinc ions are together reduced at this time. Therefore the height of the peak in curve 2 is greater than

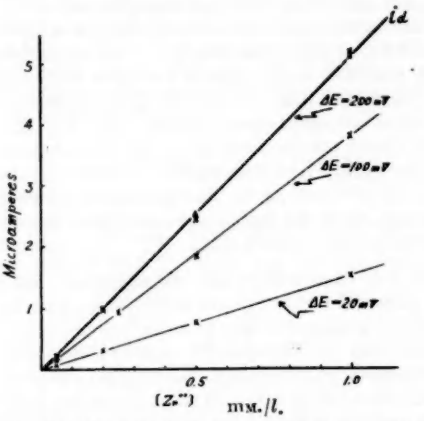

Fig. 5.—Relation between the peak current (i_h) and the diffusion current (i_d) of the zinc ion in ammoniacal solution.

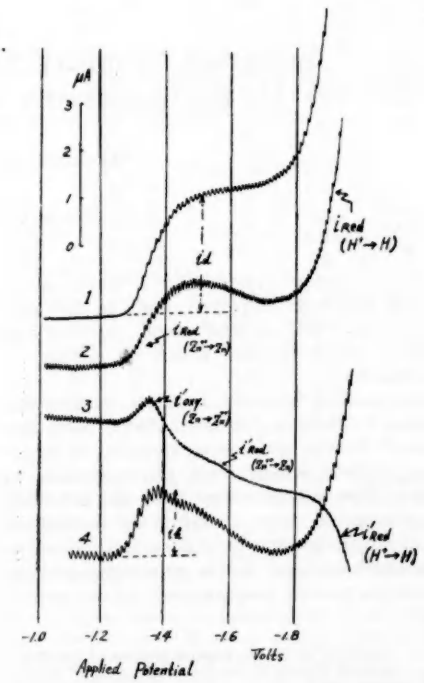

Fig. 6.—Polarograms of zinc ion in acidic tartrate solution: ΔE=100 millivolts, sensit.=1:50.

$i_d/2$ and less than i_d. Increasing the applied potential as high as the potential $E-\Delta E$ is sufficient to reduce zinc ion, the current drops to $i_d/2$ owing to the stop of supplying the ions at $E-\Delta E$. Thus the little peak appears in the curve 2 and also in the differential curve (curve 4), but differing from the case of reversible reaction, the peak current is always less than i_d. Viewed from the standpoint of quantitative analysis, such a case is the most ideal one in which the peak current is proportional to the concentration even though ΔE is small. The results obtained are shown in Fig. 5. Such irreversibility like that of zinc ammine should also be observed as to bismuth ion in tartrate solution, hydrion, many organic substances and hydrogen peroxide.[2]

(c) **A case when the dissociation rate is slow.**—In the ordinary polarogram, zinc in tartrate solution shows a wave of more gentle slope than the theoretically expected one. The differential polarogram shows only a little peak even when ΔE is taken so large. Judging from this fact, it is concluded that the rate of the dissociation of zinc ion from its tartrate complex is very slow compared with the electrodeposition of zinc from its simple ion. Fig. 6 shows from above to below, curve 1; $E\sim i$, curve 2; $E\sim i$ rot., curve 3; $E-\Delta E\sim -i'$ rot., and curve 4; $E\sim \Delta i/\Delta E$ curves. In the electrode reaction the over-voltage is required for the dissociation, and with the increase of the applied potential the dissociation is reasonably accelerated and the reduction current increases gradually to the extent of diffusion control. However, until the appearance of its influence, the potential interval is so wide that the peak becomes very low compared with the expected one. Concerning the little peak of the curve 3, it may be concluded that the electrode reaction has yet reversibility to some extent. The similar phenomena are expected in the following cases; the complex ions of nickel or cobalt and some organic substances which generate, for instance, the kinetic current. These cases are now under investigation.

Laboratory of Analytical Chemistry, Faculty of Science, Kyoto University, Kyoto

Analytical Chemistry by Means of Oxalic Acid. I. On the Quantitative Analysis of Strontium[1]

By Tamotsu MATSUMOTO

(Received July 9, 1951)

The method of determining a metal as its oxalate had been employed only in the case of calcium. The present writer applied this method to strontium, which is similar to calcium.[2]

Precipitating strontium as its oxalate was studied by Souchay, Lenssen, Herz, Muss and others[3],[4] who got various hydrates of strontium oxalate which were fairly soluble in water. The present writer tried the following experiments in order to apply the precipitate of strontium oxalate to gravimetric as well as volumetric analysis. In the gravimetric method strontium oxalate was weighed as its monohydrate, while in the volumetric determination the oxalic acid in strontium oxalate was titrated with potassium permanganate.

Experimental

Preparation of 0.1 M strontium nitrate was as follows:—Ishizu Chemicals' strontium nitrate was recrystallized. On analysing 50 ml. of the solution containing 10 g. of this salt, there were found no heavy metals, no alkali earths but strontium, and no alkalis in the sample. One litre of 0.1 M

Table 1

No.	$SrSO_4$ g.	Sr		
		Found g.	Calc. g.	Error mg.
1	0.4583	0.2186	0.2189	−0.3
2	0.4582	0.2186	0.2189	−0.3
3	0.4585	0.2187	0.2189	−0.2
mean	0.4583	0.2186	0.2189	−0.3

(1) Presented at the 6th Regular Meeting of the Chugoku-Shikoku Branch of the Chemical Society of Japan in January, 1952.
(2) Souchay and Lenssen, *Ann.*, **100**, 313 (1856).
(3) Souchay and Lenssen, *Ann.*, **102**, 35 (1857).
(4) Souchay, Lenssen, Herz and Muss, *Ber.*, **36**, 3717 (1903).

solution was prepared by dissolving 21.150 g. of this salt in distilled water, and 25 ml. of this solution was employed for each determination. In the first place the strontium in 25 ml. of this solution was determined by the ordinary sulfate method. The results are shown in Table 1.

1. Gravimetric Method.—In order to precipitate strontium as its oxalate, 5% ammonium oxalate solution was employed.

Procedure for precipitating strontium oxalate:—To 25 ml. of hot 0.1 M strontium nitrate solution which is acidified with dilute hydrochloric acid so that a small quantity of strontium oxalate precipitate once formed is redissolved, a definite quantity of hot 5% amm. oxalate solution is added and the whole is well stirred. When dilute ammonia is added drop by drop to the solution agitating strongly all the while, until the latter becomes just pink with phenolphthalein, a crystalline precipitate is produced. Now the whole is warmed in the water-bath for about 2 hrs., left to stand over night and filtered with 1.G.4. glass filter. The precipitate is washed with 1% amm. oxalate, distilled water or 50% alcohol, dried at 100—105°C. for 2 hrs. in the air-bath, and weighed.

A) Influence of washing solution.—In this case, 10 ml. of hot 5% amm. oxalate solution was employed for each determination. The precipitate was washed by decantation with one of the following washing liquids.

(1) 100 ml. of distilled water.

(2) 30 ml. of 1% amm. oxalate first, and 70 ml. of distilled water.

(3) 100 ml. of 50% alcohol.

The results are shown in Table 2.

Table 2 (Sr used is 0.2189 g.)

Washing liquid	$SrC_2O_4 \cdot H_2O$ g.	Sr	
		Found g.	Error mg.
water 100 ml.	0.4791	0.2168	−2.1
	0.4790	0.2167	−2.2
	0.4790	0.2167	−2.2
1% amm. oxalate 30 ml. and water 70 ml.	0.4810	0.2177	−1.2
	0.4812	0.2177	−1.2
	0.4813	0.2178	−1.1
50% alcohol 100 ml.	0.4837	0.2189	±0
	0.4835	0.2183	−0.1
	0.4835	0.2188	−0.1

The washing with distilled water (1) produces a remarkable negative error, the solubility of strontium oxalate being fairly large, while 50% alcohol (3) is found to be most effective, better results being given than by the ordinary sulfate method (Table 1). The error found in the case of washing with 1% amm. oxalate and water (2) is about the mean value of (1) and (3).

For the above reason, in the case where 50% alcohol is employed as the washing liquid, the determination of strontium can be carried out quantitatively.

Solubility of strontium oxalate.—The precipitate of strontium oxalate prepared by the above process and completely washed in hot water is put in a 300 ml. Erlenmeyer flask together with 200 ml. of solvent. The whole is set in a thermostat and shaken till the solution is saturated. After a definite time the solution is filtered, 50 ml. of the filtrate is put in the beaker and evaporated to dryness in the water-bath. The residue is dried at 100—105°C for 1 hr. and weighed. Table 3 shows the solubilities of strontium oxalate in distilled water, and 50% alcohol at 25—26°C.

Table 3

Solvent	Time in contact with solvent and precipitated, hr.	$SrC_2O_4 \cdot H_2O$ dissolved in 50 ml. mg.	Solubility (25-26°C) mg./l.	mol/l.
water	8	2.0		
	24	2.4	43.5	2.5×10^{-4}
	35	2.3		
50% alcohol	8	0.2		
	24	0.3	3.6	—
	35	0.2		

B) Influence of amount of amm. oxalate.—To find out the most suitable amount of amm. oxalate for precipitation of strontium oxalate and also to study the influence of dilution of the sample solution, a series of experiments were carried out, the results of which are shown in Table 4. In these experiments 100 ml. of 50% alcohol was employed as the washing solution.

Table 4 (Sr used is 0.2189 g.)

Water added ml.	5% Amm. Oxalate ml.	5% Amm. Oxalate molar ratio to Sr	$SrC_2O_4 \cdot H_2O$ g.	Sr found g.	Error mg.
—	10	1.4	0.4835	0.2188	−0.1
—	20	2.8	0.4836	0.2188	−0.1
—	40	5.6	0.4835	0.2188	−0.1
—	80	11.2	0.4838	0.2189	±0
50	10	1.4	0.4835	0.2188	−0.1
100	10	1.4	0.4834	0.2187	−0.2

The amounts of amm. oxalate and the partial dilution of the sample solution do not affect the exactness of the analysis.

C) Influence of *p*H.—To 25 ml. of 0.1 M strontium nitrate, a suitable indicator is added, and *p*H of the solution is adjusted to a certain value with dilute ammonia or hydrochloric acid. Then, with 10 ml. of hot 5% amm. oxalate solution the precipitate of strontium oxalate is formed.

From the results shown in Table 5, it is evident that the precipitation is completely carried out if the *p*H value of the sample solution is larger than 3.

Table 5 (Sr used is 0.2189 g.)

pH (Indicator)	$SrC_2O_4 \cdot H_2O$ g.	Sr g.	Error mg.
11.0 (Nitramine)	0.4835	0.2188	−0.1
8.2 (Phenolphthalein)	0.4835	0.2188	−0.1
6.3 (Methyl red)	0.4837	0.2189	±0
3.1 (Methyl orange)	0.4835	0.2188	−0.1
1.2 (Thymol blue)	0.4778	0.2162	−2.7
0.1 (Methyl violet)	none	—	—

D) Influence of various salts present.—The influence of various salts such as sodium chloride, potassium chloride, potassium nitrate, ammonium chloride or ammonium nitrate was examined. In each experiment, 25 ml. of 0.1 M strontium nitrate solution was mixed with a definite quantity of the salt, and this solution was treated in the manner described before. The results are shown in Table 6.

Table 6 (Sr used is 0.2189 g.)

salt	Mixed g.	$SrC_2O_4 \cdot H_2O$ g.	Sr g.	Error mg.
NaCl	2	0.5998	0.2714	+52.5
KCl	1	0.5324	0.2409	+22.0
KNO_3	2	0.5381	0.2435	+24.6
NH_4Cl	2	0.4833	0.2187	− 0.2
NH_4NO_3	2	0.4836	0.2188	− 0.1

Sod. chloride, pot. chloride, and pot. nitrate seem to be adsorbed in the precipitate of strontium oxalate so that the value of strontium is made very high. Amm. chloride and nitrate have no influence.

2) Volumetric Method.—When the strontium oxalate prepared by the above method is decomposed by sulfuric acid, oxalic acid is formed in the solution. By titrating this oxalic acid with potassium permanganate, the amount of strontium in the sample solution can be determined. The present writer applied this method to the volumetric analysis of strontium, and compared the results with those obtained by the gravimetric method.

Procedure:—From 25 ml. of 0.1 M strontium nitrate solution the precipitate of strontium oxalate is prepared under the best condition required in the former method. When 6 N sulfuric acid is added to the precipitate in a glass filter, strontium sulfate is formed and it is filtered out with suction, being stirred continuously with a glass rod. As the strontium sulfate probably adsorbs the oxalic acid, it should be washed well with distilled water. All the filtrate is kept in a measuring flask and diluted accurately to 250 ml. The 25 ml. of the filtrate, acidified with sulfuric acid, is titrated with 0.1 N potassium permanganate and from its volume the amount of strontium may be calculated.

Table 7 (Sr used is 0.2189 g.)

Gravimetrically		Volumetrically		
$SrC_2O_4 \cdot H_2O$ g.	Sr g.	0.1N-$KMnO_4$ (factor=1.0046) ml.	Sr found g.	diff. to grav. mg.
0.4837	0.2189	49.70	0.2188	−0.1
0.4835	0.2188	49.66	0.2186	−0.2
0.4835	0.2188	49.71	0.2188	±0

The results are shown in Table 7. Judging from the fact that the amount of strontium determined by the volumetric method is nearly equal to that given by the gravimetric, it may be said that the volumetric analysis by means of oxalic acid brings on satisfactory results.

Summary

1. Quantitative precipitation of strontium as its oxalate monohydrate is made possible by employing 50% alcohol as the washing solution and by drying the precipitate at 100-105°C for 2 hrs., and as a consequence a new method for determining strontium gravimetrically was established.

2. It was found that strontium can be determined volumetrically by titrating with potassium permangante the oxalic acid which is formed when the strontium oxalate prepared by the above method is decomposed with sulfuric acid.

The writer wishes here to express his hearty thanks to Prof. Masayoshi Ishibashi at Kyoto Univ. and Prof. Koichi Emi at Okayama Univ. for their kind guidance and encouragement. The expenses of this research were defrayed by the Grant in Aid for Fundamental Scientific Research from the Department of Education, to which the writer's thanks are due.

Chemical Institute, Faculty of Science, Okayama Univ.

A Study on the Mechanism of the Catalytic Action of Manganese Dioxide on the Decomposition of Potassium Chlorate by Use of Heavy Oxygen as an Isotopic Tracer

By Shouzow FUKUSHIMA, Yoshio HORIBE and Toshizo TITANI

(Received March 15, 1952)

Introduction

It is a well-known fact that various metallic oxides, especially manganese dioxide, show a remarkable catalytic action for the thermal decomposition of potassium chlorate.(1) Thus, the potassium chlorate, which melts at 370°C. without chemical change in the absence of catalyst, decomposes at such low temperature as 235~290°C.(2), when it is mixed with manganese dioxide which alone does not evolve oxygen gas below 520°C.

Ever since the reaction was studied by Döbereiner(3) in 1832, various hypotheses have been proposed for the mechanism of the catalytic action of manganese dioxide. But among these hypotheses the one which postulates the formation of an intermediate compound is presumably most probable.(4) According to this hypothesis, primarily an unstable intermediate compound is formed between potassium chlorate and manganese dioxide, and the subsequent decomposition of this intermediate compound is accompanied by the evolution of oxygen gas and the production of potassium chloride, manganese dioxide being regenerated. Although this hypothesis seems very probable from the recent point of view about the general mechanism of catalytic reactions, only few direct verifications for this mechanism have been found in the literatures so far as we know.

If, however, oxygen is evolved through the intermediate formation of an unstable compound between potassium chlorate and manganese dioxide, the evolved oxygen must contain oxygen atoms which are originated not only from potassium chlorate but also from manganese dioxide used as catalyst. And this may easily be shown by an isotopic analysis of the evolved gas, if either the oxygen atoms of potassium chlorate or those of manganese dioxide are labeled with heavy oxygen as an isotopic tracer. From this point of view, we studied the isotopic composition of oxygen gas evolved when potassium chlorate labeled with heavy oxygen was decomposed in the presence of an ordinary manganese dioxide.

Experimental

The potassium chlorate labeled with heavy oxygen was prepared by the anodic oxidation of potassium chloride in the solution of heavy water, of which content of heavy oxygen had been whose increased above its natural abundance by fractional distillation.

The product was purified by repeated recrystallizations in aqueous solution of ordinary water for the exchange reaction of oxygen atoms between water and chlorate ion can be ignored.(5)

The heavy potassium chlorate prepared in such a way was decomposed by heating in the presence of an ordinary manganese dioxide under various conditions as described below and the evolved oxygen was converted into the form of water by recombining with an ordinary tank hydrogen by the aid of a copper catalyst. At the same time a part of the same heavy potassium chlorate was non-catalytically decomposed in the absence of manganese dioxide catalyst by heating at 650°C. and the evolved oxygen gas was converted into the form of water in the same way as above, using the same tank hydrogen.

Another sort of water was also prepared by reducing, with the same tank hydrogen, a part of the same manganese dioxide which was used for the decomposition of heavy potassium chlorate as the catalyst. Although in this case manganese dioxide was to be reduced only to manganese monoxide, the isotopic separation between oxygen atoms contained in the produced water and those which remained in manganese monoxide was ignored.

The densities of these three sorts of water were then compared by the ordinary sinker

(1) Gmelin, "Handbuch der anorganischen Chemie", Kalium **22**, 473; Chlor, **6**, 342.

(2) Brown, Burrow and McLaughlin, *J. Am, Chem. Soc.*, **45**, 1343 (1923): Neville, ibid., **45**, 2331 (1923): Burrow and Brown, ibid., **48**, 1790 (1926): Balarew, *Kolloid-Z.*, **66**, 317 (1934).

(3) Döbereiner, *Ann.*, **1**, 236 (1832).

(4) McLeod, *J. Chem. Soc.*, **55**, 184 (1889); Sodeau, *J. Chem. Soc.*, **81**, 1066 (1902): *Proc. Chem. Soc.*, **18**, 136(1903); Dhar, *J. Phys. Chem.*, **28**, 953 (1924): Deniges, *Bull. trav. Soc. pharma. Bordeauz*, **74**, 93 (1936); Bhatnagar, et al, *J. Indian Chem. Soc.*, **17**, 124 (1940).

(5) T. Titani and K. Goto, This Bulletin, **13**, 667(1938).

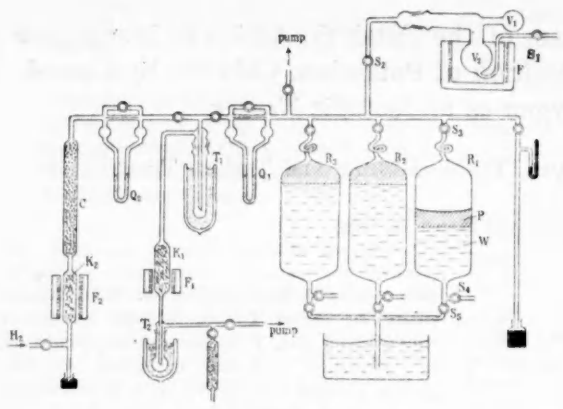

Fig. 1.

method, after a careful purification by heating with a small quantity of caustic soda and potassium permanganate and vacuum distillations. For each measurement, 0.5~0.8 ml. of water was needed.

The apparatus used for the thermal decomposition of heavy potassium chlorate in the presence and the absence of manganese dioxide is shown in Fig. 1 and the details of each run of the experiments are given below, where $KClO_3$* denotes the potassium chlorate whose oxygen is labeled with heavy oxygen, and $MnO_2 \cdot H_2O$ the manganese dioxide used as catalyst, because the manganese content of the catalyst determined by pyrophosphate method corresponds to that of this formula.

Exp. I.—Carefully powdered samples of 0.051 mole of $KClO_3$* and 0.045 mole of $MnO_2 \cdot H_2O$, were placed separately in V_1 and V_2. $KClO_3$* was dried in a vacuum for three hours at 20°C. and $MnO_2 \cdot H_2O$ was dried first in dry air current passed through S_1 and S_2 for two hours at 320°C. then in a vacuum for three hours at 20°C. Then, two reagents were mixed thoroughly in V_2 in a vacuum and the mixture was heated carefully by means of an electric furnace F at the desired temperature, which was measured by a thermocouple placed closely to the wall of the reaction vessel V_2. Oxygen gas was found to evolve at moderate rate at 320°C. and it took about fifty minutes until the reaction was completed, during this period the temperature inside the furnace being kept constant within a range of ±3°C. All of the evolved oxygen was collected in receiver R_1 by opening stopcocks S_2, S_3 and S_5. A thick layer of liquid paraffin P was placed to cover the surface of water W in the receiver in order to isolate the sampled oxygen from the air dissolved in the water. Then the oxygen gas was pushed out of R_1 to the catalyst tube K_1 through the flowmeter Q_1 and the dry ice trap T_1 by applying a hydropressure through S_4. The catalyst tube K_1 was filled with copper catalyst and heated at 400°C. in an electric furnace F_1. On the other hand, an excess quantity of tank hydrogen, which was freed from oxygen and water vapor by passing through the heated copper catalyst tube K_2 and the calcium chloride tube C and the dry ice trap T_1, was introduced into the catalyst tube K_1, the flow rate being checked by flowmeter Q_2. And thus the water, which was formed in the catalyst tube K_1 by the combination of the sample oxygen and the tank hydrogen, was collected in the ice water trap T_2.

Exp. II.—The experimental procedures and conditions were the same as Exp. I, except that 0.053 mole of $KClO_3$* was taken.

Exp. III.—The experimental procedures of this Exp. III, where 0.093 mole of $KClO_3$* and 0.095 mole of $MnO_2 \cdot H_2O$ were taken, were different from preceding Exps. I and II in two respects. In the first place $MnO_2 \cdot H_2O$ used in this experiment was pretreated under more severe conditions than in the preceding experiments. It was at first desiccated in the current of dry air for two hours at 480°C. and then treated for three hours in a vacuum at 320°C. By this severe treatment the catalytic activity of $MnO_2 \cdot H_2O$ seemed to be somewhat injured, for with this $MnO_2 \cdot H_2O$ the moderate rate of oxygen evolution was not observed until the temperature was raised up to 345°C. which is much higher than 320°C. the temperature used in the preceding experiments. The second characteristic of the procedure of this run was that the fractions of oxygen gas which were evolved at three different stages of the reaction were collected separately in three receivers, namely, the first fraction (1.05 l.) in R_1, the middle fraction (1.05 l.) in R_2 and the last fraction (0.35 l.) in R_3, and these three fractions of sampled oxygen were separately converted to water by use of the same tank hydrogen.

Exp. IV.—The purpose of this experiment was quite different from the purposes of the preceding Exps. I, II, and III and it is to investigate the possibility of a supposed secondary exchange reaction of oxygen atoms between manganese dioxide and gaseous oxygen which is evolved by the decomposition of potassium chlorate.

A gaseous oxygen which has the same isotopic composition as that of $KClO_3$* was prepared by the non-catalytic thermal decomposition of $KClO_3$*. The prepared heavy oxygen gas was then passed slowly through a reaction vessel which contains $MnO_2 \cdot H_2O$ pad at 350°C. and at the rate of 1.85 l. per hour. The $MnO_2 \cdot H_2O$ used in this experiment was preliminarily dried in the same way as in Exps. I and II, and the temperature of the reaction vessel (350°C.) was chosen much higher than the temperature (320°C.) at which the reaction mixture was heated in Exps. I and II. The heavy oxygen gas after being passed through the reaction vessel was converted to water in the same way as in the preceding experiments.

Results and Discussions

Results of the experiments are shown in Table 1; the third column gives the excess densities of recombined water due to the enrichment of heavy oxygen above the tap water in Osaka city,[6] and the last column the same, but with sample 1 taken as the standard. It will be seen from this table, by comparing the excess densities of samples No. 1 and 2, that the oxygen in $KClO_3$* is 47.5 p. p. m. heavier than that in $MnO_2 \cdot H_2O$. Accordingly the oxygen gas, which is evolved by the thermal decomposition of the mixture of $KClO_3$* and $MnO_2 \cdot H_2O$, must show the same excess density as that of $KClO_3$*, if the gas is exclusively originated from $KClO_3$*. But in fact the evolved gas has a much lower excess density than that of $KClO_3$*, as is seen from samples No. 3 to 5. On the other hand, the possibility of the secondary exchange reaction between evolved oxygen gas and $MnO_2 \cdot H_2O$ can be excluded by the result of Exp. IV, where the heavy oxygen, which was prepared by the noncatalytic decomposition of $KClO_3$* and passed over the same $MnO_2 \cdot H_2O$ as used in Exp. I and II, at higher temperature than that in these experiments, showed the same excess density as that of $KClO_3$* (see sample No. 8 in Table 1). From these experimental results, it can be concluded that a part of the oxygen gas, which is evolved by the catalytic decomposition of potassium chlorate in the presence of manganese dioxide, originates from the latter, presumably through an unstable compound, formed intermediately between the two substances. The result obtained in Exp. III is highly interesting, because it has been found there that the first fraction of the oxygen, which is evolved at the beginning of the reaction, shows the lower excess density than that of $KClO_3$*, as is seen in the preceding Exps. I and II, whereas the densities of the middle and last fractions agree with that of $KClO_3$* within the limit of the experimental error (see samples No. 5, 6 and 7 in Table 1). This result can, however, be explained under the following assumptions.

Table 1

Results of the Experiments

Number of the sample	Sample	Excess density due to heavy oxygen in the sample[6] (in p. p. m.)	Density difference (in p.p.m.)
1	$KClO_3$*	48.3±0.8	Standard
2	$Mn_2O \cdot H_2O$	0.8±0.5	−47.5
3	Oxygen gas evolved in Exp. I	32.6±1.0	−15.7
4	Oxygen gas evolved in Exp. II	34.6±1.0	−13.7
5	Oxygen gas evolved in the first stage of Exp. III	37.8±0.2	−10.5
6	Oxygen gas evolved in the middle stage of Exp. III	48.5±0.3	+ 0.2
7	Oxygen gas evolved in the last stage of Exp. III	46.5±2.6	− 1.8
8	Oxygen gas after exchange reaction in Exp. IV	48.0±0.2	− 0.3

Although the oxygen is liberated through the decomposition of the intermediate compound, which is formed between potassium chlorate and manganese dioxide, only a small part of the manganese dioxide has the activity to form such an intermediate compound, with potassium chlorate. It follows therefore that an isotopic exchange equilibrium is quickly established between the oxygen atoms contained in this active part of manganese dioxide and those of potassium chlorate through the repeated formation and decomposition of the intermediate compound between the two substances, when a limited quantity of manganese dioxide is heated with potassium chlorate. And when this equilibrium is once attained, the oxygen liberated from the mixture of both substances must have the same isotopic composition as that of potassium chlorate, whereas a part of the gas originates from manganese dioxide. This may be the reason why in Exp. III the oxygen, evolved after a certain period of the reaction, has the same excess density as that of potassium chlorate.

If it is so, the ratio of the number N of oxygen atoms contained in the active part to the total number N_0 of oxygen atoms contained in the whole manganese dioxide can be calculated from the quantity of potassium chlorate and manganese dioxide used in the experiment and the isotopic composition of the liberated oxygen and that contained in the potassium chlorate. The results of the calculation are shown in Table 2.

Although nothing can be said on the exact nature of this active part of manganese dioxide without further study, it may be a reasonable assumption that it would be a thin layer on the surface of each manganese dioxide particle. It has been found further by a microscopic observation that the manganese dioxide particles used in the present experiment may be

(6) Corrected for the difference in the isotopic composition of hydrogen between the tank hydrogen and tap water.

Table 2

Ratio of the Active Part and Thickness of Active Layer of Manganese Dioxide

Sample	N/N_0	Thickness of active layer ($m\mu$)
$MnO_2 \cdot H_2O$ used in Exp. I	0.37	2.2
$MnO_2 \cdot H_2O$ used in Exp. II	0.32	1.8
$MnO_2 \cdot H_2O$ used in Exp. III	0.072	0.4

regarded as a sphere having a mean diameter of 30 μ. The thickness of the active layer given in the last column of Table 2 has been calculated by using the ratio N/N_0 given in the second column of the table, under the assumption that the active part forms a complete shell layer on the surface of a spherical particle of manganese dioxide having a diameter given above. From the figures given in Table 2, it will be seen that the active part of $MnO_2 \cdot H_2O$ used in the last Exp. III is much smaller than those used in Exps. I and II. This result is, however, in good accordance with the experimental fact that $MnO_2 \cdot H_2O$ used in Exp. III has a much weaker activity than those used in the other experiments as has already been stated. And if it is taken into consideration that $MnO_2 \cdot H_2O$ used in Exp. III has been pretreated under more severe conditions than in other experiments, namely, heated in a vacuum at much higher temperatures than others, it may be concluded that a large portion of the active part of manganese dioxide catalyst has been lost or destroyed by this severe treatment.

Summary

By use of heavy oxygen as an isotopic tracer, the following facts have been found;

1. At the catalytic decomposition of potassium chlorate in the presence of manganese dioxide, an unstable compound is formed between potassium chlorate and manganese dioxide, and oxygen gas is liberated by the decomposition of this intermediate compound.
2. The active part of manganese dioxide capable of composing such an intermediate compound with potassium chlorate is only a limited small portion of the particle.
3. Such an active part is readily destroyed by such a severe treatment as the heating of the catalyst in a vacuum at high temperature.

A part of the expense for the present research has been defrayed by the Scientific Research Encouragement Grant from the Ministry of Education, to which the authors' thanks are due.

Department of Chemistry, Faculty of Science, Osaka University, Osaka

Über die Reinigung des Rubidiums. — Umkrystallisation des Rubidiumtetraoxalates —

Von Airi SUETUNA

(Eingegangen am 25 Dezember, 1951)

Einleitung

Die Reinigung des Rubidiums wurde durch Umkrystallisation des Rubidiumtetraoxalates[1],[2] an Stelle des Rubidiumbitartrates versucht, welches als das entsprechende Cäsiumsalz weit schwerer löslich in Wasser ist und darum bisher für die Entfernung des Cäsiums von Rubidiumsalz oft benutzt wurde. Die Löslichkeit der Tetraoxalate wurde nun von neuem bestimmt, und somit wurde die Tatsache gefunden, daß trotz der Literaturenangabe der Löslichkeitsunterschied zwischen Tetraoxalaten des Cäsiums

(1) Neulich erschien eine Abhandlung von J. D'ans (*Angew. Chem.*, **62**, 118 (1950)), der für die Abscheidung des Rubidiums aus dem reinen Rubidiumcarnallit die Oxalsäure an Stelle von Weinsäure benutzte. Man saugt das abgeschiedene Rubidiumtetraoxalat ab und krystallisiert es aus Wasser um. Nach einer kurzen Fraktionierreihe geht das Cäsium als die leichter lösliche Komponente in die Mutterlauge.

(2) J. Formánek (*Österr. Chem. Ztg.*, **2**, 309 (1899)) benutzte die Normaloxalate zur Trennung von Kalium, Rubidium und Cäsium. Dabei ist wohl das Kaliumoxalat das wenigst lösliche

und des Rubidiums leider nicht so groß sei. Um diesen Nachteil zu überwinden, wurde die Umkrystallisation des Rnbidiumtetraoxalates so oftmals wiederholt, daß ganz unerwartet nicht nur das Cäsium sondern auch das Kalium dabei zugleich entfernt und das reine Rubidiumpräparat erhalten wurde. Dies stellt wirklich einen neuen Typus der Reinigung des Rubidiums dar.

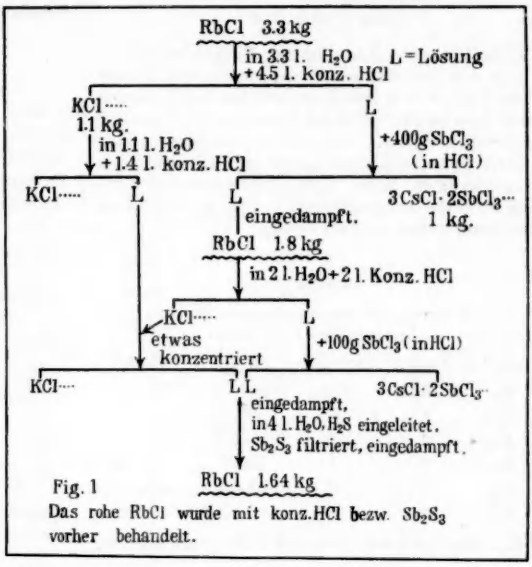

Fig. 1 Das rohe RbCl wurde mit konz. HCl bezw. Sb_2S_3 vorher behandelt.

(A) Löslichkeit der Tetraoxalate in Wasser

Ältere Angaben stehen in Tabelle 1.

Tabelle 1

Löslichkeit der Tetraoxalate.
g. Salz/100 g. H_2O (Ältere Angaben)

Salz	21°	25°	30°
$KH_3(C_2O_4)_2 \cdot 2H_2O$	4.96[3] (20.6°)	3.16[4] 5.2[5]	5.05[6]
$RbH_3(C_2O_4)_2 \cdot 2H_2O$	2.1[7]		
$CsH_3(C_2O_4)_2 \cdot 2H_2O$		25[8]	

Unter den Hydrooxalaten des Kaliums, des Rubidiums und des Cäsiums lassen sich nur die Tetraoxalate $MH_3(C_2O_4)_2 \cdot 2H_2O$ unverändert aus Wasser umkrystallisieren. Die Löslichkeit der Tetraoxalate wurde hier folgenderweise bestimmt: das reine Präparat der Tetraoxalate wurde in mäßiger Menge Wasser heiß aufgelöst, die Lösung in einem Thermostaten unter Schütteln abgekühlt, und einige Zeit stehen gelassen, dann ein Teil Mutterlauge gewogen und das darin vorhandene Oxalat-ion mit Kaliumpermanganatlösung titriert. In Tabelle 2 stehen die so erhaltenen Resultate. Die Werte sind die Mittel von je 2 bis 4 Messungen. Der Fehler beträgt bei jedem Falle höchstens 1%.

Tabelle 2

Löslichkeit der Tetraoxalate. g. Salz/100 g. H_2O (von neuem bestimmt)

Salz	21°	25°
$KH_3(C_2O_4)_2 \cdot 2H_2O$	2.46	
$RbH_3(C_2O_4)_2 \cdot 2H_2O$	2.03	
$CsH_3(C_2O_4)_2 \cdot 2H_2O$	4.34	5.93

(3) J. J. Pohl. *Ber. Wien. Akad.*, **6**, 397 (1851).
(4) H. Hartley, J. Drugman, usw. *J. Chem. Soc.*, **103**, 1747 (1913).
(5) berechnet aus dem Diagramm des Systems $K_2C_2O_4$-$H_2C_2O_4$-H_2O bei 25° von H. W. Foote, I. A. Andrew. *Am. Chem. J.*, **34**, 162 (1905).
(6) I. Koppel, M. Cahn. *Z. anorg. Chem.*, **60**, 106 (1908).
(7) F. Stolba. Sitzungsber. Böhm. Ges. Wissensch., 278 (1877).
(8) berechnet aus dem Diagramm des Systems $Cs_2C_2O_4$-$H_2C_2O_4$-H_2O bei 25° von H. W. Foote, I. A. Andrew. *Am. Chem. J.*, **34**, 162 (1905).

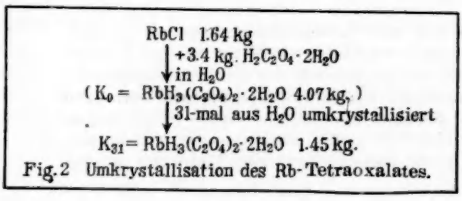
RbCl 1.64 kg
+3.4 kg. $H_2C_2O_4 \cdot 2H_2O$
in H_2O
(K_0 = $RbH_3(C_2O_4)_2 \cdot 2H_2O$ 4.07 kg.)
31-mal aus H_2O umkrystallisiert
K_{31} = $RbH_3(C_2O_4)_2 \cdot 2H_2O$ 1.45 kg.

Fig. 2 Umkrystallisation des Rb-Tetraoxalates.

(B) Umkrystallisation des Rubidiumtetraoxalates

Das rohe Rubidiumchlorid, anscheinend K 15~20%, Rb 60~70%, Cs 15~20%, wurde wie üblich zur Beseitigung der Hauptteile des Kaliums und des Cäsiums mit konzentrierter Salzsäure bezw. Antimontrichlorid vorher behandelt. Fig. 1 veranschaulicht dieses Verfahren.

Das solcherweise vorbereitete Rubidiumchlorid wurde mit der berechneten Menge Oxalsäure in Wasser aufgelöst. Beim Abkühlen scheidet sich das Tetraoxalat fast ohne Verlust aus. Dies wurde durch Dekantieren von der Mutterlauge getrennt und weiter 31-mal wiederholt aus Wasser umkrystallisiert. Fig. 2 zeigt dieses Verfahren.

Das Rubidiumtetraoxalat ist äußerst günstig zur Umkrystallisation : das in kaltem Wasser wening lösliche Salz löst sich in heißem leicht und glatt, nach 31-maliger Umkrystallisation wurde 35.6% der anfänglichen Salzmenge gewonnen, und daher darf man annehmen, daß die Ausbeute 1- und 10-maliger Umkrystallisation 96.7% bezw. 71.7% betragen solle.

Weil das Salz beim Glühen leicht zerfällt und ins Carbonat übergeht, dient es sehr zweckmäßig als das Ausgangsmaterial beim Herstellen anderer Rubidiumsalze.

(C) Chemische Spektralanalyse der Produkte

Ungefähr um jede fünfte Umkrystallisation wurde ein Teil Salz zur Probe genommen, die auf einer Platinschale mäßig erhitzt, bis das Aufblasen der Schmelze sich aufhörte, und somit zur Analyse vorbereitet wurde. Die chemische, semi-quantitative Spektralanalyse wurde mit Littrowschem Spektrogramm nach Glimmschicht-spaltabbildungsmethode ausgearbeitet. Die so erhaltenen Resultate stehen in Tabelle 3.

Tabelle 3

Die Resultate der semi-quantitativen Analyse der Produkte

Produkt	Li(%)	Na(%)	K(%)	Cs(%)
K_5	0.001>	0.01	0.5~1	0.5~1
K_{10}	〃	〃	~0.5	0.1~0.5
K_{15}	〃	〃	0.1~0.5	0.05~0.1
K_{21}	〃	〃	~0.1	~0.001
K_{25}	〃	〃	0.05~0.1	~0.001
K_{31}	〃	〃	0.05~0.1	~0.001

K_n: Krystall nach n-maliger Umkrystallistation.

Wie aus dem Löslichkeitsunterschied hervorgeht, wurde das Cäsium rascher als das Kalium entfernt und gegen Ende der Umkrystallisierreihe wurde reines Rubidiumpräparat erhalten. Die letzten Mengen des Kaliums (0.05~0.1%) haften hartnäckig dem Rubidiumpräparat an und werden auch durch andere, geeignete Methoden schwer beseitigt. Wohl mag dies nicht nur auf Verbrauch der Glasgeräte zurückzuführen sein.

Zusammenfassung

(1) Die Löslichkeit der Tetraoxalate des Kaliums, des Rubidiums und des Cäsiums wurde von neuem bestimmt. Die des Cäsiumtetraoxalates wurde viel geringer als die ältere Angabe gefunden.

(2) Das rohe Rubidiumtetraoxalate wurde 31-mal aus Wasser umkrystallisiert.

(3) Die chemische Spektralalyse zeigt, daß bei der Umkrystallisation des Salzes das Cäsium sowie das Kalium in die Mutterlauge geht und allein das Rubidium im Krystall sich anreichert.

(4) Die Endprodukte stellten reines Rubidiumpräparat dar.

(5) Die Nach-und Vorteile dieser Methode werden hier nicht wiederholt erwähnt.

Herrn Prof. K. Kimura möchte ich für seine wertvollen Ratschläge bei dieser Untersuchung meinen besonderen Dank aussprechen.

Die chemische Spektralanalyse wurde von Herren H. Kakihana und M. Fujimoto durchgeführt. Dafür bin ich ihnen auch herzlich dankbar.

Chemisches Institut der Wissenschaftlichen Fakultät, Universität zu Tokyo.

Infrared Absorption Studies of Tropolone and Allied Compounds

by Kenji KURATANI, Masamichi TSUBOI and Takehiko SHIMANOUCHI

(Received March 5, 1952)

Introduction

The chemistry of the seven-membered unsaturated ring has rapidly developed in recent years. A number of new compounds with this ring have been synthesized and their structural formulas determined.[1a][1b] Of their spectroscopy, however, much work is yet to be done.[2] The present paper describes the infrared absorption spectra of tropolone and the related compounds prepared by Dr. T. Nozoe and his coworkers (Tohoku University, Sendai) who have carried out an extensive work in tropolone chemistry.[1a]

Experimental

Infrared absorption measurements were made by means of the Baird Infrared Spectrophotometer with a NaCl prism. Of the absorptions in the region above 2800 cm.$^{-1}$, measurements were also made by using a quartz spectrometer with higher resolving power, which was described in a previous paper.[3] The absorption curves obtained are shown in Figs. 1—6. Names, and

(1a) Nozoe, *Sci. Pap. Tohoku Univ. Ser.* **1**, **34**, 199 (1950). *Proc Japan Acad.*, **26**, 30 (1950). Nature, **167**, 1055 (1951). *Chem. and Ind.* (Chem. Soc, Japan), **4**, 348 (1951).

(1b) Cook and London, *Quart. Res.*, **5**, 99 (1951). Johnson, *Sci Progr.*, **39**, 405 (1951).

(2) Scott and Tarbell, *J. Am. Chem. Soc.*, **72**, 240 (1950). Doering and Knox, *J. Am. Chem. Soc.*, **73**, 828 (1951).

(3) Tsuboi, this Bulletin, **22**, 215 (1949).

melting points of the compounds examined are listed in Table 1. On dissolving the dried sample

Table 1

Substances	Melting points °C.	Absorption curves	References
tropolone	50—51	a	(i)
o-isopropyltropolone	33.2—34	b	(ii)
m-isopropyltropolone	51—52	c	(iii)
p-isopropyltropolone	77—78.5	d	(iv)
o-methyltropolone	49.5—50.5	e	(v)
m-methyltropolone	75—76	f	(v)
p-methyltropolone	108—110	g	(v)
o-bromotropolone	107—108	h	(i)
p-bromotropolone	190—191	i	(i)
o, *o'*-dibromotropolone	159—160	j	(vi)
o, *o'*, *p*-tribromotropolone	125—126	k	(i)
tropolone methyl ether	b.p. 125/5 mm.	l	(vii)
tropolone methyl ether+$^1/_2H_2O$	40.5	—	(vii)
tropolone acetate	69.5—70.5	m	(viii)
2-phenyltropone	85.8—86.5	n	(ix)
2-aminotropone	106—107	o	(x)

(i) Nozoe, Seto, Kitahara, Kunori and Nakayama, *Proc. Japan Acad.*, **26** (1950), 38.
(ii) Nozoe, Yasue and Yamane, *Proc. Japan Acad.*, **27** (1951), 15.
(iii) Nozoe and Katsura, *J. Pharm. Soc. Japan*, **69** (1944), 181.
(iv) Nozoe, Seto, Kikuchi and Takeda, *Proc. Japan Acad.*, **27** (1951), 146.
(v) Nozoe, Mukai and Matsumoto, *Proc. Japan Acad.*, **27** (1951), 110; Nozoe, Mukai and Matsui, *Proc. Japan Acad.*, in press.
(vi) Nozoe, Kitahara, Yamane and Yoshikoshi, *Proc. Japan Acad.*, **27** (1951), 18.
(vii) Nozoe, Seto, Ikemi and Arai, *Proc. Japan Acad.*, **27** (1951), 102.
(viii) Nozoe, Seto and Sato, to be published.
(ix) Nozoe, Mukai and Mineguchi, *Proc. Japan Acad.*, **27** (1951), 419.
(x) Nozoe, Seto, Takeda, Morosawa and Matsumoto, *Proc. Japan Acad.*, **27** (1951), 556.

of tropolone methyl ether in carbon tetrachloride or carbon disulphide, special care was taken to prevent it from being moistened because of its highly hygroscopic property.

Hydrogen Bond and Conjugated Double Bonds in the Tropolone Ring.—That tropolone has an intramolecular hydrogen bond of the form:

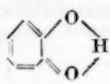

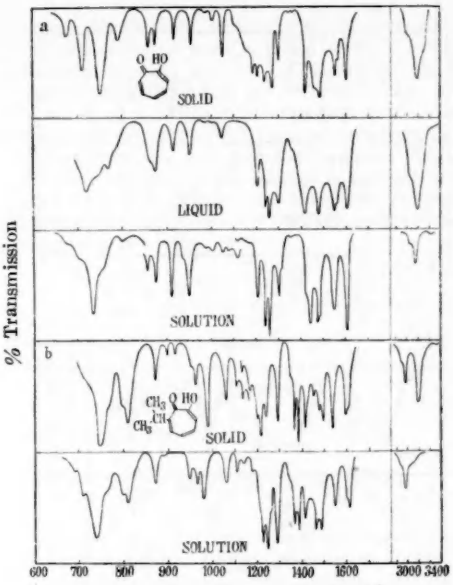

Fig. 1 A.—Infrared spectra of tropolone and *o*-isopropyltropolone.
Spectra in solids: samples molten and solidified between the two sylvine plates.
Spectra in solutions: 1300—630 cm.$^{-1}$, about 5% CS_2 solutions 4000—900 cm.$^{-1}$, about 5% CCl_4 solutions, cell thickness 0.1 mm.

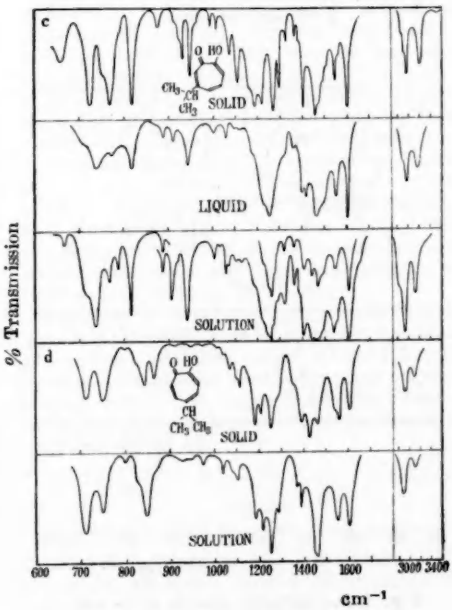

Fig. 1 B.—Infrared spectra of *m*- and *p*-isopropyltropolone.

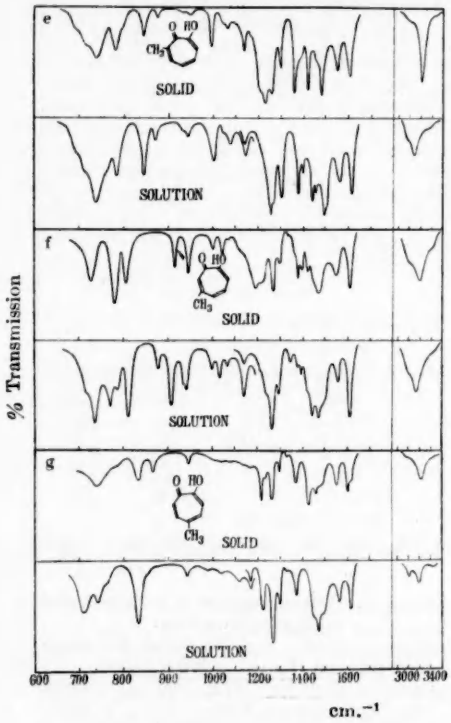

Fig. 1 C.—Infrared spectra of *o*-, *m*- and *p*-methyltropolone.

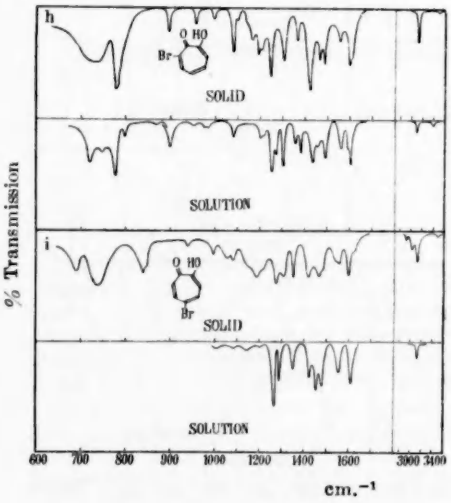

Fig. 1 D.—Infrared spectra of *o*- and *p*-bromotropolone.

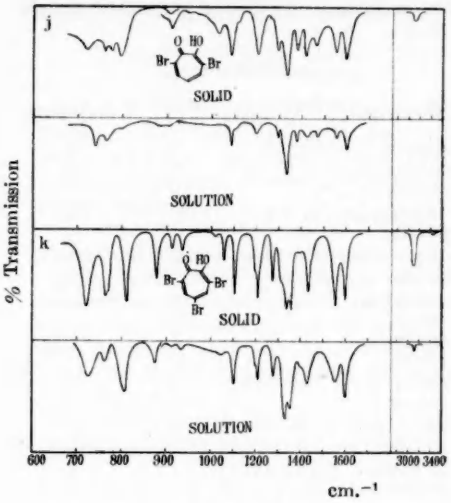

Fig. 1 E.—Infrared spectra of di- and tribromotropolone.

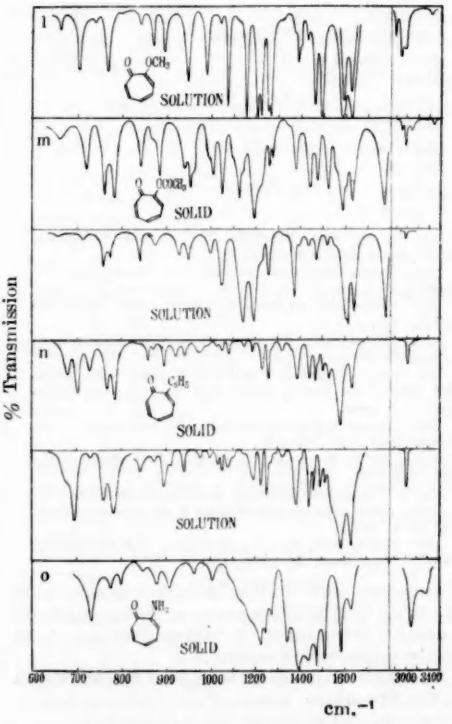

Fig. 1 F.—Infrared spectra of tropolone methyl ether, tropolone acetate, phenyltropone, and aminotropone.

has already been shown from the result of its dipole moment measurement[4] and from its infrared spectra.[5] The present studies have afforded further evidence for this conclusion. Thus, the O—H stretching band of tropolone observed in 0.01 mol./l. carbon tetrachloride solution is located at 3.2 μ (Fig. 2A), a position much displaced from that of the free O—H band, 2.8 μ,

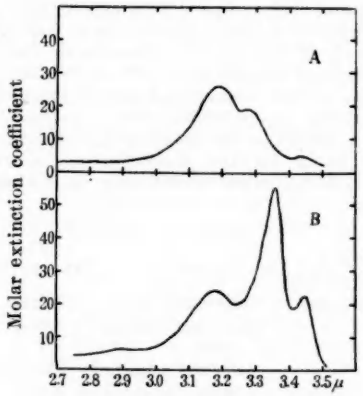

Fig. 2.—Near infrared absorption curves for (A) tropolone and (B) hinokitiol in 0.01 mol./l. CCl_4 solutions.

showing that the OH is hydrogen-bonded. Further, no change has been observed in the feature of the spectrum at all, even the concentration of the solution was changed from 0.004 to 0.1 mol./l., indicating that the hydrogen bonding is intramolecular. The unusually great shift of the O—H band of tropolone from that of free O—H band shows that the hydrogen bonding is correlated with the conjugation of the double bonds in tropolone—in other words, there is a kind of so-called "conjugated chelation"[6] in tropolone molecule. It may also be seen that the chelation in tropolone is stronger than those of *o*-substituted phenols (with O—H band at about 3.1 μ) and is weaker than those of the enol-forms of acetyl acetone and acetoacetic ethyl ester (with O—H band at about 3.7 μ[6]).

The C—H stretching absorption of tropolone is found at 3.3 μ but not in the 3.4—3.5 μ region Fig. 2A). This is consistent with the wellknown fact that all the carbon atoms in the tropolone molecule are unsaturated.

The near infrared spectra of *m*-isopropyltropolone (hinokitiol) and *o*- and *p*-isopropyltropolone (α- and γ-thujaplicin) (Fig. 1, b and d) are similar to that of tropolone in most respects, except the presence of the 3.4—3.5 μ bands in the former, which are due to the isopropyl group. Bromotropolones (Fig. 1, h, i, j, and k) exhibit their hydrogen-bonded O—H band 3.2 μ and unsaturated C—H band at 3.3 μ, just as tropolone does. On the other hand, tropolone methyl ether, 2-phenyltropone, and tropolone acetate exhibit no band at 3.2 μ, corresponding to the fact that they have no O—H group. Moreover tropolone methyl ether containing 1/2 H_2O shows its O—H band at 2.86 μ (Fig. 3).

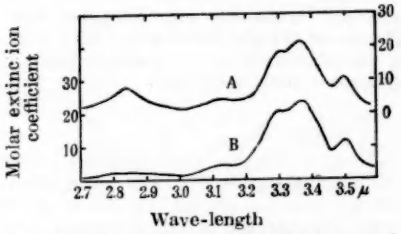

Fig. 3.—Near infrared absorption curves for (A) tropolone methyl ether with $^1/_2$ H_2O and (B) dried tropolone methyl ether in 0.02 mol./l. CCl_4 solutions.

Special attention is called to the double bond region (1700—1500 cm.$^{-1}$) of the absorption spectra of troponoid[7] compounds. In tropolone methyl ether as well as tropolone acetate and 2-phenyltropone, the stretching vibrations of the C=O and C=C bonds are found, respectively, at 1630 and 1580 cm.$^{-1}$ (Fig. 1, l, m, and n), instead of at their normal positions which are respectively at 1720 and 1660 cm.$^{-1}$. This may be ascribed to the conjugation between the C=C and C=O bonds. Further, in tropolone as well as methyl-, isopropyl- and bromo-tropolones with the intramolecular hydrogen bonds the C=C and C=O frequencies appear in still lower frequency regions ——*i.e.* respectively at 1610 and 1560 cm.$^{-1}$ (Fig. 1, a-k). This fact may be taken as indicating that the intramolecular hydrogen bonding affects the electronic state of the tropolone ring, and, accordingly, affects the force constants of the C=C and C=O bonds in the ring.

The effect of intramolecular hydrogen bonding upon the electronic state of tropolone ring is also shown from the observation of its ultraviolet spectrum. Tropolone methyl ether and tropolone acetate exhibit one strong absorption band at about 320 mμ in the near ultraviolet region, while tropolone anion:

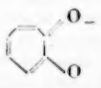

exhibits two bands at 330 and 393 mμ. The ultraviolet absorption spectra of tropolone and

(4) Kurita, Nozoe and Kubo, this Bulletin, **24**, 10 (1951).
(5) Koch, *J. Chem. Soc.*, 512 (1951).
(6) Rasmussen, Tunnicliff and Brattain, *J. Am. Chem. Soc.*, **71**, 1068 (1949).
(7) Dr. Nozoe gives a name "troponoids" to the allied compounds of tropone.

hinokitiol with intramolecular hydrogen bond possess features intermediate between those of tropolone methyl ether (or tropolone acetate) and tropolone anion, indicating that they are intermediate in electronic state.[8]

The Proton-Accepting Powers of Tropolone Methyl Ether and Hinokitiol Methyl Ether.—As has been mentioned above, tropolone has the stronger intramolecular hydrogen bond than *o*-substituted phenols. In order to obtain further information about the hydrogen-bond-forming powers of the compounds with the seven-membered unsaturated ring, the methyl ethers of tropolone and hinokitiol were compared with benzaldehyde as to their proton-accepting powers, by the method described in a previous paper.[9] The hydrogen-bonded complexes:

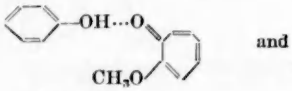

and

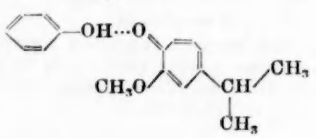

exhibit O—H bands at 3.00 and at 3.02 μ in dilute carbon tetrachloride solutions respectively (Fig. 4), while the complex:

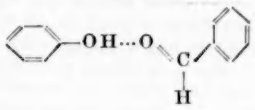

exhibits O—H band at 2.89 μ. From the amount of these complexes in the solutions (estimated from the intensity measurement of these O—H bands) and from the amount of shifting of these O—H bands from free-phenol O—H band (2.77 μ), it is concluded that the proton-accepting powers of the methyl ethers of tropolone and hinokitiol are stronger than that of benzaldehyde.

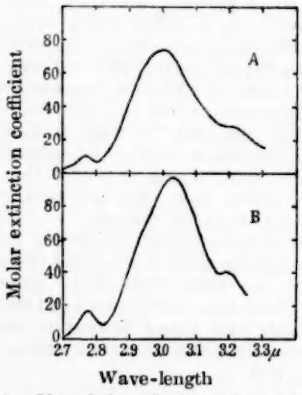

Fig. 4.—Near infrared absorption curves of phenol in (A) phenol (0.01 mol./l.)+tropolone methyl ether (0.02 mol./l.)+CCl_4 and in (B) phenol (0.01 mol./l.)+hinokitiol methyl ether (0.02 mol./l.)+CCl_4

The Vibrational Spectra and the Structure of Troponoid Compounds.—Corresponding to the arrangement of the substituent groups of benzene, characteristic absorption bands due to the out-of-plane C—H deformation vibrations are found in the region of 900—750 $cm.^{-1}$.[10] In the case of sevenn-membered unsaturated ring compounds, similar strong characteristic bands are found as shown in Table 2. The data given in the table will be useful for the determination of the structural formulas of the tropolone derivatives.

Table 2

Types of substitutions	Examples	Frequencies
1, 2-substituted	tropolone	735 $cm.^{-1}$
	tropolone methyl ether	770
	tropolone acetate	750 or 770
1, 2, 3-substituted	*o*-isopropyltropolone	800
	o-methyltropolone	782
	o-bromotropolone	770
1, 2, 4-substituted	*m*-isopropyltropolone	820
	m-methyltropolone	812
1, 2, 5-substituted	*p*-isopropyltropolone	850
	p-methyltropolone	830
	p-bromotropolone	850

Spectra of Troponoids in the Solid State.—Infrared spectra of tropolone and isopropyltropolones in the solid state are considerably different from those in solutions (Fig. 1, a—d). When they are brought from the solutions into the solid state, some of their absorption bands increase in relative intensity (for example, 1190—1210 $cm.^{-1}$ bands probably due to O—H deformation vibrations contained in them) and some become doublets (Fig. 1, b and c). The hydrogen-bonded O—H bands become, on solidification, stronger (in comparison with the C—H bands) and sharper, and at the same time shift towards shorter wave lengths (Fig. 1, b, e, f, g; Fig. 2 and 5). This indicates that the correlation between conjugation and hydrogen bonding in tropolonoid molecules is less remarkable in solid states than in solutions. According to the private communication of Prof. I. Nitta and Dr. K. Osaki, the presence of ring dimer with intermolecular double hydrogen bonds:

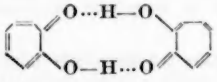

(8) Ultraviolet absorption studies of troponoids will be published elsewhere.

(9) Tsuboi, this Bulletin, **25**, 60 (1252).

(10) For example, Colthup, *J. Opt. Soc. Am.*, **40**, 397 (1950).

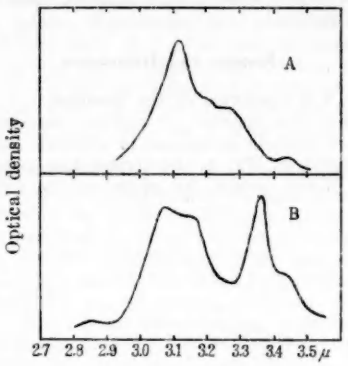

Fig. 5.—Near infrared absorption curves for (A) tropolone and (B) hinokitiol in solid states.

in tropolone crystal is recently proved from its x-ray analysis. Since tropolone in solutions has an intramolecular hydrogen bond and is in monomeric state, there must be a change in the behavior of hydrogen-bonding on its solidification. The observed changes in the spectra of tropolone and the allied compounds may be attributed to such changes in the behavior of hydrogen-bonding. A fact, perhaps worthy of note in this connection, is that the spectra of tropolone and hinokitiol in liquid states are closer to those in solutions than to those in the solid state, as may be seen from the comparison of the absorption curves shown in Fig. 1, a and c. The infrared spectra of some of the bromo-substituted tropolones are almost independent of their phase changes (Fig. 1, h—k).

Spectrum of Aminotropone.— Aminotropone exhibits two N—H stretching absorption bands at 2.83 μ (3530 cm.$^{-1}$) and 2.97 μ (3360 cm.$^{-1}$) (Fig. 6). This fact may be explained from the structure of this compound:

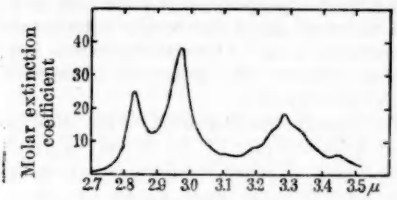

Fig. 6.—Near infrared absorption curve for aminotropone in 0.02 mol./l. CCl_4 solution.

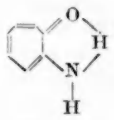

the former band being assigned to the free N—H vibration and the latter to the hydrogen-bonded N—H vibration. On the other hand, double-bond absorption bands observed for this compound are situated at 1624 and 1590 cm.$^{-1}$ (Fig. 1, o)——positions not much displaced from those observed for tropolone methyl ether. This shows that the internal hydrogen bond of aminotropone is weak.

In conclusion the writers wish to express their sincere thanks to Professor San-ichiro Mizushima for his kind guidance in this work, and to Professor Tetsuo Nozoe, Shuichi Seto, Yoshio Kitahara, Toshio Mukai, and other members of the Laboratory of Organic Chemistry, Faculty of Science, Tohoku University for their placing the samples at the writers' disposal and for their valuable suggestions. The cost of this work has been partly defrayed by a grant from the Ministry of Education.

Department of Chemistry,
Faculty of Science, University of Tokyo.

Dichroisms of Benzene Rings. III. The Dichroism of *m*-Nitronitrosobenzene Monomer

By Kazuo NAKAMOTO

(Received March 6, 1952)

Introduction

In the previous works, the dichroisms of aromatic compounds[1],[2] and molecular compounds[3] have been measured, and the general rules about the π-band have been found in respective cases. Throughout these works, however, the band at the longest wave length side

(1) K. Nakamoto, *J. Am. Chem. Soc.*, **74**, 390 (1952).
(2) K. Nakamoto, ibid., **74**, 392 (1952).
(3) K. Nakamoto, ibid., **74**, 1739 (1952).

was always superposition of the strong π-band and the weak band due to the substituents of the benzene ring. Accordingly, it was impossible to observe the dichroism characteristic of the substituents.

To measure the dichroism of the substituent band independently of the intense π-band, it is necessary to select a substance whose spectrum in crystalline state shows the band of the former, far apart from the latter in the ultraviolet region. As was shown in the spectrum of anthraquinone crystal,[2] the carbonyl band is superposed on the intense π-band, although they show definite peaks in solution. So the substance, which has both the bands far apart in the spectrum of the solution, is suitable for our purpose.

Nitrosobenzene derivatives have, generally, their characteristic bands due to the nitroso group at 700~800 mμ, and the π-bands due to the benzene ring at 300~400 mμ. They are therefore expected to appear separately even in the crystalline state.

In the present study, the spectra of *m*-nitronitrosobenzene monomer in crystalline state as well as in solution have been measured, and the results have been discussed in comparison with that of *m*-dinitrobenzene which had been reported before.[2]

Experimental

Material.—*m*-Nitronitrosobenzene was prepared by reduction of *m*-dinitroboenzene according to the method of Alway and Gortner.[4] Colourless powder (dimer). It melts at 91° to become a green liquid (monomer). For the purpose of getting fine crystals suitable for the measurement of dichroism, the ordinary method of recrystallization from the solution is not available, because the substance is unstable and apt to polymerize. By mixing the alcoholic solutions of *m*-nitronitrosobenzene and *m*-dinitrobenzene in the molar ratio of 1:1, light green acicular crystals were obtained. They are isomorphous to pure *m*-dinitrobenzene crystal, and have similar properties to it. Spectroscopic measurement, described later, revealed that they are composed of 25 per cent nitroso compound and 75 per cent dinitro compound. They show straight extinction, and dichroic property; light green by linearly polarized light with the electric vector vibrating parallel to the c-axis (needle axis), and light yellow, by the light with those vibrating perpendicular to it (b-axis).

Measurements.—Absorption spectra in solution were measured by the rotating sector method. Dichroism of the crystal was measured by the microscopic method mentioned in the former work.[1] Throughout these experiments, infrared sensitive photo-plates were used to measure the green region.

(4) F. J. Alway and R. A. Gortner, *Ber.*, **38**, 1900 (1905).

Results and Discussion

(1) The Spectrum of the Solution

Absorption spectra of *m*-dinitrobenzene and pure *m*-nitronitrosobenzene in alcoholic solutions are shown in Fig. 1. Numerical data characterizing these spectra are given in the following table.

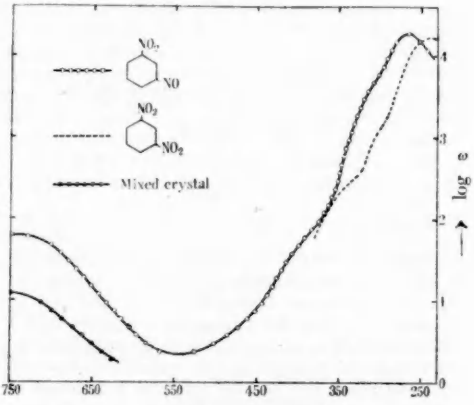

← Wave length, mμ.

Fig. 1.—Absorption spectra of *m*-nitronitrosobenzene, *m*-dinitrobenzene and their mixed crystal in alcoholic solutions.

	Nitroso band	Nitro band	π-band	σ-band
m-Dinitrobenzene		330(2.5)	300(3.1)	250(4.2)
m-Nitronitrosobenzene	750(1.8)	390(1.8)	320(3.4)	265 (4.25)

Here the $\lambda_{max.}$ is expressed in mμ, and the log $\varepsilon_{max.}$ is given in brackets, respectively.

As is shown above, the substitution of one of the nitro groups by the nitroso group causes the occurrence of the nitroso band at about 750 mμ, and gives bathochromic and hypochromic effects to the nitro band. But the same substitution gives only small bathochromic and hyperchromic effects to the π- and σ-bands in the ultraviolet region. These changes in the spectrum can be easily explained by the facts that the nitroso group is more unstable than the nitro group, and a substitution of an unstable group for a stable group gives, generally, bathochromic and hyperchromic effects to all the bands in a molecule.

The absorption spectrum of an alcoholic solution of the mixed crystal is also shown in Fig. 1. From the comparison of log ε at 750 mμ in these two curves, the crystal was estimated to contain as much *m*-nitronitrosobenzene as 25 per cents.

(2) The Dichroism of the Crystal

The crystal used for the measurement contains

25 per cent nitroso compound, as spectroscopically shown before. Practically, two components can mix at any ratio in crystal, and, moreover, no colour change can be seen at the mixing of their solutions. These chemical facts suggest that in the crystal used, the two components exist merely in a mixed state and not as a molecular compound.

So far, its crystal structure is unknown, although that of pure *m*-dinitrobenzene has been thoroughly studied.[2] So the Debye-Scherrer photographs of both the crystals have been taken, as shown in Fig. 2. The resemblance of the two photographs means that the two crystals have similar structure and so, its crystal structure can be presumed as follows: the planar molecules* of *m*-nitronitrosobenzene in *m*-dinitrobenzene crystals are piled up along the needle axis (c-axis), making their molecular planes almost parallel to the a-axis and inclined by about 20° to the b-axis, as graphically shown in Fig. 3.

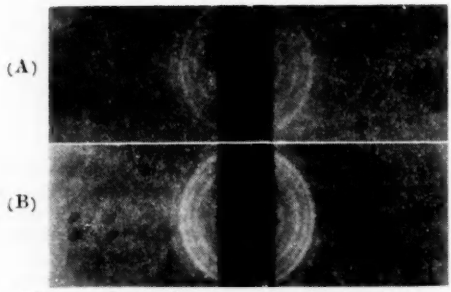

Fig. 2.—Debye-Scherrer photographs of pure *m*-dinitrobenzene (A) and the mixed crystal (B)

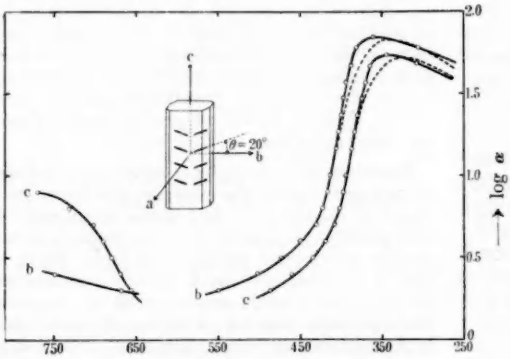

Fig. 3.—Absorption spectra of the mixed crystal (solid lines) and *m*-dinitrobenzene (broken lines) in crystalline states.

Absorption curves by linearly polarized lights with the electric vectors vibrating parallel to the b- and c-axes are shown in Fig. 3. As the angle θ between the molecular plane and the b-axis is only 20° and smaller than 45°, the light with the electric vector parallel to the b- (or c-) axis is abundant with the parallel (or perpendicular) component to the molecular plane. Conforming to these discussions with the experimental result, we can reach the conclusion that the $\parallel$-absorption in the ultraviolet region is bathochromic and hypsochromic to the $\perp$-absorption, whereas the former in the visible region is remarkably hypsochromic to the latter.

(3) The Dichroisms of pure *m*-Nitronitrosobenzene Monomer

If the absorption due to pure *m*-dinitrobenzene is reduced from the above results, the dichroism of pure *m*-nitronitrosobenzene is obtained.

(i) Visible Region

As is clearly shown in the former work, *m*-dinitrobenzene has no absorptions in the visible region. So the above result in this region is exclusively due to pure nitroso compound. Thus, it is concluded that the $\perp$-absorption is hypsochromic to the $\parallel$-absorption. The origin of this band is the nitroso group in the molecule, as is definitely shown in the spectrum of the solution. As a result, the absorption responsible for the green colour of *m*-nitronitrosobenzene is concluded to be due to the electronic transition polarized perpendicularly to the C—N—O bond. Recently Fenimore[5] obtained the same result as above. He, however, used the assemblage of many microcrystals which orientated practically parallel to each other, and measured the dichroism in the narrow range between 700~800 mμ. Whereas, we used only one single crystal, and measured in a wider range between 750~250 mμ.

(ii) Ultraviolet Region

Broad bands seen in the ultraviolet region consist mainly of the π-absorption, as already discussed in the former paper.[2] In Fig. 3 is shown the present result (solid lines) along with the dichroism of *m*-dinitrobenzene (broken lines). Both spectra are very similar to each other, except that the former is slightly bathochromic in comparison with the latter. This result suggests that both substances have similar dichroic property, and the dichroism of the π-band does not suffer any considerable change, even if *m*-dinitrobenzene in the crystal is replaced by *m*-nitronitrosobenzene.

Thus, we conclude that the $\parallel$-absorption in pure *m*-nitronitrosobenzene is bathochromic and hypsochromic to the $\perp$-absorption. If both molecules formed a molecular compound, the feature of the spectrum would be quite different.[3] This result, along with the above mentioned chemical facts, confirms the theory that the crystal observed here is only a mixed crystal, and not a molecular compound.

* The steric configuration of nitrosobenzene derivatives is a subject of much discussion. None of these crystals, however, have ever been studied by X-ray analysis. So, in the present paper, the C-N-O bond is assumed to be nearly linear and coplanar with the benzene plane.

(5) C. P. Fenimore, *J. Am. Chem. Soc.*, **70**, 3114 (1948).

Summary

Absorption spectra of *m*-nitronitrosobenzene monomer in crystalline state as well as in solution have been measured quantitatively in the visible and the ultraviolet regions. In its π-band of the ultraviolet region, the general rule about the π-band of the benzene ring was found to hold also for the present case. In regard to the nitroso band of the visible region, the absorption by linearly polarized light with the electric vector vibrating perpendicular to the C—N—O bond was hyperchromic to the absorption by the light with those vibrating parallel to it. This result suggests that the green colour of *m*-nitronitrosobenzene is due to the electronic transition polarized perpendicularly to the C—N—O bond.

The author wishes to express sincere thanks to Prof. R. Tsuchida for his kind guidance and Mr. H. Matsuda for his help in X-ray work.

Department of Chemistry, Faculty of Science, Osaka University, Osaka

The Infrared Dichroism of Amides

By Kenji KURATANI

(Received February 26, 1952)

The measurement of the infrared dichroism is a useful method of determining the position of hydrogen atoms in molecules. With regard to the structure of amide groups this technique was first applied to urea by Keller[1] and then to acetanilide by Brown and Corbridge.[2] The author suggested in a previous paper[3] that Keller's conclusion was inaccurate and that the correct determination of planarity of urea should be made, using the dichroism of NH stretching vibrations. Recently using the grating spectrometer, Waldron and Badger[4] measured the dichroism of NH stretching vibrations and the planarity of urea molecule was accurately proved. In this paper, the infrared absorption spectra of trichloroacetamide and deuterated monochloroacetamide were measured and the observed vibrational frequencies of amide groups were assigned. With this result together with the measurement of infrared dichroism of benzamide and monochloroacetamide, the position of hydrogen atoms in these molecules is discussed.

Experimental

Infrared spectra of trichloroacetamide and deuterated monochloroacetamide were measured with a Baird spectrophotometer. Infrared dichroism of benzamide and monochloroacetamide were measured with the apparatus described in our previous papers,[5] though we also used a selenium reflexion polarizer (the incident angle about 70°) to provide plane polarized infrared radiation. The direction of the electric vector of the incident radiation was parallel to the entrance slit.

A small amount of the solid was molten between a pair of sylvine plates. The specimens were cooled in such a way as to induce as far as possible the crystallization in oriented linear fashion. Absorption intensities of these specimens were measured with the direction of the orientation of crystals either parallel or perpendicular to the electric vector of the incident plane-polarized radiation.

Materials.—The samples of amide were obtained as follows: benzamide was recrystallized from water (m.p. 127—8°), and monochloroacetamide was prepared from ethyl monochloroacetate and ammonia and then recrystallized from water by Mr. I. Nakagawa (m.p. 120°). Deuterated monochloroacetamide was obtained by repeating the exchange reaction with heavy water, and trichloroacetamide was prepared from ethyl trichloroacetate and ammonia by Mr. T. Sugita (m.p. 140°).

Results

Infrared absorption spectra of deuterated

(1) Keller, *J. Chem. Phys.*, **16**, 1003, (1948).
(2) Brown and Corbridge, *Nature*, **162**, 72 (1948).
(3) Kuratani, *J. Chem. Soc. Japan*, **71**, 22 (1950).
(4) Waldron and Badger, *J. Chem. Phys.*, **18**, 566 (1950).
(5) Shimanouchi, Tsuruta and Mizushima, *Sci. Pap. I. P. C. R.*, **42**, 165 (1945).

monochloroacetamide and trichloroacetamide are given in Fig. 1. and 2.

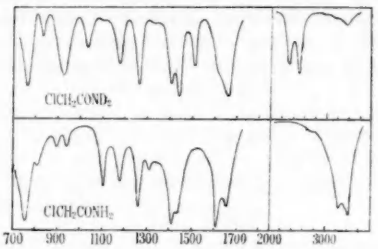

Fig. 1.—Infrared spectra of monochloroacetamide and partially deuterated monochloroacetamide.

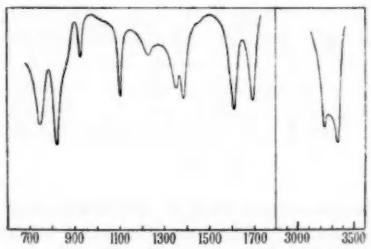

Fig. 2.—Infrared spectrum of trichloroacetamide.

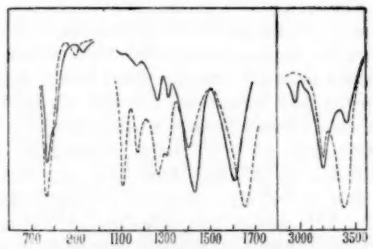

Fig. 3.—Polarized spectra for oriented crystals of monochloroacetamide. Electric vector of the beam is parallel (dotted curve) and perpendicular (full curve) to the direction of the crystal growth.

The absorption spectra of monochloroacetamide with the orientation of crystals parallel or perpendicular to the incident radiation are given in Fig. 3. The experimental results of the absorption spectra of benzamide were in agreement with those of Mann and Thompson.[6] The absorption peaks are summarized in Table 1, in which we have used the term

Table 1

Monochloroacetamide		Benzamide	
Bands	Dichroism	Bands	Dichroism
766 s	∥	768 s	⊥
804 w	⊥ ?	790 s	⊥ ?
890 w	∥ ?	805 s	⊥ ?
924 w	⊥ ?	920 m	?
1100 m	∥	1020 m	?
1180 s	∥	1120 m	∥ ?
1265 s	∥	1140 m	∥
1310 m	∥	1300 m	∥
1410 s	∥	1405 s	⊥
1430 s	⊥	1450 m	?
1610 s	⊥	1575 s	∥
1660 m	∥	1620 s	⊥
2960 m	⊥	1660 s	∥
3200 s	⊥	3200 s	⊥
3400 s	∥	3400 s	∥

"parallel dichroism" to describe larger absorption when the ek ic vector vibrates parallel to the axis of orientation than when it vibrates in a perpendicular direction, and the term "perpendicular dichroism" which is the reverse. Benzamide has other weaker bands, i. e., 843, 995, 1070, 1175, 1250 and 1495 cm.$^{-1}$, but the dichroism of these bands have not been determined.

Discussion

a) Vibrational Modes of Amide Group.—In the 9 vibrational modes of $-CONH_2-$ group, OCN skeletal deformation vibration is not dealt with since this vibration lies beyond the observed frequency region. The remaining 8 modes are indicated in the first column of Table 2.

Table 2

Vibrational Modes	Notations	Assignment
NH_2 symmetric stretching	$\nu(NH_2)_s$	−3400 cm.$^{-1}$
NH_2 antisymmetric stretching	$\nu(NH_2)_a$	−3200
C=O stretching	ν(C=O)	−1660
C−N stretching	ν(C−N)	−1400
NH_2 symmetric deformation	$\delta(NH_2)$	−1600
NH_2 rocking, NH_2 wagging, NH_2 twisting	NH_2 rocking*	$\gamma(NH_2)$	−1150, —, —

(* The distinction of these 3 bands is not necessary for the following discussion.)

The characteristic vibrational frequencies of amide groups, i. e., the vibrational frequencies which are commonly found in amide groups are 3400, 3200, 1660, 1600, 1400, and 1150 cm.$^{-1}$.

(6) Mann and Thompson, *Proc. Roy. Soc.* (*London*), **A. 192**, 489 (1948).

These absorption frequencies are also observed in the case of trichloroacetamide which has no C—H bond (see Fig. 2). There is no doubt about the assignment of the first 3 bands and, therefore, only the assignment of the last 3 bands is discussed.

Based on the numerous experimental results, Randall[7] assigns the 1400 cm.$^{-1}$ band to ν(C—N) vibration. This conclusion is also supported by the presence of 1385 cm.$^{-1}$ band in trichloroacetamide (see Fig. 2), since in this case there is no possibility of the presence of $\delta(CH_3)$ vibration. (In general $\delta(CH_3)$ and $\delta(CH_2)$ vibrations are found in 1380—1480cm.$^{-1}$ region.)

The weakness of absorption bands at 1600 and 1100 cm.$^{-1}$ and the appearance of the bands at 830, 925 and 1030 cm.$^{-1}$ in the spectrum of deuterated monochloroacetamide, support the assignments of 1600 and 1100 cm.$^{-1}$ to NH_2 bending vibrations. These assignments are also confirmed by the frequency shift of 1600 and 1150 cm.$^{-1}$ bands in $CO(NH_2)_2$ to 1250 and 990 cm.$^{-1}$ in $CO(ND_2)_2$,[8],[9] and the shift of 1150 cm.$^{-1}$ band in CH_3CONH_2 to lower frequency region in CH_3COND_2.[10] The fact that primary amines have 1600 and 1150 cm.$^{-1}$ bands and secondary amines have only 1150 cm.$^{-1}$ band proves the assignments of 1600 cm.$^{-1}$ band to symmetric deformation vibration, and 1150 cm.$^{-1}$ band to NH_2 or NH rocking vibration. This conclusion is consistent with the assignment of Axford, Janz and Russel[11] on methylhydrazine, and that of Kahovec and Kohlrausch[12] on the Raman lines of various amides. Cleaves and Plyler[13] made the same assignment for 1625 and 1150 cm.$^{-1}$ bands of methylamine measuring the band contours of these bands. These considerations confirm the assignment of vibrational bands of amide groups as indicated in the right column of Table 2.

b) Relation between the Molecular Structure and Infrared Dichroism.—In the first place let us discuss the cofiguration of CNH_2 groups of amide molecules. For CNH_2 group, we may consider 2 configurations, in one of which C—N bond is almost perpendicular to the plane of NH_2 group as in the case of methylamine molecule, and in the other the C—N bond is in the NH_2 plane as in the case of urea molecule.

When the C-N bond is nearly perpendicular to the plane of NH_2 group, the vibrational modes of 1600 and 1150 cm.$^{-1}$ bands become as shown in Fig. 4.[14] In this case the direction of the dipole moment change of ν(C—N) mode coincides with that of $\gamma(NH_2)$ mode and, therefore, ν(C—N) shows the same dichroism as $\gamma(NH_2)$. However, the direction of the dipole moment change of $\delta(NH_2)$ is perpendicular to that of ν(C—N) and the dichroism of $\delta(NH_2)$ is opposite to that of ν(C—N).

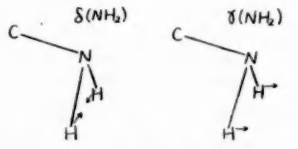

Fig. 4.—Vibrational modes for the nonplanar form.

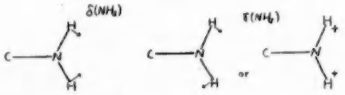

Fig. 5.—Vibrational modes for the planar form.

On the other hand, when the 2 hydrogen atoms lie on the same plane with carbon and nitrogen atoms as in the case of urea molecule, the vibrational modes of 1600 and 1150 cm.$^{-1}$ bands become as shown in Fig. 5.[14] In this case ν(C—N) band shows the same dichroism as $\delta(NH_2)$ and the opposite dichroism as $\gamma(NH_2)$. Accordingly the planarity of C—NH_2 group, i. e., whether C—NH_2 group is more similar to methylamine or to urea, is determined from the dichroism of 1600, 1400, and 1150 cm.$^{-1}$ bands. Of course, the accurate angle between C—N bond and NH_2 plane will be determined from the measurement of the pleochroism of these bands, but in the present experiment only the dichroism was measured and only the more favorable form was determined.

Monochloroacetamide.—Since chloroacetyl chloride, bromoacetyl chloride and bromoacetyl bromide[15] have their CH_2 deformation frequencies in the range of 1390—1400 cm.$^{-1}$, the

(7) Randall, Fowler, Fuson and Dangl, "Infrared Determination of Organic Structures" New York (1949).
(8) Kellner, *Proc. Roy. Soc.* (*London*), **A. 177**, 456 (1941).
(9) Otvos and Edsall, *J. Chem. Phys.*, **7**, 632 (1939).
(10) Lenormant, *Compt. rend.*, **228**, 1861 (1949).
(11) Axford, Janz and Russel, *J. Chem. Phys.*, **19**, 709 (1951).
(12) Kahovec and Kohlrausch, *Z. phys. Chem.*, **B. 51**, 49 (1942).
(13) Cleaves and Plyler, *J. Chem. Phys.*, **7**, 563 (1939).
(14) Since 1150 cm.$^{-1}$ Raman line of formamide is a polarized one, vibrational modes of this frequency are confined to these figures.
(15) Mizushima and Nakagawa, to be published shortly.

1410 and 1430 cm.$^{-1}$ bands of monochloroacetamide are most reasonably interpreted as being a CH_2 deformation and a C—N stretching vibration, respectively. The propriety of the planar structure as shown in Fig. 5 is deduced from the fact that 1430 and 1610 cm.$^{-1}$ bands have the same dichroism and 1100 cm.$^{-1}$ band has the dichroism opposite to them.

This conclusion is verified by the experiment in the 3 micron region. The same dichroism of ν(C—N) and $\nu(NH_2)_s$, i. e., 1430 and 3200 cm.$^{-1}$ bands, is the excellent evidence of the planarity of C—NH_2 group.

Benzamide.—The opposite dichroism of 1400 and 1140 cm.$^{-1}$ bands assigned, respectively to ν(C—N) and $\gamma(NH_2)$ vibrations of benzamide, prefers the planar structure without the discussion of the dichroism of $\delta(NH_2)$ vibration. The same dichroism of ν(C—N) and $\nu(NH_2)_s$ vibrations confirms this conclusion.

On account of the planarity of carbon, nitrogen and hydrogen atoms, remaining possibilities of amide structure are confined to 2 forms. In one of these, NH_2 group lies on the same plane with C—O—N skeleton (form I), and in the other, CNH_2 plane intersects the plane of C—O—N skeleton at right angles (form II). (Only the more symmetrical forms are considered.)

The depolarization degree of Raman lines assigned to NH_2 stretching vibrations will be useful to distinguish the 2 forms, because in structure I both Raman lines due to NH_2 symmetric and antisymmetric stretching vibrations are polarized, while in structute II, the depolarized Raman line due to NH_2 antisymmetric stretching vibration should be observed. However, the depolarization degree of Raman lines of amides has not yet been measured.

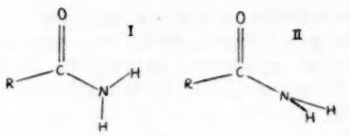

Fig. 6.

The direction of the dipole moment change of $\nu(NH_2)_a$ vibration is parallel to that of ν(C=O) vibration in structure I, and perpendicular in structure II. Therefore from the relation between the dichroism of $\nu(NH_2)_a$ and ν(C=O) (3400 and 1660 cm.$^{-1}$ bands), we can determine whether the structure of amides is consistent with I or II. The experimental result supports structure I for monochloroacetamide and benzamide molecules.

The writer wishes to express his sincere thanks to Professor San-ichiro Mizushima, and Assistant Professor Takehiko Shimanouchi for their kind guidance. The writer also thanks to Messrs. Tatsuo Miyazawa, Tadao Sugita, and Ichiro Nakagawa for their kind assistance throughout this work. The cost of this work has been partly defrayed by a grant from the Ministry of Education.

Institute of Science and Technology,
Tokyo University, Tokyo

The Change of Molecular Weight of Egg Albumin in Aqueous Solutions

By Kazuo SHIBATA and Koichi MURAI

(Received September 13, 1951)

Heller and Klevens[1] have recently measured the molecular weight of egg albumin in aqueous solutions by the light transmission method, and obtained a value of 47,000 immediately after the preparation of the sample at 4°C. With the lapse of time after the preparation, however, the value obtained gradually increased, namely 64,000 after 24 hours and 81,000 after 72 hours. This phenomenon was considered to be due to the occurence of aggregation, but the details of the process were not relevantly worked out by these authors. The purpose of this study is to elucidate the nature of the process, with special reference to the effect of temperature upon the phenomenon in question.

(1) W. Heller and H. B. Klevens, *Phys. Rev.*, **67**, 61 (1945). W. Heller, Ibid., **68**, 5 (1945).

The solution used was a 0.3% aquous solution of egg albumin, which was prepared by dissolving egg albumin (preparation of Takeda Pure Chemicals LTD.) in distilled water. The relative value of the molecular weight of egg albumin in aqueous solution was measured by determining the turbidities of solutions, using a Pulfrich photometer provided with a special device for measuring the scattered light. The change of the molecular weight was observed at several intervals of time in the aqueous solution of egg albumin, which was immersed in the water baths regulated at 30°C., 40°C. and 50°C., respectively.

The results obtained are shown in Fig. 1, where the abscissa is the time in hours and the ordinate is relative value W of the weight average molecular weight, assuming the value immediately after the preparation of the solution as unity. As will be seen from this figure, the value of W increased rapidly within a few hours and reached the maximum value in four hours. In one experiment observation was continued over night, but from the fifth hour on, the value W was found to remain practically unchanged. To one of the samples (200 cc.), in which W had already reached its maximum value at 30°C., 5 cc. of 10 N urea solution were added, whereby no change of W could be observed. The rise of temperature caused both the increase of the initial velocity and the increase of the maximum value of W.

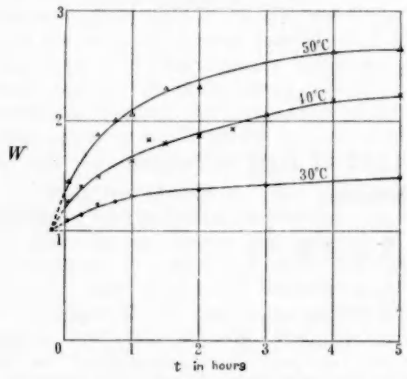

Fig. 1.

As was suggested by Heller and Klevens, the observed increase of molecular weight may be due to the process of aggregation. Let us assume that the aggregation takes place in the manner of the following polymerization reaction.

$$M_1+M_1 \xrightarrow{k} M,\ M_1+M_2 \xrightarrow{k} M_3,\ M_1+M_3 \xrightarrow{k} M_4,\ \ldots\ldots$$
$$M_2+M_2 \xrightarrow{k} M_4,\ M_2+M_3 \xrightarrow{k} M_5,\ \ldots\ldots\ldots\ldots$$
$$\ldots\ldots\ldots\ldots\ldots\ldots\ldots\ldots\ldots\ldots$$
$$M_i+M_i \xrightarrow{k} M_{2i},\ \ldots\ldots M_i+M_j \xrightarrow{k} M_{i+j},\ \ldots\ldots$$
$$\ldots\ldots\ldots\ldots$$

where M_1, M_2..... indicate monomer, dimer and so on, i and j being assumed to be any integer. The velocity constant for each step of aggregating reactions is assumed to be the same. For such a type of multistep reactions, a theory had already been developed by Flory,[2] according to whom, the number of moles of i-mers, N_i, which has been formed at the time t, is given by the following equation;

$$N_i = N_0 p^{i-1}(1-p)^2 \qquad (1)$$

in which

$$p = \frac{kt}{2+kt}.$$

N_0: Total number of moles of the monomer at the beginning. It has already been shown by Doty, Zimm and Mark[3] that whereas osmotic pressure measurements yield a number average molecular weight, turbidity measurements give a weight average. Therefore, the value W which we have observed is the relative value of weight average molecular weight M to the molecular weight of the monomer M_0. Hence,

$$W = M/M_0$$
$$= \frac{1}{M_0} \cdot \frac{\sum_i (iM_0)^2 Ni}{\sum_i iM_0 Ni}$$
$$= \frac{\sum i^2 Ni}{\sum iNi}$$
$$= \frac{\sum i^2 p^{i-1}}{\sum ip^{i-1}} \qquad (3)$$

Using the relations

$$\sum_i ix^{i-1} = (1-x)^{-2} \qquad (4)$$

$$\sum_i i^2 x^{i-1} = (1-x)^{-3}(1+x), \qquad (5)$$

equation (3) becomes

$$W = \frac{1+p}{1-p}$$

(2) P. J. Flory, *J. Am. Chem. Soc.*, **58**, 1877 (1936); **59**, 241 (1937); **61**, 1518, 3334 (1939); **62**, 1057, 1561, 2255, 2261 (1940); **63**, 3083, 3091, 3096 (1941).

(3) P. M. Doty, B. H. Zimm and H. Mark, *J. Chem. Phys.*, **13**, 159 (1945).

$$=1+kt. \qquad (6)$$

This equation indicates that the initial velocity of the increase of W is k. The value k for each temperature can be evaluated from the data of our experiments. Based on the temperature dependency of k, the activation energy of the reaction was calculated to be 7 kcal./mole.

If we further assume that each reaction step has the same equilibrium constant (K), then the following relation must hold for the number fractions $m_i=N_i/N_0$;

$$K=\frac{m_{i+j}}{m_i \cdot m_j}.$$

This equation must hold for any choice of i and j, but the equations thus obtained are not necessarily independent of each other. Actually, the relation ($i=2$, $j=2$) can be derived from the equations for ($i=1$, $j=1$), ($i=1$, $j=2$) and ($i=1$, $j=3$). As will be seen from this example, the independent relationship will be the following;

$$m_i K=x^i, \qquad (7)$$

in which

$$x = Km_1.$$

Using equations (4), (5) and (7), the relative value of weight average molecular weight at equilibrium may be expressed by

$$W=\frac{1}{M_0}\cdot\frac{\sum_i (iM_0)^2 Ni}{\sum_i iM_0 Ni}$$

$$=\frac{\sum i^2 mi}{\sum imi}$$

$$=\frac{\sum i^2 x^i}{\sum ix^i}$$

$$=\frac{1+x}{1-x}. \qquad (8)$$

For obtaining the relation between K and W, we shall use the following relation;

$$\sum_i im_i=1, \qquad (9)$$

which must be true according to the definition of m. Substituting equation (7) in (9), we have

$$K=\frac{x}{(1-x)^2}. \qquad (10)$$

Since we have equation (8) relating x to W, we can express K in terms of W at equilibrium; that is

$$K=\frac{1}{4}(W^2-1). \qquad (11)$$

Using this equation, we evaluated K at each temperature, and calculated the change of heat content from the temperature dependency of K, which amounted to 7 kcal./mole. If we extrapolate our result of analysis to the case of lower temperatures, the value of W at equilibrium is calculated to be 1.04 at 0°C., which shows that almost no egg albumin molecules will aggregate at 0°C. Whether or not this conclusion is valid, it remains to be checked by further investigations.

The author is much indebted to Dr. Hiroshi Tamiya for his constant help and advice.

Tokugawa Institute for Biological Research

Synthetic Studies on the Δ^2-Derivatives of Selenazolines

By Yutaka MIZUHARA

(Received March 18, 1952)

The possible heterocyclic syntheses according to the schema which follow

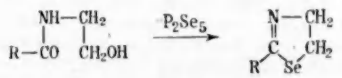

were pursued in our laboratory, with the desire to obtain selenium-containing ring compounds.

From N-acylethanolamine, H. Wenker[1] synthesized Δ^2-oxazolines and Δ^2-thiazolines.

(1) H. Wenker, *J. Am. Chem. Soc.*, **57**, 1080 (1935).

The procedure was not applied for the preparation of Δ^2-selenazolines.

Recently A. Van Dormael[2] made report on the formation of 2-methylselenazoline by a similar method to Wenker's procedure for the preparation of 2-methylthiazoline.

Hitherto 2-methylselenazoline has been prepared from diacetyldiaminoethyl-β-diselenide hydrochloride and phosphorus pentachloride.[3] It has also been synthesized from bromoethylamine hydrobromide and selenoacetamide.[4]

Unintentionally I have investigated also the reaction between N-acyletanolamine and phosphorus pentaselenide, which was found later to be similar to A. Van Dormael's procedure. This report* describes five homologues of Δ^2-selenazolines, three of which are 2-alkyl derivatives—2-methylselenazoline, 2-ethylselenazoline, and 2-*n*-propylselenazoline; and two of which are 2-aryl derivatives—2-phenylselenazoline, 2-benzylselenazoline. I found that the 2-aryl derivatives were solid and did not give picrates. Contrarily, the 2-alkyl derivatives were liquid and gave picrates easily. In the three 2-alkyl derivatives, the boiling point rises according to the increase of alkyl group weight. However the relation between the melting point of their picrates and the boiling point of free bases is reverse. The higher homologues are more stable and the yields are better.

This procedure is much simpler than the methods which so far have been devised and is convenient to obtain Δ^2-derivatives of selenazolines.

Experimental

Phosphorus pentaselenide.—Phosphorus pentaselenide was prepared by the methods described by W. Bogen[5] and by W. Muthmann & A. Clever.[6]

N-Acylethanolamines. — N-Acylethanolamines were synthesized by the double decomposition of ethanolamines and acid esters. The boiling points of the acylethanolamines used here were as follows:

Acetylethanolamine, b.p. 161°/4.5 mm. Hg,
Propionylethanolamine, b.p. 155—156°/7 mm. Hg,
Butyrylethanolamine, b.p. 159.5°/5 mm. Hg,
Benzoylethanolamine, b.p. 202—203°/4 mm. Hg,
Phenylacetylethanolamine, b.p. 207~209°/6.5 mm. Hg.

Δ^2-Selenazolines

(i) 2-Propylselenazoline.—The procedure described here for 2-propylselenazoline was also used for the preparation of the other two 2-alkylselenazolines. In a 500 cc. Claisen distilling flask N-butyrylethanolamine (20 g.) and phosphorus pentaselenide (20.9 g., 5:1.5 mol.) were placed. The flask was connected with a condenser set for downward distillation. A Y-type adaptor was attached tightly at the place between the lower end of the condenser and a receiver. A tube then ran from the side arm of the adaptor to some bottles of granular sodium hydroxide and strong caustic soda to dissolve and decompose any hydrogen selenide which might be formed. The mixture was heated gently in an oil bath to 70—90°, when the reaction commenced violently with a rapid evolution of hydrogen selenide. The heat source was withdrawn until the reaction moderated. After the vigorous reaction had subsided, the flask was arranged for distillation under diminished pressure. The yellow-green liquid was collected at 110—135°/120—150 mm. Hg. During the distillation the bath temperature was maintained at about 200—230°. The liquid collected weighed 16.9 g. (yield 63%). By repeated redistillation 2-*n*-propylselenazoline, a light green liquid (8.7 g., yield 32.4%) which boiled at 116°/70.5 mm. Hg was obtained. The picrate was obtained by adding the base to a saturated alcoholic solution of picric acid. When this material was recrystallized from hot alcohol, it was often decomposed. The crude picrate was recrystallized from chloroform-ligroin, yellow crystals, m.p. 100.5—101°. (Found: C, 35.62; H, 3.33; N, 13.60. Calculated for $C_{12}H_{14}O_7N_4Se$: C, 35.56; H, 3.48; N, 13.82%).

(ii) 2-Ethylselenazoline.—The procedure for 2-ethylselenazoline was similar to the procedure described above in the preparation of 2-*n*-propylselenazoline. The yellow orange liquid (2.4 g., yield 34.8%) distilled at 70—90°/60—70 mm. Hg (bath temperature of 180—190°) was made from propionylethanolamine (5 g.) and phosphorus pentaselenide (5.85 g., 5:1.5 mol).

The redistillation of the crude material gave light green liquid which boiled at 110—111°/135 mm. Hg (1.3 g., yield 19.4%). The picrate was labile in alcoholic solution. The recrystallization of the crude picrate from chloroform-ligroin yielded yellow prisms, m.p. 127—127.5° (Found: C, 34.07; H, 3.03; N, 14.25. Calculated for $C_{11}H_{12}O_7N_4Se$: C, 33.77; H, 3.09; N, 14.32%).

(iii) 2-Methylselenazoline.—By the same procedure as mentioned above, the orange-yellow liquid (6.8 g., yield 18.2%) distilled at 80—92°/50—60 mm. Hg (bath temperature of 160—175°) was made from N-acetylethanolamine (26 g.) and phosphorus pentaselenide (34.4 g., 5:1.5 mol.). Repeated redistillation gave a light yellow liquid

(2) A. Van Dormael, *Chem. Abstr.* **44**, 144 (1950).
(3) W. Michels, *Ber.*, **25**, 3048 (1892).
(4) F. L. White, *Chem. Abstr.* **27**, 5350 (1933); *Brit. Pat.* 392,410.
* The present paper was read at the 4th Annual Meeting of the Chemical Society of Japan in Tokyo held in April 6, 1951.
(5) W. Bogen, *Ann.*, **124**, 57 (1862).
(6) W. Muthmann and A. Clever, *Zeit. anorg. Chem.*, **13**, 191 (1897).

(5.2 g., yield 13.9%) which boiled at 102°/145 mm. Hg. This boiling point coincided with b.p. 160—162°/752 mm. Hg,[3] 71—72°/35 mm. Hg[4] shown in the literatures. The crude picrate recrystallized from chloroform, yellow crystals, m.p. 159—159.5°, which also coincided with the melting point in the literature.[3]

(iv) **2-Phenylselenazoline.**—N-Benzylethanolamine (5 g.) and phosphorus pentaselenide (2.75 g., 5:1 mol.). were placed in a flask. The thermometer was inserted nearly to the bottom of the flask. The reaction started at about 80°, proceeded rapidly at about 120° with the evolution of white smoke, and the temperature rose spontaneously to about 140—160°. Soon the reaction ended. The yellow transparent resinous product was dissolved in chloroform, first washed with about 60 cc. of 5% sodium hydroxide solution and then washed with distilled water. White needles crystallized in the chloroform solution. The chloroform was distilled off under reduced pressure, leaving white yellow solid (3 g.). The recrystallization from benzene (70 cc.) gave white needles, m.p. 116—118°, softening at 105° (2.3g., yield 36.2%). (Found: C, 51.69; H, 4.39; N, 6.72. Calculated for C_9H_9NSe; C, 51.45; H, 4.32; N, 6.67%). The crystals obtained here did not give picrate, differing from the 2-alkylselenazolines.

(v) **2-Benzylselenazoline.**—By the same procedure as mentioned in 2-phenylselenazoline, a yellow-brown transparent resin was obtained from N-phenylacetylethanolamine (5 g.) and phosphorus pentaselenide (2.55 g., 5:1 mol.). The resinous mass was dissolved in chloroform (10 cc.), washed with 5% sodium hydroxide solution (50 cc.) and with distilled water. The chloroform was distilled under reduced pressure, leaving a yellow solid (3.45 g.). The recrystallization from benzene (100 cc.) gave yellow crystals, m.p. 122—124°, softening at 117°. Recrystallization thrice from benzene raised the melting point to 123—126°, softening at 122° but without being decolourized. The elementary analysis showed a fair coincidence with the theoretical value. (Found: C, 53.55; H, 5.30; N, 6.19. Calculated for $C_{10}H_{11}NSe$: C, 53.58; H, 4.95; N, 6.25%). The crystals also did not give picrate.

Summary

(i) Several derivatives of Δ^2-selenazolines were synthesized from N-acylethanolamine and phosphorus pentaselenide.

The larger the alkyl group was, the better the yield became.

(ii) 2-Arylselenazolines were solid and did not give picrates, differing from 2-alkylselenazolines.

The above results are largely due to the kind guidance of Professor Sumio Umezawa and the assistances of Kazuo Suzuki, and Yoshiro Itō who have helped me. Many thanks for their continual kindness.

Department of Applied Chemistry, Engineering Faculty of Keiō University, Tokyo.

Walden Inversion of Amino Acids. VI. The Synthesis of D-Surinamine (N-Methyl-D-tyrosine)

By Nobuo IZUMIYA and Atsuo NAGAMATSU

(Received March 27, 1952)

The synthesis of L-surinamine was carried out by Fischer and Lipschitz[1] from L-tyrosine through *p*-toluenesulfonyl derivatives. Recently, Corti[2] treated L-tyrosine with dimethyl sulfate and obtained L-surinamine. But no synthesis of D-surinamine has yet been attempted. The present study was undertaken to accomplish the synthesis of D-surinamine, and the reactions utilized were as follows:

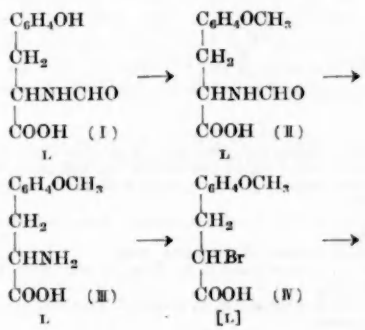

(1) E. Fischer and W. Lipschitz, *Ber.*, **48**, 360 (1915).
(2) U. A. Corti, *Helv.*, **32**, 681 (1949).

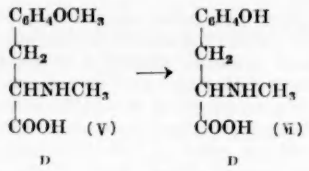

(V) (VI)

D D

One of us (N. I.) has reported the results of his studies on Walden inversion of some amino acids,[3] such as δ-benzoyl-L-ornithine, ε-benzoyl-L-lysine, L-methionine, S-methyl-L-cysteine, S-butyl-L-cysteine, S-benzyl-L-cysteine, O-methyl-L-threonine, β-methoxy-DL-norvaline and 1 (or 3)-benzyl-L-histidine, and recognized a certain regularity in the case of amination and methylamination at 0 and 100° of the [L]-α-bromo acid prepared by the action of nitrosyl bromide on L-amino acid.

O-Methyltyrosine produced by the action of ammonia on the bromo acid (IV) at 100° was racemic, but O-methyltyrosine obtained at 0° was of D-form and showed the occurrence of Walden inversion. In the case of methylamination either at 100 or 0°, the obtained O, N-dimethyltyrosine was of D-form. But it must be noted that Rivers and Lerman[4] synthesized O-methyl-D-tyrosine before we did by the reaction of ammonia on bromo acid (IV) at 0°.

Though N-formyl-L-tyrosine was synthesized by Fischer[5] in 1907, we obtained a good yield of the substance by the method of Fruton and Clarke.[6] O-Methyl-L-tyrosine had already been prepared by Behr and Clarke[7] by methylation and subsequent hydrolysis of N-acetyl-L-tyrosine, and by Rivers et al.[4] by catalytic reduction of O-methyl-N-carbobenzoxy-L-tyrosine. But, the method adopted by the present authors seems preferable to the existing methods described above in the yield and the procedure. The compound (III) had $[\alpha]_D^{17}=-5.7°$ (the authors), $[\alpha]_D^{29}=-5.9°$[7] and $[\alpha]_D^{17}=-10.0°$.[4] Therefore, it was expected that we might obtain a partly racemized product after formylation. But actually, L-tyrosine obtained by the hydrolysis of our -O methyl-L-tyrosine and D-surinamine by the methylamination of bromo acid (IV) and subsequent hydrolysis were optically pure substances.

(3) N. Izumiya, *J. Chem. Soc. Japan, Pure Chem. Sect.*, **71**, 560 (1950), **72**, 26, 149, 445, 550, 702, 1050 (1951); The result of concerning, 1 (or 3)-benzyl-L-histidine is unpublished.

(4) R. P. Rivers and J. Lerman, *J. Endocrinol.*, **5**, 223 (1948).

(5) E. Fischer, *Ber.*, **40**, 3716 (1907).

(6) J. S. Fruton and H. T. Clarke, *J. Biol. Chem.*, **106**, 667 (1934).

(7) L. D. Behr and H. T. Clarke, *J. Am. Chem. Soc.*, **54**, 1630 (1932).

Experimental

N-Formyl-L-tyrosine (I).—L-Tyrosine (18.1 g.), having m.p. 314~316° (decomp.) and $[\alpha]_D^{10}=-12.1°$ (c=2.81, 3N HCl), was treated with 85% formic acid (220 cc.) and acetic anhydride (65 cc.) by Fruton and Clarke's method of formylation. At the end of the reaction, the solution was evaporated under reduced pressure. An ice cold N-hydrochloric acid was added to the remaining product to dissolve tyrosine not reacted on, and the compound (I) was collected by filtration, and washed with a small amount of cold water. It was recrystallized from water, and obtained 16.3 g. (yield 78%). It had no crystal water and remained as a non-hydrated compound even when exposed to the air for a long time. It has m. p. 170~171° and $[\alpha]_D^{10}=+89.4°$ (c=1.74, ethyl alcohol). Found: N, 6.64%; neut. equiv., 213. Calculated for $C_{10}H_{11}O_4N$: N, 6.70%; neut. equiv., 209.1.

Fischer[5] has described this substance as having one mole of crystal water, m. p. 171° and $[\alpha]_D^{25°}=+84.8°$ (dried substance, c=2.20, alcohol).

O-Methyl-N-formyl-L-tyrosine (II).—The compound (I) (20.9 g.) was dissolved in 4N-sodium hydroxide (50 cc.). The solution was then treated alternately with 4N-sodium hydroxide (10 cc.) and dimethyl sulfate (4.76 cc.) with mechanical stirring, the temperature being held at 30~35° by cooling; the addition was repeated four times in all. Stirring was continued for two hours at room temperature after all of the dimethyl sulfate had been added. The solution was acidified with 8N-nitric acid, and the crystal was collected and recrystallized from water. 20.3 g. was obtained (yield 91%). It had m. p. 152~154° and $[\alpha]_D^{10}=+94.7°$ (c=2.11, alcohol). Found: N, 6.31%; neut. equiv., 226. Calculated for $C_{11}H_{13}O_4N$: N, 6.28%, neut. equiv., 223.1.

The compound (I) was methylated with methyl iodide and sodium hydroxide in the usual way,[1] and the product obtained had m. p. 151~154°, showing correct elementary analysis. But, in this case, the fact that the product contained a small amount of the compound (I) was recognized in the paper chromatogram of the hydrolysate of this product.

O-Methyl-L-tyrosine (III).—The compound (II) (11.2 g.) was hydrolysed with 3N-hydrochloric acid (100 cc.) for 2 hours. The solution was evaporated under reduced pressure, and the concentration was repeated with the addition of water. The residue was dissolved in a small amount of water and neutralized with ammonia. After cooling, the resulting crystal was collected. This was recrystallized from hydrochloric acid and ammonia, and 8.6 g. was obtained (yield 88%). It had m. p. 263~265° (decomp.) and $[\alpha]_D^{17}=-5.7°$ (c=2.02, 3N HCl). Its phenylhydantoic acid had m. p. 176° and $[\alpha]_D^{15}=+127.5$ (c=3.89, alcohol).

Its *p*-toluenesulfonyl derivative had m. p. 66~

67° and $[\alpha]_D^{15}=+32.8°$ (c=3.34, alcohol). Found: N, 3.88%. Calculated for $C_{17}H_{19}O_5NS$: N, 4.01%.

The compound (III) was converted into L-tyrosine by the action of hydroiodic acid. The resulting L-tyrosine was confirmed as optically pure, and had $[\alpha]_D^{10}=-11.9$ (c=2.57, 3N HCl).

Behr et al.[7] have reported the compound (III) as having m. p. 264~265° (decomp.) and $[\alpha]_D^{20}=-5.9°$ (2% in N HCl), and its phenylhydantoic acid as having $[\alpha]_D^{21}=+123.6°$ (4% in alcohol). Rivers et al.[4] have reported the compound (III) as having m. p. 259~260° (decomp.) and $[\alpha]_D^{17}=-10.0°$ (2% in N HCl).

[L]-α-Bromo-β-(p-methoxy phenyl) propionic acid (IV).—The compound (III) (0.1 mol.) and potassium bromide (0.35 mol.) were dissolved in 2.5N-sulfuric acid (0.52 mol.). To the mixture was added sodium nitrite (0.16 mol.) in the usual way.[3] The resulting pale yellow crystal was collected, washed with water. The yield was 84 %. It had m. p. 85~89° and $[\alpha]_D^{10}=+13.8°$ (c=1.74, alcohol). It became oily when it was recrystallized from alcohol and water. Found: Br, 29.4%. Calculated for $C_{10}H_{11}O_3Br$: Br, 30.8%.

Rivers et al.[4] have reported it as having m. p. 98~99°.

O-Methyl-DL-tyrosine.—The brome acid (IV) (5.18 g.) was dissolved in 60 cc. of ammonia (saturated at 0°) and heated in a sealed tube at 100° for 1 hour. The solution was evaporated to dryness under reduced pressure, and the residue was collected by the aid of a small amount of cold water. It was recrystallized from hydrochloric acid and ammonia, and 3.20 g. was obtained (yield 82%). This had m. p. 285~287° (decomp.) and no rotation. Found: N, 7.24%. Calculated for $C_{10}H_{13}O_3N$: N, 7.18%. Its phenylhydantoic acid had m. p. 192~193° and showed no appreciable rotation. Found: N, 9.07%. Calculated for $C_{17}H_{18}O_4N_2$: N, 8.92%.

Dakin[8] has reported O-methyl-DL-tyrosine as having m. p. 295° (decomp.).

O-Methyl-D-tyrosine.—The bromo acid was dissolved in ammonia in the manner described above and kept at 0° for 7 days. The yield was 79%. It had m.p. 262~263° (decomp.) and $[\alpha]_D^{10}=+5.4°$ (c=2.11, 3N HCl). Its phenylhydantoic acid had m. p. 176° and $[\alpha]_D^{10}=-124.6°$ (c=2.84, alcohol).

O, N-Dimethyl-D-tyrosine (V).—(A) The bromo acid (5.18 g.) was dissolved in 36 cc. of aqueous methylamine (33%) and heated in a sealed tube at 100° for 30 minutes. The solution was concentrated under reduced pressure, and the residue was collected. It was recrystallized from hydrochloric acid and ammonia, and 2.38 g. was obtained (yield 57%). It had m. p. 247~248° (decomp.) and $[\alpha]_D^{10}=-3.9°$ (c=2.02, 3N HCl). Found: N, 6.74%. Calculated for $C_{11}H_{15}O_3N$: N, 6.70%. (B) The bromo acid was treated in the manner described above and kept at 0° for 5 days. The yield was 64%. It had m. p. 247~249° (decomp.) and $[\alpha]_D^{10}=-3.8°$ (c=2.54, 3N HCl). Found: N, 6.77%. Calcd.: N, 6.70%.

D-Surinamine (VI).—(A) The compound (V) (2.09 g.), $[\alpha]_D^{10}=-3.9°$, was dissolved in 20 cc. of hydroiodic acid (saturated at 0°) and warmed in a sealed tube at 70° for 30 minutes. The solution was concentrated under reduced pressure repeatedly by adding some water each time. The residue was dissolved in a small amount of water and neutralized with ammonia. The resulting product was recrystallized from hydrochloric acid and ammonia, and 1.74 g. was obtained (yield 89 %). It had m. p. 273~274° and $[\alpha]_D^{15}=-18.9°$ (c=1.74, 3N HCl). Found: N, 7.07%. Calculated for $C_{10}H_{13}O_3N$: N, 7.18. (B) In the manner described above, D-surinamine was obtained from the compound (V) ($[\alpha]_D^{10}=-3.8°$). It had m. p. 273~275° (decomp.) and $[\alpha]_D^{15}=-19.1$ (c=2.02, 3N HCl).

Fischer et al.[1] have reported L-surinamine as having $[\alpha]_D^{21}=+19.8°$ and Corti[2] as having m. p. 273° (decomp.) and $[\alpha]_D^{19}=+19.1$~19.3.

Rf values of paper chromatography.—The composition of each solvent was as follows:—phenol: water=100:15, collidine:lutidine=2:5 (saturated with water); acetic acid-*n*-butanol:water=1:4:1. The figures denote the volumes. The amino acids were dissolved in N-hydrochloric acid and tested.

Amino acid	Solvent		
	Phenol	Collidine + Lutidine	Acetic acid + Butanol
L-Tyrosine	0.57	0.61	0.60
D-Surinamine	0·83	0.66	0.66
O-Methyl-L-tyrosine	0.77	0.59	0.70
O, N-Dimethyl-D-tyrosine	0.86	0.64	0.78

This work was carried out partly by the aid of the Scientific Research Funds of the Ministry of Education. The authors wish to thank Prof. Dr. R. Hirohata for his guidance in carrying out this work, and also Mr. S. Saeki for his microanalysis of the substances.

Department of Medical Chemistry, Faculty of Medicine, Kyushu University, Fukuoka

(8) H. D. Dakin, *J. Biol. Chem.*, **8**, 20 (1911).

Dichroic Study on Polyvinylalcohol Fiber. II. Effect of the Crystallinity and Moisture Content of the Fibers on Their Deformation

By Saburo OKAJIMA and Yasuji KOBAYASHI

(Received February 11, 1952)

Introduction

The authors studied previously the deformation of the regenerated cellulose fiber,[1] so now the Polyvinylalcohol (PVA) fibers are being studied. The chain molecule of PVA is considered to be very flexible as compared to that of the cellulose and this difference may be expected to appear also in the deformation course. Moreover, the mechanical properties of PVA gel changes remarkably with the crystallinity and the moisture content, and the crystallinity itself can be controlled easily by the heat treatment.[2] The study of these effects of inner structure upon the deformation is considered to be very important and very interesting not only from the theoretical standpoint but also as the basic phenomena in the synthetic fiber industry, especially of Japanese vinylon.

As to the method of study of the orientation degree changed by the deformation, the X-Ray method is not necessarily effective as the crystallinity of the non-heat-treated PVA is very poor and only the dichroic method is useful for the quantitative study, because it gives the orientation of the PVA molecules by using that of a direct dye as a parameter. The dichroic data of Congo Red has already been studied by the authors[3] in the case of the cellulose fibers. PVA fibers can be dyed with direct dyes.

The double refraction and the refractive indices methods are not useful at present as their basic data of PVA fiber of ideal orientation has not been found. These data will possibly be found in the future when the orientation of PVA fiber will be determined dichroitically.

Experiment

(1) Preparation of the isotropic PVA filament.—The isotropic model filament of PVA is prepared by melt-spinning as described in the first report;[4] A sample of PVA powder containing 50% moisture was melted at 140—150°C under 4 atm. and extruded through a glass nozzle in the air of room temperature. The obtained filament has a circular cross section and a smooth surface. The diameter is about 0.17 mm and nearly equal to that of the glass nozzle.

As to the isotropy of the filament it is not perfect, but it has a slight anisotropy and the outer layer of the filament has a positive double refraction and the core a negative one as P. H. Hermans described in the case of the cellulose fiber.[5] But this anisotropy is so slight that it can be used in the following study.

(2) Crystallization of the filament.—In the two series B and C the samples were partially crystallized by heating at 140°C for one hour in the aqueous solutions of 40 and 50% ammonium sulfate respectively. The autoclave required 30 min. to be heated to 140°C from the room temperature and also to be cooled from the same temperature. The treated filaments were washed thoroughly with water and air-dried.

(3) Stretching of the isotropic filaments.—The isotropic filaments, both the non-heat-treated seires A and the heat heat-treated B and C, were dyed with Congo Red and then conditioned and stretched. The dyeing conditions are described in the next section.

The conditioning was carried out in three desiccators at 20°C for 48 hours. The desiccators contained water and the saturated solutions of Na_2SO_4 10 H_2O and $(NH_4)_2SO_4$ and the relative humidities in each desiccator are 100, 93 and 81% respectively at 20°C. It has been confirmed by a preliminary test that the 48 hours' conditioning was sufficient to get the equilibrium states.

The conditioned samples were then stretched from l_0 to l (ca. 26 cm) and then air-dried after being placed in each desiccator for 48 hours more. The degree of stretching is given by $v=l/l_0$. In this case the change of the filament volume caused by stretching was so small that the correction in the value of v was not necessary.

The middle part of the stretched filament was

(1) S. Okajima and others, *J. Soc. Chem. Ind. Japan*, **48**, 85, 86 (1945); **49**, 52, 168 (1946); S. Okajima and Y. Kobayashi, This Bulletin **24**, 85 (1951); S. Okajima and S. Hayama, ibid., **24**, 90 (1951).

(2) I. Sakurada and K. Futino, *Bull. Inst. Phys. and Chem. Research, Japan*, **21**, 1077 (1942).

(3) S. Okajima, *Japan Science Review*, **1**, No. 2, 71(1950).

(4) S. Okajima and Y. Kobayashi, *J. Soc. Chem. Ind. Japan*, **52**, 794 (1951).

(5) P. H. Hermans, Physics and Chemistry of Cellulose Fiber, Elsevier, 1949, p. 387.

placed on the deck glasses, A and B in Fig. 1, and fixed on them at the points F with celluloid solution. Cutting off the filaments at C, A and B were used as the preparates for the measurement of D.

PVA filament can be stretched at its maximum to some 6-fold under the appropriate conditions as shown below and in this case the diameter of the sample decreased and became so thin that a special device was necessary to prevent the slippage at the clamps.

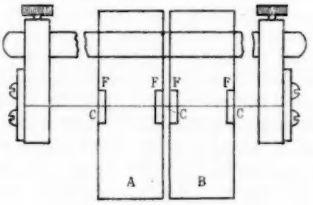

Fig. 1.

Dyeing condition of PVA filament for the dichroic study

As already shown,[3] it is necessary to dye the fiber suitably to obtain the reasonable value of D as the over-dyeing lowers the value enormously. This condition has already been determined in the case of the cellulose fibers, but the properties of PVA are so remarkably different from that of the cellulose that the composition of the dyeing bath was newly determined as below after many trials:

Congo Red: 0.025%,

Solvent: 50% Ethanol aqueous solution.

The filament was dyed in this bath for 48 hours at room temperature. The 48 hours' dyeing was confirmed to be necessary for the complete penetration of the dye in our filament. The ethanol solution was used to prevent the swelling of the non-heat-treated PVA filament.

The sample was taken out of the dye bath and air-dried by hanging in the room air after rinsing with water.

The fixed filament on a deck glass as above was mounted in Tricresylphosphate and the two principal coefficients of absorption, $K_{\parallel}$ and $K_{\perp}$, were determined as previously described.[3] $K_{\parallel}$ and $K_{\perp}$ are the coefficients of absorption of the dyed filament for D-line, oscillating parallel and perpendicular to the fiber axis, and $D=K_{\parallel}/K_{\perp}$ is a measure of the orientation degree of the filament.

Now dyeing to various deepnesses by controlling the dye concentration in the bath and plotting the values of $K_{\parallel}$ and $K_{\perp}$ of these filaments which have been stretched by 6-fold (the maximum stretching), the points appear as shown in Fig. 2. In the figure the points are likely to belong to a linear relation (1) till $K=0.5$, but for the larger values of $K_{\parallel}$ they deviate remarkably (over-dyeing).

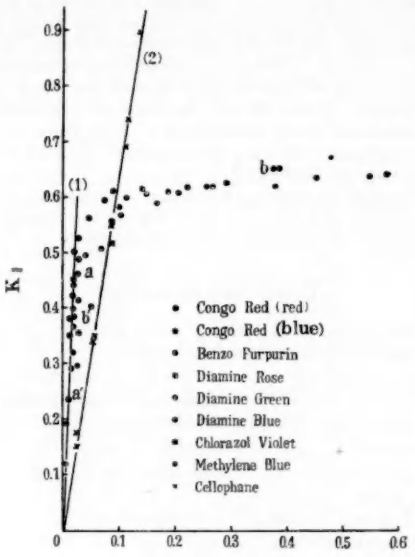

Fig. 2.

This phenomenon is the same as already shown in the case of the cellulose fibers.[3] In order to determine the value of D exactly the value of $K_{\perp}$ must be measured accurately and for this purpose it is desirable that the range of linear relationship extends sufficiently. So the similar experiments were repeated by using the following direct dyes: Diamine Rose, Diamine Green, Diamine Blue, Chlorazol violet, Benzopurpurine, and Methylen Blue. But the results are negative and the observed points begin to deviate from the same value of $K_{\parallel}$ as in the case of Congo Red. The filaments dyed with Congo Red are usually red but change to blue when they come in contact with HCl vapor and, at the same time, their coefficients of absorption increase, even when the $K_{\parallel}-K_{\perp}$ relation is kept unchanged.

A point (a) of a red filament, which has a larger $K_{\parallel}$ but is still on the line, moves to the point (b) when the filament changes to blue, but the point (a') of smaller $K_{\parallel}$ goes to (b') on the line unless $K_{\parallel}$ of (b') is smaller than 0.5. This change is reversible and the points come back to the initial points when the filaments are exposed to NH_3-gas.

The reason of this phenomenon is that the critical values of $K_{\parallel}$ and $K_{\perp}$ are the functions of the specific coefficients of absorption of the filament and not of the total absorption. The linear relationship seems to extend more in the case of the thicker filament of smaller specific absorption coefficient than the thinner filament of larger specific coefficient of absorption even though their total absorption are equall to each other.

This is proved experimentally as shown by a

line (2) in Fig. 2. In this case the values of $K_{\parallel}$ and $K_{\perp}$ were controlled by piling the strips of cellophane, which had been dyed with Congo Red and stretched. The specific coefficient of absorption of this cellophane ($K_{\parallel}$) is 0.16 and smaller than that of the above filament so the linear relationship holds good for $K_{\parallel}$ larger than 0.5. Of course the relation can be expected from the previous calculation.(5)

From these results the dyeing was carried out in this experiment so that $K_{\parallel}$ of the filament stretched to maximum did not exceed 0.5.

Results and discussion

Six series of stretching were carried out as shown in the next table:

Treatment	Relative humidity at the stretching at 20°C		
	100%	93%	81%
A. non-treated	A−1	A−2	A−3
B. heated in 40% $(NH_4)_2SO_4$ soln.	B−1		
C. heated in 50% $(NH_4)_2SO_4$ soln.	C−1	C−2	

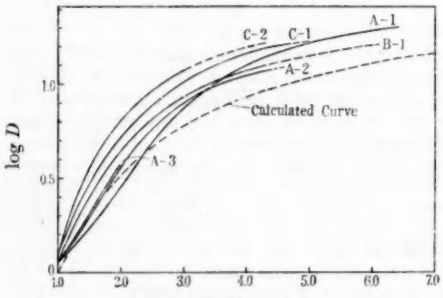

Fig. 3.

Fig. 3 shows $\log D$ as the measure of the orientation degree caused by the stretching given on the abscissa. The broken curve is the calculated one with the assumption of the first theory of O. Kratky.(6) The starting point of each curve does not coincide with the origin because of the slight anisotropy of the original filament. The curves are the mean of the several experiments.

From the figure some interesting facts can be observed as follows.

A-series. In this case the curves are slightly sigmoid but the tendency becomes slighter as the moisture content of the sample decreases, and, at the same time, the maximum degrees of stretching also decrease in the order from A−1 to A−3. The maximum stretching of A−1 is 6.4 and those of A−2 and −3 are 4.5 and 2.0 respectively, and the corresponding values of $\log D$ are 1.31, 1.09 and 0.57 respectively. The orientation degree of $\log D = 1.3$ is almost comparable to that of the ramie as reported previously(3) and, therefore, the orientation of A−1 can be said to be almost complete, while the filament of lower moisture content breaks at the lower degree of orientation.

It is well known that the moistened gel of PVA has a rubber-like elasticity but it loses the high elasticity and becomes rigid as it dries. This behaviour can be considered to be due to the decreasing microbrownian motion with the lowering of the moisture content. The above phenomena in the stretching may be due to the same cause, and therefore, generally speaking, the polymer having a more flexible chain molecule can be oriented more completely by stretching.

The authors repeatedly(7) maintained that in the case of the regenerated cellulose fiber the orientation degree at break is far from the complete orientation. This is because the chain molecule of the cellulose is too rigid to be arranged parallel in the ordinary processing. But this flexibility of the chain molecule is affected by many factors and even in the case of PVA it becomes rigid as said above because of the decaying microbrownian motion and the growing coherent force between the segments. And indeed, the deformation process of A−3 is very similar to that of the cellulose fiber. So, on the contrary, the isotropic cellulose fiber may possibly be stretched to a more highly oriented state in the properly selected conditions.

B−1. The curve is the saturation type in this case. The change is steep at first but later becomes inferior to that of A−1. The maximum value of v and $\log D$ are 6.1 and 1.21 respectively.

C-series. The curves are also the saturation type and very similar to that of B−1, and the changes of these are steeper than of the latter. But in this case the anisotropy of the original sample increased slightly by the heat-treatment, so correcting this factor, the difference between B−1 and C−1 becomes very slight although the above tendency also remains unchanged. The effect of the moisture content is also seen in this series.

Now an interesting observation will be added. It has been observed that when an isotropic fiber of regenerated cellulose is stretched higher under some conditions it appears milky due to the occurrence of a number of small lateral crackings. According to one of the authors' experiment on the cellulose fiber, this milkiness occurred in the dry stretching only and it was seen that the higher the stretching, the more anisotropic the original fiber was.

The same phenomena also appeared in the present study. The table below shows the degrees of stretching when the filaments began to appear

(6) O. Kratky, Kolloid, Z. 64, 213 (1933).

(7) S. Okajima, *J. Soc. Chem. Ind. Japan*, **49**, 168 (1946); *Bulletin of the Yamagata University, Natural Science*, No. 1, 21 (1951).

milky under their conditions, from which it is clear that even in dry stretching the phenomenon

A-1	A-2	A-3	B-1	C-1	C-2
—	4.4	—	4.3	4.7	3.1

is difficult in the moist state (A-1, not occurred) but becomes easy as the filament is demoistened (C-1, C-2) and crystallizes (C-1). The broken curves of A-2, B-1, C-1 and C-2 in Fig. 3 indicate the occurrence of this milkiness.

Conclusion

From the above results it is concluded that the relation of $\log D$ versus v of PVA filament is nearly saturation type as the first theory of Kratky requires. The demoistening and the partial crystallization of the filament does not change the tendency, but the former affects remarkably the degree of maximum stretching and the corresponding orientation, while the latter lowers the maximum stretching degree but not the degree of orientation.

Of course dichroism can indicate the orientation of the amorphous region and not the state in the crystallite. The crystallinity of the series A is very poor, so the orientation of this series may be given reasonably by $\log D$. But in the case of the filaments of higher crystallinity, the problem is not so simple because it is not yet proved whether the orientation of the amorphous part is not different from that in the crystalline region in the case of PVA. The study must await the future work. So the above results must be considered from the present stage of our knowledge.

The authors are indebted to Dr. S. Yazawa for the sample of PVA used. The cost of this research has been defrayed by the Grant in Aid for Fundamental Scientific Research from the Ministry of Education, to which the author's thanks are due.

Faculty of Engineering, Yamagata University, Yonezawa

Heterogeneous Structure of Rayon. I. Some Observations of the Heterogeneous Acetylation of Rayon

By Saburo OKAJIMA, Shigeru HAYAMA and Koichiro KOBAYASHI

(Received February 11, 1952)

It has long been known that the viscose rayons have the skins whose microstructures differ from those of the cores, but until recently there was no attempt to clear up these differences by studying the microstructures of the skin and core separately, excepting a short report by Nakayama,[1] who studied separately their orientation degrees by preparing a longitudinal section of rayon.

But this method requires extreme skill, so the authors studied the same problem since 1950 with a completely different method and have gained some interesting results. Recently the authors learned that some papers referring to the same problem have already appeared since 1946 by Elöd,[2] Preston,[3] and Hermans,[4] among which we could read the original papers by Preston and Hermans, according to which the similar experiments seem to be carried out by Elöd to get some similar results. But some discrepancies are thought to exist between the results of these authors, including the authors of this present paper, so our data are also reported here.

Consideration about the heterogeneous acetylation suitable for peeling-off the rayons

A method can easily be considered to trace radially the heterogeneous structure by peeling-off the rayon from the surface toward the center. And the authors also tried this chemically by acetylating the outer layers of the filament to the various depths by acid-catalyzed heterogeneous

(1) T. Nakayama, *Textile Review, Japan*, **40**, 60 (1949).
(2) E. Elöd & H. G. Fröhlich, *Melliand Textilb.*, **27**, 103 (1946); *Textile Research J.*, **18**, 487 (1948).
(3) J. M. Preston, *J. Textile Inst.*, **39**, T 211 (1948); **40**, T 327 (1949).
( ) P. H. Hermans, *Textile Research J.*, **20**, 553, (1950).

reaction by keeping the fibrous state and subsequent dissolution of the acetylated shell. The topochemical acetylation of the cellulose fiber was precisely studied by I. Sakurada,[3] who concluded that the acetylation is also a micelle-heterogeneous reaction and the fiber must be swollen for the sake of the rapid and smooth acetylation.

But for our present purpose, it is desirable that the penetration velocities of the acetylation reagents through the inter-micellar region be as equal as possible to that through the micell itself, although then the acetylation velocity may necessarily be very much smaller. So the heterogeneous acetylation of rayons was tried under the deswollen states in the following experiments.

Nitration, which is more speedy than acetylation, may also be used instead of acetylation for the above purpose, on which the study is now in progress.

Experiment

(1) Sample.—Five rayons were used as samples:

V-1: a viscose rayon on the market, 120/25 denier.

V-2: a viscose rayon, manufactured some 15 years ago, 120/25 denier.

V-3: an old viscose rayon, manufactured on trial some 40 years ago by Prof. Hata, who was one of the famous pioneers of the Japanese rayon industry.

T: a viscose tire cord.

C-1: a cuprammonium rayon on the market.

These samples were extracted with ether for 10 hours, washed with hot distilled water (60°C) repeatedly. The purified samples were vacuum-dried and acetylated; in some experiments the air-dried samples were also used. The effect of the moisture content of the sample will be discussed in the following paper.

(2) Acetylation.—1 gm. of a sample was poured into an acetylating bath, contained in an ordinary test tube stoppered lightly by a cork stopper and acetylated at the constant temperature. Four bath compositions shown in Table 1 were tried, among which the bath A is the most suitable and was used successfully for the most experiments at 40 ~60°C. At 100°C the integration of the fiber was too remarkable for bath A to be used.

Table 1

Bath composition	A	B	C	D
Benzol	30 g.	30 g.	30 g.	
Acetic anhydride	10 g.	10 g.	10 g.	40 g.
Sulfuric acid (1.84)	0.05cc.	0.025cc.	0.10 cc.	
Potassium acetate				12 g.
Glacial acetic acid				10 g.

The bath C contains too much sulfuric acid and disintegrated the fiber considerably, although the reaction proceeds rapidly in this case; when B is used, on the contrary, the reaction is too slow due to the too small content of the catalyst. These two baths are, therefore, not suitable. In the bath D, the fiber form was retained completely even when it was used at 100°C, but the acetylated product did not dissolve in any usual solvents and this was abandoned.

When the samples had been acetylated for the desired time (0.5~1160 hours), they were taken out, washed with benzol, and with hot distilled water (60°C) repeatedly and air-dried at room temperature.

(3) Measurement of the acetic acid content.—0.5 g. of the acetylated product was poured into a 20 cc. of $\pi/2$ NaOH aq. solution in a tightly closed flask and saponified for 48 hours at the room temperature, after which the consumed alkali was titrated and acetic acid content was calculated as usual. The saponification was ascertained to be enough and it needed to be continued for 48 hours under the present conditions.

The observation of the acetylation process

(1) Partial dissolution of the fiber during the acetylation.—If W g. of a sample is acetylated under an ideal condition and if we obtain W_A g. of the partially acetylated product, whose degree of acetylation is x mole. per glucose residue and the acetic acid content is 100 A%, then

$$A = 60x/(162+42x) \tag{1}$$

and therefore,

$$x = 162\,A/(60-42\,A), \tag{2}$$

and

$$W_A = \frac{W}{162}(162+42x) = \frac{W}{1-0.7A}. \tag{3}$$

But the observed value of W_A was always smaller than that calculated from the relation (3), and this decrease in weight became larger and larger as the acetylation time elongated and A also grew larger. This is thought to be due to the partial dissolution of the acetylated part of the rayon.

Now this partially dissolved cellulose, actually dissolving as triacetylcellulose, is assumed to be L_1 g, them

$$W_A = (W-L_1)/(1-0.7\,A). \tag{4}$$

So L_1 can be calculated from W_A, W and A.

Fig. 1 shows the relations of L_1 and A of the samples V-1 and V-3, acetylated under various conditions (see the next report), according to which L_1 grows linearly but slowly with A, (α-range), and beyond a certain point K the curve is very steep (β-range). Similar phenomena are also seen in the cases of the other samples as shown in

(3) I. Sakurada, *J. Soc. Chem. Ind. Japan*, **35**, 123 B, 283 B, (1932); **36**, 280 B, 299 B, (1933); **37**, 53 B, 509 B, (1934).

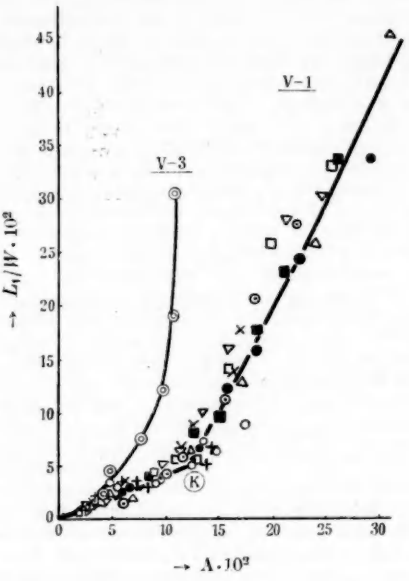

Fig. 1.

Fig. 2. In the α-range the fluctuation of the points is comparatively small, and its slope is independent upon the type of the rayon, while they are dispersed in the β-range and the slopes also vary from sample to sample. The position of K and the slopes of the curves in the β-range are characteristic to each sample, but not remarkably affected by the acetylating conditions. The characteristic of the curve will be described in the following paper. Because of these facts, acetyl content A did not obey the diffusion formula as suggested by I. Sakurada,[5] but after a certain time of reaction, the acetylation velocity increased again.

(2) Microscopic observation of the acetylated fibers.—As well known, many stripes running parallel to the fiber axis can be seen under a microscope on the surface of our viscose samples (Fig. 3 A), but as the acetylation proceeds the surface of the fiber becomes very rugged and many small cracks which cover the stripes appear on them (Fig. 4). But when the yarn is poured

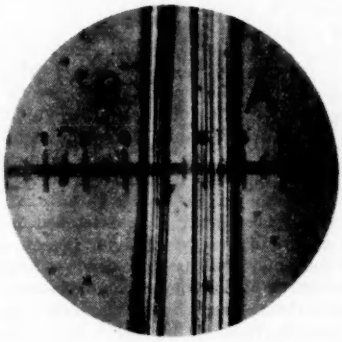

Fig. 3.

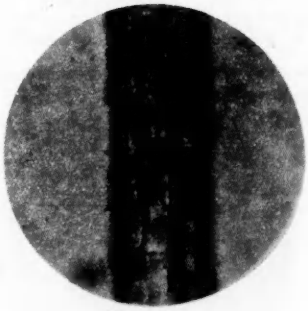

Fig. 4.

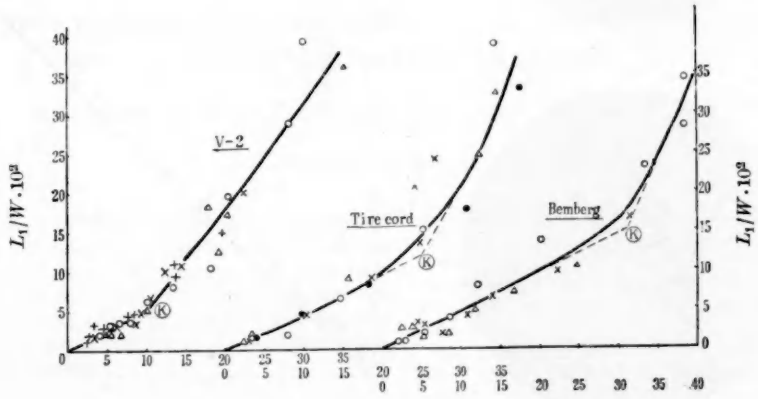

Fig. 2.

into chloroform and warmed at 60°C for 3—4 hours, the stripes reappear again and at the same time the fiber becomes transparent and the external appearance recovers, excepting that its diameter becomes slender (Fig. 3 B). This observation can be clearly explained by considering that the outer layer of a certain thickness, corresponding to the acetylation time, changed to triacetyl cellulose. These acetylated layer depolymerized considerably during the acetylation, so it is partly soluble in the acetylation bath and also its mechanical strength is also very poor and it cracks as the result of the mechanical shocks. This layer can be removed by treating with chloroform. If the acetylation proceeds fiber-heterogeneously the dissolution by chloroform occurs concentrically and, again, the stripes can be seen on the new surface of the rayon, and of course, then, the fiber becomes slender.

The fiber shown in Fig. 5 is an example of the partially acetylated yarn stretched a little, where a part of the peeled layer is seen, and in Fig. 6 the outer shell is more clearly shown.

The degrees of polymerisation of the acetylated shell and the non-acetylated core are separately measured in Table 2, in which DP of the acetylated part was measured viscometrically by dissolving in chloroform and that of the core in cuprammonium solution. The extremely low degree of polymerisation of the acetylated layer allows us to consider its poor mechanical property. As shown in Figs. 1—2 the larger dispersion of the points in the β-range may partly be due to the mechanical removing during the treatment as well as the extraction with the solvent. On the contrary the core is thought not to be degraded to some extent. This is very important when we discuss the mechanical properties of the skin and core separately by such a peeling-off method. But this problem requires further precise study.

Table 2

Sample	Degree of Peeling-off, %	Degree of Polymerization		
		Original rayon	Acetylated shell	Core
V-1	18.8	250	—	270
	19.3	240	60	230
	11.8	240	55	220
V-2	10.0	270	75	250

(3) Solubility of the acetylated product.—If the acetylation proceeds from the outer layer concentrically as considered above, the amount of cellulose, L_2, which changed to triacetylcellulose and remained undissolved during the reaction and the corresponding weight of triacetylcellulose, L_A, can be calculated from the value of A as follows:

$$L_A = \frac{291}{162} L_2 = 1.778\, L_2 \qquad (5)$$

And the value of L_1+L_2 can be also obtained directly by measuring the difference between W and the residue after extracting the acetylated shell with chloroform followed by saponification

Fig. 5.

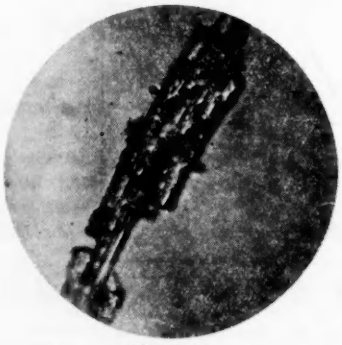

Fig. 6.

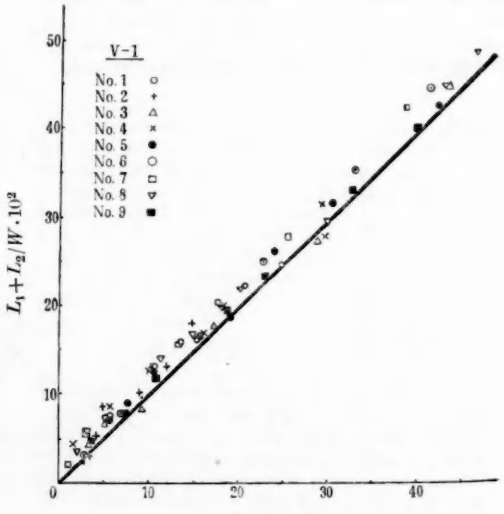

Fig. 7.

with N/5 NaOH aq. solution. If this is denoted by L_T, it must be equal to L_1+L_2, provided that the fiber is acetylated completely heterogeneously. And indeed this is nearly true as shown in Fig. 7. In the figure $(L_1+L_2)/W$ is plotted against L_T/W, where a nearly theoretical relation can be seen (a line in the figure is bisecting between the coordinates), although there is a tendency that the former values are slightly (1—2%) larger than the latter ones, which may probably be due to the incomplete extraction. There is necessarily a continuous distribution of the acetyl groups between the outer layer of triacetylcellulose and the completely unchanged core, and therefore, the smaller part of the acetyl groups remain unextracted.

The Fig. 7 shows the case of V-1 as an example; in the other cases the same relation holds good, excepting values larger than 50%, where the relation is inverse and L_T/W is larger than $(L_1+L_2)/W$, which may perhaps be due to the disintegration of the sample and the loss during the treatments, as the fiber becomes too slender.

Observing th fibers, which were extracted with only chloroform and not treated with dilute alkali, the refractive indices, $n_\parallel$ and $n_\perp$, are equal to these of the extracted one followed by saponification, in spite of the fact that the remarkable difference of the refractivity has been known between the cellulose and triacetylcellulose. So the surface layer of the core containing acetyl group is considered to be very thin in other words, the acetylated layer can be removed almost quantitatively. In order to ascertain this point the next experiment was carried out.

Two samples of V-1 were acetylated at 60°C for 6 (P) and 15 (Q) hours. Their respective acetyl contents are 3.06 and 6.14% and the thickness of the acetylated layers are estimated to be nearly 0.8 and 2.9% of their radius respectively (see the next paper). The denier of the single filament in this case is 5.04 and its mean diameter is nearly 10 micron. Therefore the thickness of the acetylated layers are 900 and 3000 A. respectively.

Observing the sample Q under a microscope existence of a thin layer of different refractivity can be clearly recognized on the surface of the fiber by the appearance of the two Becke's lines. But in the case of P, a single Becke's line appears ordinarily and the outer layer can not be recognized. Therefore, it is thought that the unextracted acetyl content of some 1—2% does not cover the refractivity of cellulose itself. This observation can support the above consideration. The critical thickness of this diffuse layer may be the order of the wave length.

Conclusion

The acetylation type of the not-swollen rayon is fiber-heterogeneous and it proceeds concentrically from the outer surface and the acetylated layer can be removed nearly quantitatively by chloroform. This reaction may be suitable for the peeling-off the rayons.

The cost of this research has been defrayed by the Grant in Aid for Fundamental Scientific Research from the Ministry of Education, to which the authors' thanks are due.

Faculty of Engineering,
Yamagata University, Yonezawa

Heterogeneous Structure of Rayon. II. Orientation Degree of the Skin and Core of Rayons

By Saburo OKAJIMA, Shigeru HAYAMA and Koichiro KOBAYASHI

(Received February 11, 1952)

In the previous report a possibility of peeling-off the rayon fiber by a heterogeneous acetylation was recognized. So now the orientation degrees of the skin and core are measured optically, applying this method, and the effect of the conditions of acetylation upon them is discussed.

Experiment

Five samples of rayon were acetylated by using the bath A as already described in the preceding report. In some cases the other bath compositions were used, where only the diluent benzol was substituted by carbon tetrachloride or toluol. The moisture content of the sample was also controlled.

The acetylated fiber was extracted with chloroform, treated with N/5 NaOH aq. solution, washed with distilled water and air-dried. The refractive indices, $n_\parallel$ and $n_\perp$, of the peeled-off fiber were measured with the Becke's method and the observed values were corrected on the

standard value of $n_{iso}=1.5356$ with the authors' method.[1] $n_{\parallel}$ and $n_{\perp}$ are the refractive indices for the plane-polarized D-line, oscillating parallel and perpendicular to the fiber axis; then the intrinsic double refraction Γ is given by $n_{\parallel}-n_{\perp}$.

The amount of the peeled-off cellulose is expressed by P_r %, which indicates the thickness of the peeled-off shell. If the sectional area and the length of the single fiber are denoted by S_0 and l, then its weight is

$$W=S_0ld,$$

and

$$L_T=(S_0-S)ld,$$

where d is the density of the original fiber and S_0 and S are the cross sectional areas before acetylation and after acetylation and extraction, followed by saponification respectively, providing, of course, that the length is very long compared to S_0, the form of the cross section remains similar during the peeling-off process, and the density is equal through the cross section. Then

$$1-L_T/W=S/S_0.$$

Therefore,

$$(S/S_0)^{1/2}=(1-L_T/W)^{1/2}=r/r_0,$$

and

$$P_r=1-r/r_0=1-(1-L_T/W)^{1/2},$$

where r_0 and r are the radii before and after the peeling-off.

The above assumptions are not thought to hold exactly good in the actual case, and P_r is, therefore, only an apparent representation, although it is right in the dimension.

Conditions of treatment

The results obtained are given in Figs. 1—4, from which some interesting phenomena can be seen.

(1) Effect of moisture of the sample.—The moisture content of the sample poured into the acetylation bath does not affect the orientation of peeled-off fiber according to P. H. Hermans,[2] but in our data the effect is clearly seen. Some of the examples are given in Fig. 1, where the samples V−1 and −2 were acetylated under the following conditions; the vacuum-drying was carried out at 60°C in each case.

Table 1

Conditions of Acetylation

Sample		Conditioning	Acetylation temp., °C	Diluent
V−1	(1)	Air-dried	45	Benzol
	(3)	Air-dired, acetylated after immersion into benzol overnight	60	Benzol
	(4)	Vacuum-dried	60	Benzol
	(5)	Vacuum-dried	60	Toluol
	(8)	Vacuum-dried, conditioned to the moisture content of 4.23%	60	Benzol
	(9)	Vacunm-dried, conditioned to the moisture content of 14.1%	60	Benzol
V−2	(1)	Air-dried	45	Benzol
	(2)	Air-dried	60	Benzol
	(3)	Vacuum-dried	45	Benzol

The vacuum-dried samples (4) and (5) of V−1 show the existence of the outermost layers and the cores of the completely and almost constant birefringence and the transition layers between them, while in the cases of the air-dried ones Γ decreases continuously from the surface toward the core and this tendensy is more remarkable

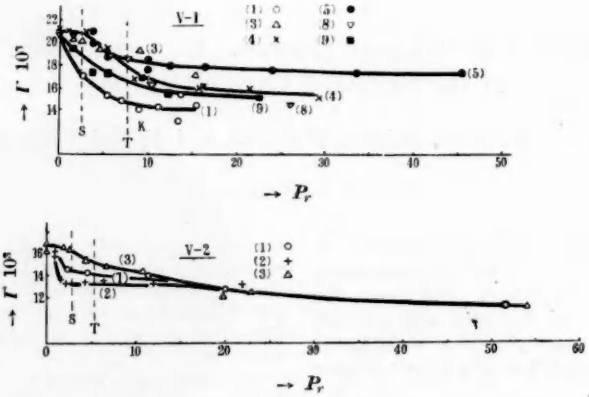

Fig. 1.

(1) S. Okajima and Y. Kobayashi, *J. Soc. Chem. Ind. Japan*, **46**, 941(1943). S. Okajima, Bull. Yamagata University, *Natural Science*, No. 1, 21(1950).

(2) P. H. Hermans, *Textile Research J.*, **20**, 553 (1950).

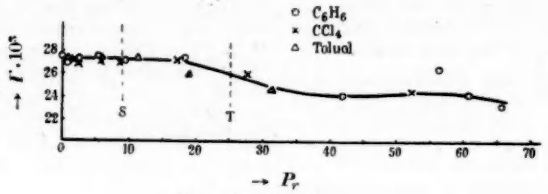

Fig. 2.—Bemberg.

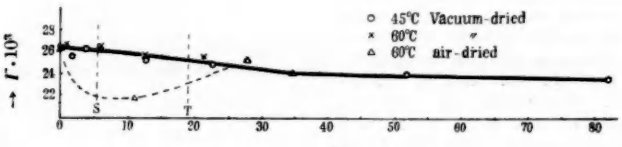

Fig. 3.—Tirecord.

the larger the moisture content of them is (rf. the samples V−1, 1, 3, 8, 9).

The cause of this phenomenon is not clear but the authors believe that the factor causing this difference is the moisture of the sample and not the vacuum-drying because the immersion of the air-dried one into benzol overnight gives the vacuum-dried type (rf. V−1, 3) and also the conditioning after the vacuum-drying gives the air-dried type again (rf. V−1, 8 and 9).

The same phenomenon can also be seen in the case of V−2, where the effect disappears as the reaction proceeds; this is because the loosely absorbed moisture is substituted by the molecules of benzol.

As the results, the moisture effect appears especially in the early stage of reaction so the vacuum-drying is thought to be necessary to recognize the existence of the outermost skin, if any, so all of the samples were vacuum-dried in the following experiments, excepting ones which were especially described.

(2) Effect of diluent.—Two samples of V−1 were peeled-off by acetylating in the bath C, but with using toluol and benzol as the diluent (rf, 4 and 5). Fig. 1 indicates that the curves are similar in shape but Γ of the core are more or less different.

A cuprammonium rayon was also examined by using benzol, toluol and carbon tetrachloride as the diluents. In this case the three curves coincide completely with each other as shown in Fig. 2, therefore, the effect of diluent seems to be negligible.

(3) Effect of the acetylation temperature.—A sample of tire cord was examined by acetylating at 45 and 60°C. Their results coincide completely as shown in Fig. 3 and, therefore, the temperature effect can be disregarded.

In the series (3) the acetylation was carried out without vacuum-drying, so the first point (P_r=10.8%) is remarkably low but the other two points are normal. The reason was already described in the section of the moisture effect.

Distribution of the orientation degree and the type of rayon

Now it is clear that the careful treatment can give the reasonable results, and observing the curves $\Gamma - P_r$ of the vacuum-dried samples, they indicate some interesting facts.

(1) The distribution of the orientation degree and the skin structure.—Observing the radial distribution of Γ of V−1, −2 and also −3 (Fig. 4), whose skin structures are clearly shown by the microscopical observation of the stained cross sections, the outermost skin, the core and the transition layer are recognized in each case. The orientation of the outermost skin, whose thickness is 2−4% of the total radius is constant, while that of the core decreases very faintly toward the center.

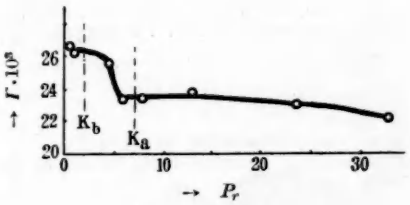

Fig. 4.—V-3.

Moreover in the case of the tire cord or the cuprammonium rayon, one of which is said to have a thickened skin and the other no skin, the similar distribution of the orientation can be seen, although the tendency is slight, as the results of the thickening of the outermost and the transition layers and also the smaller difference of orientation between the skin and core.

This difference of orientation between the skin

and core is much smaller than that which was expected from the impression hitherto given by the optical observation of its cross section.

(2) Structure of the skin.—Some of the microstructures of the skin were tested by many authors. The density of the skin has been thought to be larger according to the methacromasic[3] observation, but the result of Hermans[2] was opposite. As to this problem a phenomenon of some importance is seen in the above data.

As shown in Figs. 1 and 2 of Report I, there is a knick point K on each curve of L_1/W versus A. The curve indicate the ratio of the rate of acetylation of the fiber and the rate of dispersion of the acetylated layer in the bath, so the appearance of a knick point means the occurence of the abrupt change of this ratio, which may probably be caused by the dissolving away of the skin, providing, of course, that the resistance of the skin toward the penetration of the acetylating agents and dispersing away in the bath is larger than that of the core. The behaviour is the same in the case of the air-dried sample and this seems to indicate a priori existence of the outermost skin in the original fiber.

This presumption is supported by the following consideration. If the amount of cellulose which was lost in the acetylating bath (actually as triacetylcellulose) up to the knick point K is L'_K per 100 part of the original sample and the acetic acid content at K is 10^2.A %, then the weight of the partially acetylated sample, W_K, is given by the formula (1) of Report I as follows,

$$W_K=(100-L'_K)/(1-0.7\,A) \qquad (1)$$

If the corresponding value of L_2 at K is denoted by L''_K, then

$$100-L'_K-L''_K+1.778\,L''_K=W_K \qquad (2)$$

$$L''_K=\frac{0.7A(100-L'_K)}{(1-0.7A)\times 0.778} \qquad (3)$$

The value of L_T/W is smaller than $(L'_K+L''_K)/W$ by some 1.5 according to Fig. 7 in the preceding report, therefore in this case

$$L_T=L'_K+L''_K-1.5 \qquad (4)$$

This gives the corresponding value of P_r.

The table below contains these values at the knick point, where the values of L'_K and A of each sample are obtained on each curve in Figs. 1 and 2 of the preceding paper. In the case of $V-3$, the curve is too steep to obtain the correct value of K, so K_a and K_b are used as the limiting values as shown in Fig. 5; the acutal value must be between them.

Table 2

Sample	$V-1$	$V-2$	$V-3$ (a)	$V-3$ (b)	T	C
A (%)	12	11	8.5	4	25	31
L'_K/W	5.3	6	8	1.8	12	15
L_T/W	15.0	10.5	14.1	3.9	34.5	43.8
P_r (%)	7.8	5.4	7.3	2.0	19.1	25.0

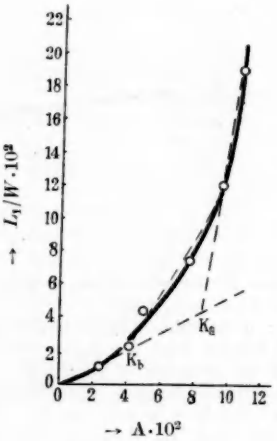

Fig. 5.—V-3.

The calculated value of P_r is indicated by a broken line (T) on each curve of $\Gamma-P_r$; then all of them seem to be in the transition layer of each sample. And in the case of $V-3$ also the transition layer is held between the above two limiting lines.

The same behaviour is also seen in the tire cord or the cuprammonium rayon. This fact is thought to support the existence of the skin structure as described above even in a case, where the existence of the skin has been denied. Of course the skin structure of these rayons are not so remarkable and correspondingly the knick points are less distinct.

These results allow us to venture to calculate the thickness of the outermost skin. If we suppose that the knick point K appears when the outermost skin of the least porosity has dispersed away in the bath liquor and the resistance for the acetylation and the dispersion have decreased abruptly, then L_1 indicates the amount of the outermost skin, which is easily calculated from the $L_1/W-A$ curve.

As shown in Figs. 1—3, in which the calculated value is indicated by a broken line (S), the above supposition is proved to be nearly true in the cases of $V-1$ and -2 and the tire cord. But the value of the cuprammonium rayon which is obtained is too thin. This is probably because the microstructure of the cuprammonium rayon is more or less different from that of the viscose rayon due to the different nature of the spinning reaction.

(3) K. Ohara, *Scientific Paper. I. P. C. R.*, **25**, 154 (1934).

As to V−3 it is very difficult to obtain exactly as already described, so it was omitted from the present discussion.

Furthermore, it is worthy to note that the slope of curve $L_1/W-A$ between the origin and K is constant but thereafter it varies according to the type of rayon, which may indicate that the microstructures of the skin of the various rayons are nearly equal to each other but not of the core.

Conclusion

A peeling-off method by the heterogeneous acetylation can give reasonably the radial distribution of the degree of orientation when it is carried out under the appropriate conditions. The skin structure is shown by this method in the cases of the tire cord and even the cuprammonium rayon. And the resistance of the skin against penetration and dispersion seems larger than that of the core.

The cost of this research has been defrayed by the Grant in Aid for Fundamental Scientific Research from the Ministry of Education, to which the authors' thanks are due.

Faculty of Engineering,
Yamagata University, Yonezawa.

LETTER

Electron Microscopic Observation of Aluminum Chloride

By Sho SUZUKI

(Received April 3, 1952)

A smoke of aluminum chloride, one of the halide catalysts of the Friedel-Crafts' type, was observed by means of electron microscopy. With regard to the same material, the electron microscopic observation has not yet been reported in the literatures I could see. This paper presents interesting micrographs obtained on the same material.

Aluminum chloride used here was prepared

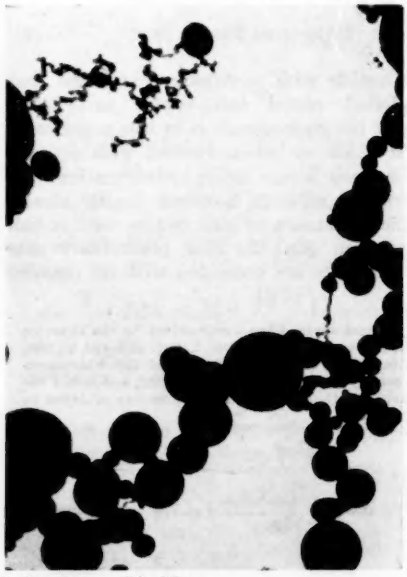

Electron micrographs of aluminum chloride.

Fig. 1.—Magnification: 20,000. Fig. 2.—Magnification: 18,000.

as follows: A stream of chlorine was flowed over pure aluminum foils (99,9%) heated at about 250°C in order to obtain the aluminum chloride smoke.

Figs. 1 and 2 show the micrographs obtained from the aluminum chloride smoke. In these micrographs there are found the two types of particles. One of them has the forms (size: 200 A.—0,2 μ) as recognizable in the case of the usual smoke of metal oxides. Another of them has spherical forms (size: 500 A.—1 μ). The spherical particles seemed to be the hydrate of chloride, because the number of these spherical particles increased always on exposure of the specimen to the air.

Since the wet aluminum chloride can not play a role of a catalyst, the spherical particles remarked in Figs. 1 and 2 will not behave as an active catalyst, but the smoke-like particles in Fig. 1 will be active in catalytic reaction.

The sample prepared by subliming the commercial aluminum chloride gave the same micrographs as are shown in Figs. 1 and 2.

Governmental Chemical Industrial Research Institute, Tokyo

A New Method of Catalytic Hydrogenation[1]

By Yoshiyuki URUSHIBARA

(Received July 4, 1952)

The author with co-workers has found that precipitated nickel and copper are active catalysts for hydrogenation in the presence of caustic alkali or when treated with aqueous caustic alkali before use in hydrogenation. In the hydrogenation in aqueous caustic alkali, metallic aluminum or zinc can be used as well as hydrogen gas. In this preliminary note some examples are presented with no detailed accounts.

Metallic nickel is precipitated by adding zinc dust to an aqueous solution of nickel chloride heated on a water bath until the supernatant liquid becomes colorless. It is washed with water by decantation, digested with 10 percent aqueous sodium hydroxide or potassium hydroxide on a water bath for one hour or two, and again well washed with water. The nickel catalyst thus prepared is shaken with hydrogen for two hours in the hydrogenating medium, aqueous caustic alkali, alcohol, or alcoholic caustic alkali, and then is ready for use as the catalyst in the hydrogenation of organic compounds by shaking with hydrogen at the ordinary temperature and pressure. Thus, estrone is reduced to estradiol either in aqueous caustic potash or in neutral alcoholic solution. Cholestenone is reduced to cholestanol in alcoholic solution, neutral or alkaline. Cinnamic acid is reduced to hydrocinnamic acid in alkaline aqueous solution. Nitrobenzene is reduced to aniline in alkaline alcoholic solution.

The time needed for hydrogenation naturally depends on the amount of nickel, and the use of a large amount seems desirable especially in the hydrogenation in the neutral medium. The metallic nickel precipitated from the chloride solution contains adsorbed chloride ions and the preparatory treatment with caustic alkali seems advantageous even in the hydrogenation in the alkaline medium, because the digestion with caustic alkali desorbs much of the adsorbed chloride. The nickel treated with caustic alkali retains a considerable quantity of adsorbed alkali even though washed several times with hot water, the washings keeping persistently alkaline to phenolphthalein, while it loses the retained alkali promptly if digested with a sodium chloride solution. The adsorbed alkali probably plays an important rôle in the hydrogenation, because the nickel not treated with caustic alkali, and the nickel treated with caustic alkali and then washed with acetic acid, are totally inactive. In conclusion, it may be added that the author has come to understand why Raney nickel is an active catalyst.

Department of Chemistry, Faculty of Science, Tokyo University, Tokyo.
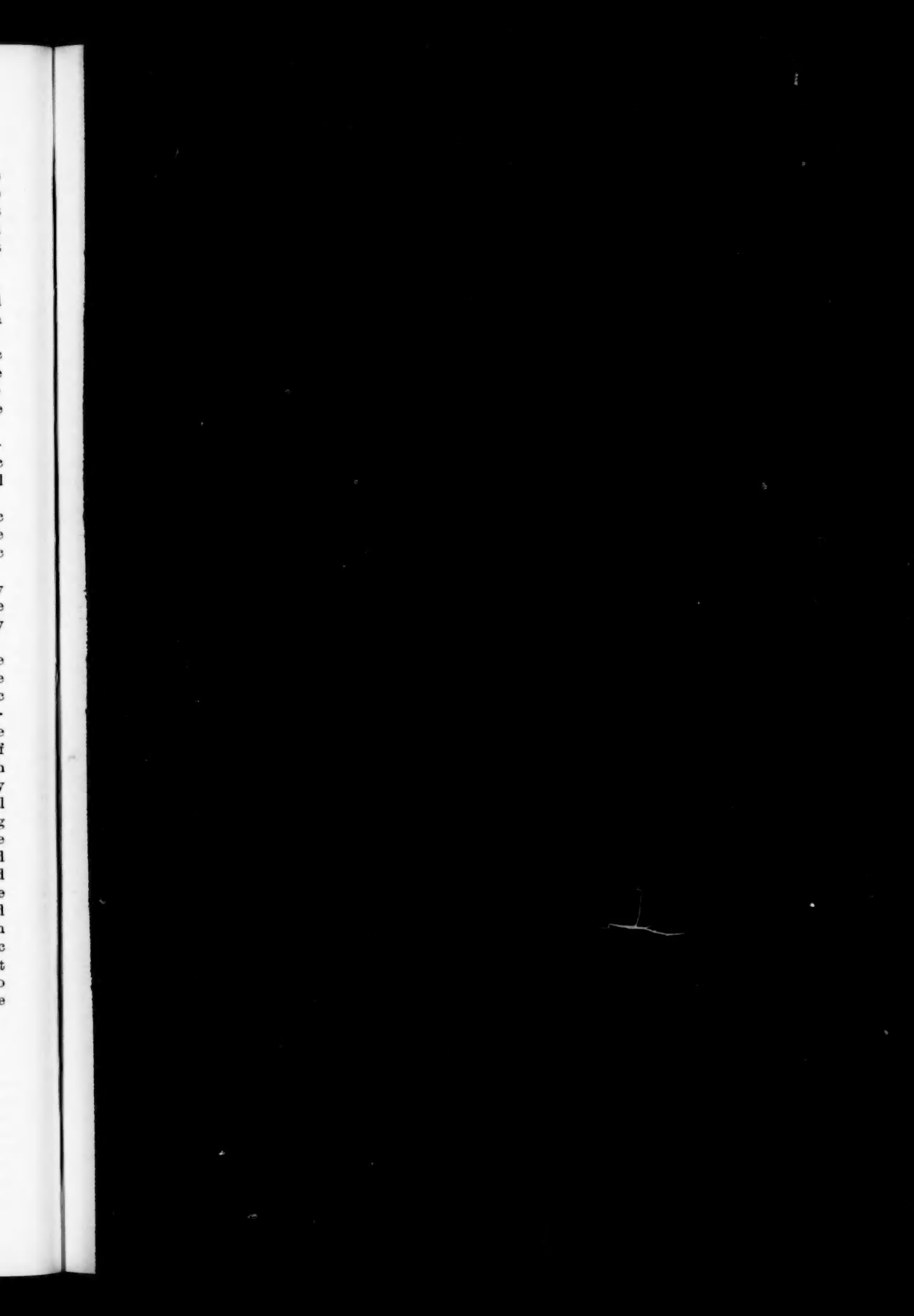
(1) Patent applications were received by the Japanese Patent Bureau: Nov. 7, 1951; Dec. 7, 1951; and Apr. 24, 1952. Read before the 5th Annual Meeting of the Pharmaceutical Society of Japan on April 30, 1952, and before the ordinary meeting of the Chemical Society of Japan on June 21, 1952.